DESIGN OF POLYMER MATERIALS TO HAVE LOWER ENVIRONMENTAL IMPACT

A Dissertation
Submitted to the Graduate Faculty
of the
North Dakota State University
of Agriculture and Applied Science

By

Andriy Popadyuk

In Partial Fulfillment of the Requirements
for the Degree of
DOCTOR OF PHILOSOPHY

Major Department:
Coatings and Polymeric Materials

June 2015

Fargo, North Dakota

North Dakota State University
Graduate School

Title

DESIGN OF POLYMER MATERIALS TO HAVE LOWER ENVIRONMENTAL IMPACT

By

Andriy Popadyuk

The Supervisory Committee certifies that this ***disquisition*** complies with North Dakota State University's regulations and meets the accepted standards for the degree of

DOCTOR OF PHILOSOPHY

SUPERVISORY COMMITTEE:

Dr. Andriy Voronov

Chair

Dr. Dean Webster

Dr. Chad Ulven

Dr. Bret Chisholm

Approved:

06/26/2015 — Date

Dr. Dean Webster — Department Chair

ABSTRACT

In today's world of emerging advanced materials, environmental impact of new technologies, as well as already well-established products, is of utmost importance. Environmental safety is as crucial as performance/price ratio for new materials. Talking specifically about polymer materials, research efforts are dedicated to enhancing material biodegradability, sustainability, manufacturing process improvements etc. It starts to become an industrial standard – to eliminate solvents from polymer production routines, reduce number of chemicals, increase biobased content and generally move towards "green synthesis" concept (use of renewable and/or reclaimed resources throughout whole production process).

The main goal of this work was to develop novel polymers and polymer materials to have potentially lower environmental impact, including new biobased polymer materials with properties and performance not sacrificed by the presence of renewable content, and demonstrate the feasibility of new polymers in industrial applications.

For the purpose of achieving the goal of this work, several approaches were attempted. The first approach lies in the development of a new polymer - poly[n-(tert-butylperoxymethyl) acrylamide-co-maleic anhydride], which combines the features of both initiator and surfactant (the inisurf), to be applied in conventional emulsion polymerization. Use of the inisurf allows for synthesis of novel, in-situ functionalized (peroxidized) latex particles, while reducing the number of chemicals involved in the process.

Another focus of this work was on the development of biobased polymer materials, from plant oils as a raw source, which would be used to substitute petroleum-based polymers.

For this, soybean based polymer surfactants (amphiphylic copolymers) were synthesized, and their potential to be applied as surfactant ingredients in shampoos was evaluated. In addition, synthesis of novel biobased monomers from sebacic (castor oil) and

caprylic (coconut, palm oils) fatty acids – dipropylene glycol acrylate caprylate and dipropylene glycol diacrylate sebacate is presented. Both monomers are shown to be applicable for development of thermosensitive latex particles for controlled encapsulation and release of fragrance in cosmetic products. Finally, a synthetic route for the fabrication of new soybean oil based acrylic monomer for free radical polymerization for making latexes for paints and adhesives is disclosed.

ACKNOWLEDGMENTS

Foremost, I would like to express my sincere gratitude to my advisor, Dr. Andriy Voronov for the continuous support of my Ph.D. study and research, for his patience, motivation, enthusiasm, and immense knowledge he willingly shared with me over the years. His guidance helped me in all the time of research and writing of this thesis. I could not have imagined having a better advisor and mentor for my Ph.D. study.

Besides my advisor, I would like to thank the rest of my thesis committee: Dr. Dean Webster, Dr. Bret Chisholm, and Dr. Chad Ulven, for their encouragement, insightful comments, and hard (but fair) questions.

Deep appreciation goes to Dr. Bret Chisholm and his research group for allowing to work with them on development of soybean based polymers and helping in solving shampoo performance issues. This was a very fruitful collaboration. Dr. H. Kalita and Dr. S. Satyabrata, without your synthetic skills, my work wouldn't exist as it is now.

My sincere thanks also goes to Dr. Stanislav Voronov, Dr. Stuart Croll, Dr. Gordon Bierwagen and Dr. Victoria Gelling, for offering me vast amount of knowledge and inspiration in my research work.

I thank my fellow lab mates, students and staff in Coatings and Polymeric Materials Department: Dr. Ihor Tarnavchyk, Dr. Ivan Hevus, James Docken Jr. and many others, for the stimulating discussions, insightful ideas and for all the fun we have had in the last three years.

I cannot find the proper way to express enormous gratitude to my beloved wife – Dr. Nadiya Popadyuk – for all the support both in research and in everyday life and being impressively wonderful soulmate.

Last but not the least, I would like to thank my family: my parents Igor and Galina Popadyuk, for supporting me spiritually (and financially too!).

DEDICATION

I dedicate this work to my most precious girls, Nadiya and Eva.

PREFACE

This thesis is a product of a hard work of numerous researchers. I happened to be in the right place and the right time to be involved in what I consider a state-of-the-art research process. Following is merely a brisk overview of the immense experimental and theoretical findings, generated in group of Dr. Andriy Voronov.

TABLE OF CONTENTS

LIST OF TABLES

LIST OF FIGURES

LIST OF SCHEMES

LIST OF ABBREVIATIONS

AIBN	Azobisisobutyronitrile
AL	Acrylic Latex
ALS	Amonium Lauryl Sulfate
ASTM	American Society for Testing and Materials
B, HB, H, 1H, 2H, 3H, 4H, 5H, 6H	European continuum pencil hardness scale: H – hardness, B – blackness
BSA	Bovine Serum Albumin
CMC	Critical Micelle Concentration
DC	Dipropylene Glycol Caprylate Diester
DEGVE	Diethylene Glycol Vinyl Ether
DGAC	Dipropylene Glycol Acrylate Caprylate
DGDS	Dipropylene Glycol Diacrylate Sebacate
DLS	Dynamic Light Microscopy
DMAP	4-Dimethylaminopyridine
DI	Deionized
DPG	Dipropylene Glycol
DS	Dipropylene Glycol Sebacate Diester
DSC	Differential Scanning Calorimetry
DVB	Divinylbenzene
ESI	Electrospray Ionization
FPP	Functional Polyperoxide
FT-IR (FTIR)	Fourier Transform Infrared Spectroscopy
GC-MS	Gas Chromatography–Mass Spectrometry
GPC	Gel Permeation Chromatography
HD	Hexadecane
HLB	Hydrophilic-Lipophilic Balance

HMAA .....N-(Hydroxymethyl) Acrylamide

HPLC .....High Pressure Liquid Chromatography

MA .....Maleic Anhydride

MEK.....Methyl Ethyl Ketone

Mn .....Number Average Molecular Weight

NMR .....Nuclear Magnetic Resonance Spectroscopy

PDI.....Polydispersity Index

PEGEVE.....Penta(Ethylene Glycol) Ethyl Vinyl Ether

PM.....N-[(Tert-Butylperoxy)Methyl]Acrylamide Peroxide Monomer

PM-MA .....Poly[N-(tert-Butylperoxymethyl)Acrylamide-co-Maleic Anhydride]

PSA .....Poly(Stearyl Acrylate)

SA.....Stearyl Acrylate

SB.....Styrene-Butadiene Latex

SBA .....Soybean Oil-Based Acrylic Monomer

SBPS .....Soybean-Based Polymeric Surfactants

SEM (FE) .....Scanning Electron Microscopy (Field Emitting)

SLS .....Sodium Lauryl Sulfate

St.....Styrene

TBHP .....tert-Butyl Hydroperoxide

TEA .....Trimethylamine

TEG .....Triethylene Glycol

TEGEVE.....Tri(Ethylene Glycol) Ethyl Vinyl Ether

TEM.....Transmission Electron Microscopy

TGA.....Thermogravimetric Analysis

THF .....Tetrahydrofuran

Tm .....Melting Temperature

Ts-DEGMEE .....Tosylate of di(Ethylene Glycol) Monoethyl Ether

Ts-TEGEE.....Tosylate of tri(Ethylene Glycol) Ethyl Ether

USDA.....United States Department of Agriculture

UV-vis-NIR .....Ultraviolet-Visible-Near Infrared

VOC.....Volatile Organic Compound

VAZO-67.....2,2'-Azobis(2-Methylbutyronitrile)

2-VOES.....2-(Vinyloxy)Ethyl Soyate

2-VOES-ran-TEG .....Poly[2-(Vinyloxy)Ethyl Soyate-ran-tri(Ethylene Glycol) Ethyl Vinyl Ether]

WMP.....Waterborne Polymer Materials

CHAPTER 1. INTRODUCTION

1.1. Vegetable oil potential as a raw material for polymer production

Being one of the major industrial sectors, the coatings industry consumes a sizable amount of petroleum-based materials in the process of paint manufacturing, specifically for the production of resins. Polymeric in nature, resins form the backbone of paint formulations and therefore pose strict requirements as to mechanical and chemical properties, environmental resistance and aesthetics that they result in the final coating [1].

Given the finite nature of crude oil [2], alternatives are being sought with ever increasing intensity. The most promising candidates to supplement chemical industry, with the oncoming shortage of crude oil are plant oils – soybean, palm, corn, cottonseed, rapeseed, sunflowerseed oil etc. [3]. The benefits of vegetable oils include the relative ease of their extraction from plants and vast production volumes, which greatly surpasses their food market capacity, leaving millions of bushels of oil available for chemical reprocessing. According to United States Department of Agriculture (USDA) every year more than 17 million metric tons of edible vegetable oils are left as end stocks [4], adding to the volume of non-edible oils that are available for the chemical industry. Vegetable oils are used to make soaps, skin products, candles, perfumes and other personal care and cosmetic products as is or with minor chemical alterations [5]. Some oils are particularly suitable as drying oils, and are used in making paints and a variety of wood treatment products [6].

That being said, the majority of vegetable oil-derived polymers are yet to become competitive due to their lackluster mechanical and chemical properties, as compared to petroleum-based analogues. Consequently, the design of high-performance biobased polymers from renewable resources, including vegetable oils, represents a promising platform to partially substitute petroleum-based polymers and provide new materials with industrially viable properties and a positive environmental impact [7, 8].

Since the beginning of the XX century, vegetable oils are readily used in the coatings industry as a raw material for polymer production, most prominent use being alkyd resin technology [9]. Ever since alkyd resins were introduced, no other significantly utilized polymers for coating usage are produced on the basis of vegetable oils. Some of the reasons for stagnation in vegetable oil use in polymer production include:

- Composition variation of fatty acids in vegetable oil triglycerides (Figure 1.1) [10, 11];
- Complex physical and chemical transformations/refining required for production of useful chemicals out of vegetable oils [12, 13];
- Lack of vegetable-derived monomers capable of producing linear polymers and, consequently, thermoplastic resins [14, 15];
- Very few systems exist that can accept highly hydrophobic vegetable-based monomers, oligomers or polymers without need to introduce additional solvents [16, 17];
- Inherent autooxidative reactions for unsaturated fatty acids reduce the appeal for coating use, causing yellowing and loss of appearance quality [18, 19];

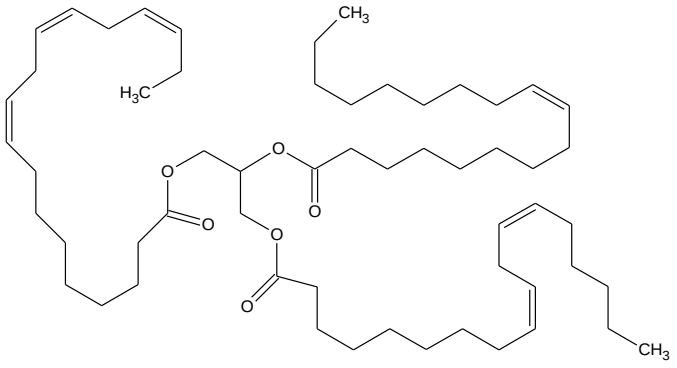

Figure 1.1. Chemical structure of a typical vegetable oil triglyceride, including: linoleic, oleic and alpha-linolenic fatty acid residues (soybean oil).

Chemical transformation of vegetable oils is a growing field which showcases more and more new approaches to the synthesis of both monomers and polymers [20-22]. The majority of fatty acids, comprising vegetable oil triglycerides, have at least two types of

functional groups – alkene unsaturation (one or more) and carboxylic group; only some specialty vegetable oils possess other functional groups, like for example hydroxyl group in 12-hydroxy-octadec-9-enoic acid (ricinoleic) [23]. With this limitation, or rather opportunity, decades of research have been spent on the development of monomers and polymers from fatty acids, mostly by further functionalizing existent functional groups in order to generally produce more readily reactive materials. For example, extensively studied reactions for producing polymers from vegetable oils include:

i) copolymerization in presence of styrene and divinyl benzene [24, 25]:

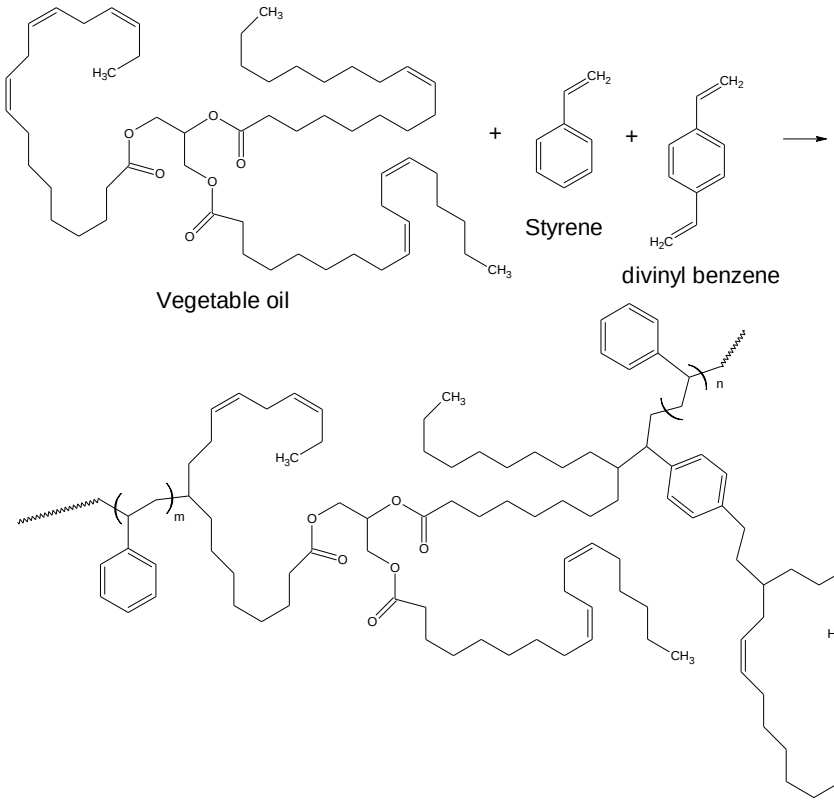

Figure 1.2. Simplified scheme of vegetable oil copolymerization with styrene/divinyl benzene.

ii) epoxidation of unsaturated double bonds and further ring-opening reactions for additional modification or cross-linking [26, 27]:

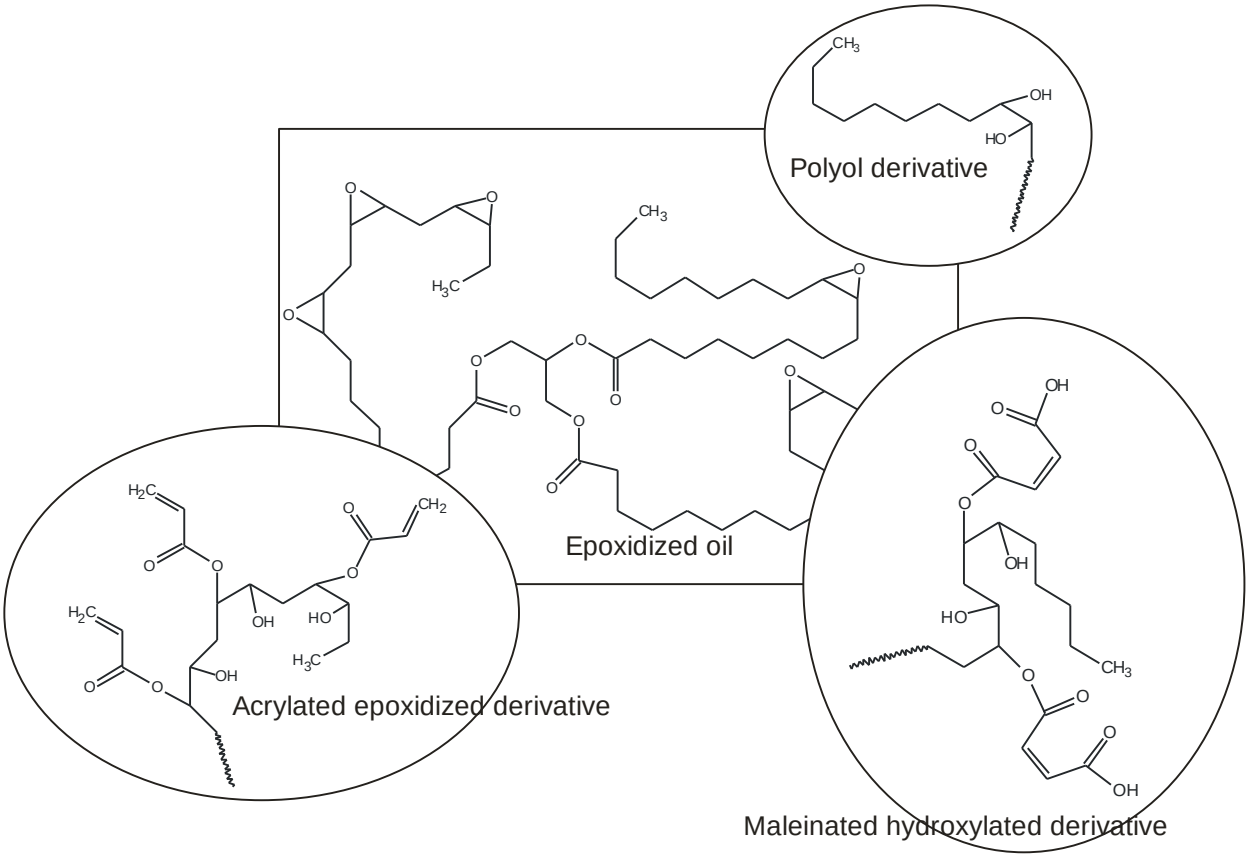

Figure 1.3. Specific products derived from epoxidized vegetable oils.

iii) esterification and transesterification of fatty acids with other reactants to yield monomers for further polymerization/cross-linking [28]:

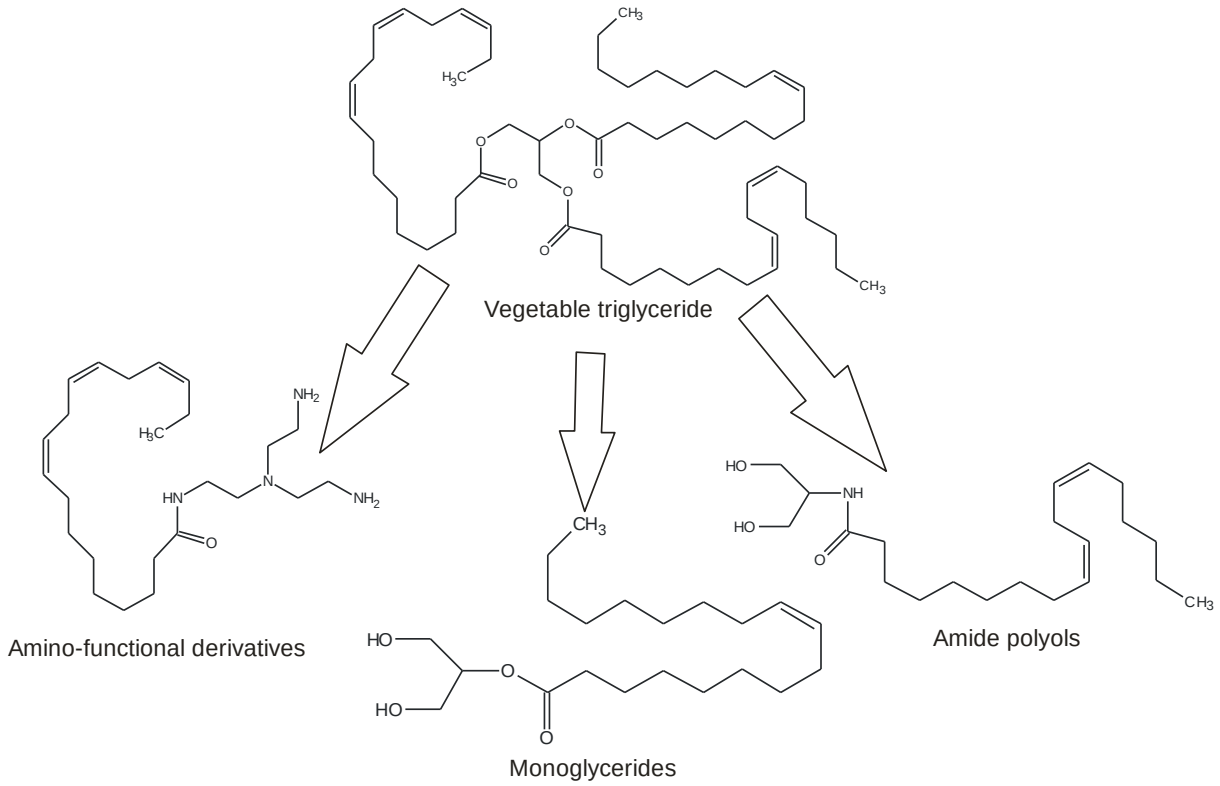

Figure 1.4. Scheme of fatty acid transesterification/amidation products.

iv) cross-linking of unsaturated polyesters, resulting from microbial treatment of vegetable oils and fatty acids [29].

Resulting materials can be further used in polyesterefication (polyols, monoglycerides), polycondesation (epoxy derivatives) and free radical cross-linking (maleate esters, acrylated epoxy derivatives) to produce thermoset resins.

Coherent coating films can be formed from plant oil-based polymer/monomer materials via autooxidative cross-linking of unsaturated fatty acids induced by oxygen and light irradiation (Figure 1.5).

Thus, chemically modified vegetable oils have found a large application niche in alkyd coating systems [9]. Consequently, a great variety of alkyd systems have been formulated, that use linseed oil-based resins, mono-/diglyceride derivatives and polyols, and unsaturated polyesters/polyacrylates based on vegetable oils, etc. [30-33].

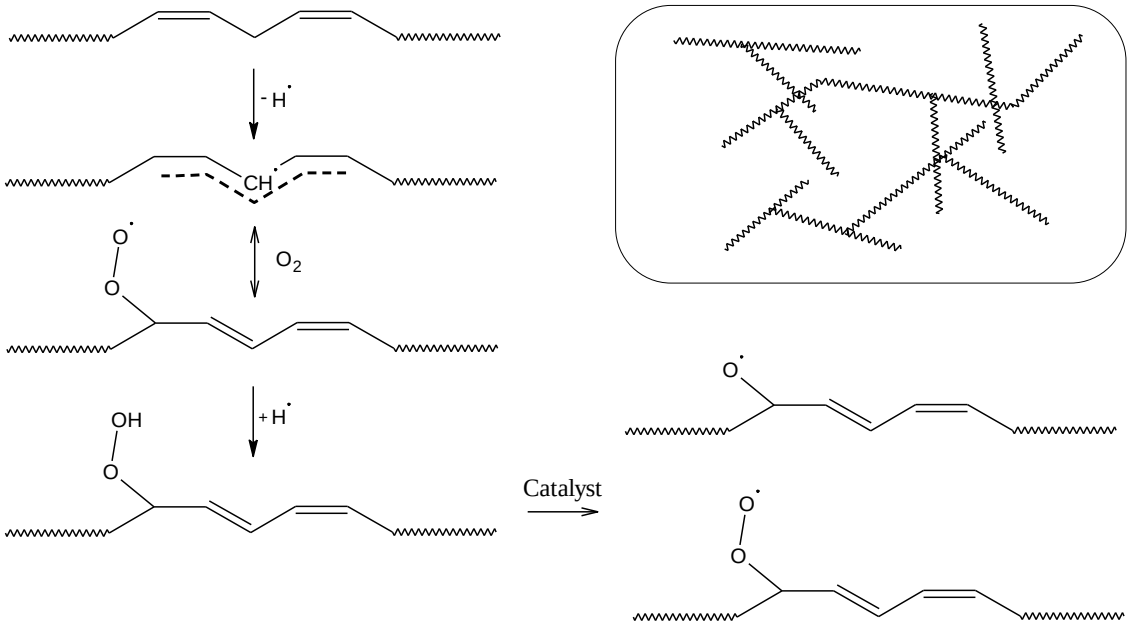

Figure 1.5. Simplified scheme of autooxidative reactions leading to cross-linking in alkyd-type resins (inset shows example of final network).

Autooxidative cross-linking of alkyd-type resins can be accelerated by the introduction of complexion catalysts (so-called "driers") [34]. This brings high potential utility to plant oil-based polymeric binder systems, allowing for a tough, cross-linked coating layer. Additionally, modification of vegetable oil-based materials allows for enhancement of specific properties of the final coating. For example, hybrid acrylic-alkyd (or polyurethane-alkyd) resins exhibit superior weathering resistance, mechanical properties and appearance of acrylics (or polyurethanes) while also benefiting from possible reinforcement via oxidative alkyd-type cross-linking [35-37].

Since the introduction of alkyd-type resins, vegetable oil-based polymers have been successfully used in a variety of varnishes, enamels and architectural coatings. However, the majority of such products have been and still are solvent-based, which decreases their marketability, with more environment-friendly waterborne coating formulations steadily taking over [38]. Consequently, a number of water-based alkyd systems were formulated [39, 40]. However, these systems still require substantial amount of organic solvents during

preparation and hinder a zero-VOC (Volatile Organic Compound) waterborne alkyd system development, or significantly limit the total content of vegetable oil-derived materials used.

To this date, only a handful of competitive technologies exist that are able to produce thermoplastic polymers from vegetable oil, and those available require some unorthodox approaches, limiting large volume production at industrial scale levels [41-43]. There are extensive reviews available in literature on the topics of vegetable oil utilization for polymer production; authors conclude that '*recent developments clearly show that there is still a large potential for interesting new monomers, polymeric materials as well as model systems in all described areas of research*' [44] and '*In recent years, natural oils have become the center of attraction for their potential use as starting materials for the preparation of polymers. This is an alternate route, which has the potential to augment the use of petroleum-based polymers*' [45].

Alongside the benefits of being bio-derived, all plant oil-based polymers and monomers inherently exhibit high hydrophobicity, which presents both positive and negative effects on the utilization of such materials. Most polymer composites, coating binder systems, inks and adhesives tend to benefit from having higher hydrophobicity, which can be attained by use of plant oil-based polymers. However, practical issues concerning product manufacturing limit the use of highly hydrophobic materials. With recent trends in reducing solvent use in technological step for chemical production, waterborne systems for polymer synthesis are receiving particular interest. The same is true for water-based polymer materials, such as latex polymers, providing great challenges for developing hydrophobic systems that are inherently incompatible with water.

There exist few processes capable of producing large volumes of waterborne polymers, including dispersion, emulsion and miniemulsion polymerization, phase inversion process etc. [46, 47]. However, as will be explained in this chapter, the majority of such processes cannot process highly hydrophobic monomers into polymers [48]. Therefore,

even if the technology was developed to produce monomer and resulting thermoplastic polymers out of vegetable oil raw material, considerable effort is still required to effectively implement such material into the industrial sector. In this work we will explore how the application of colloidal chemistry can open venues to incorporate highly hydrophobic oil-derived materials into commercially viable technology.

1.2. Waterborne polymer syntheses

One of the most common industrial routes for waterborne polymer latex production is emulsion polymerization. Emulsion polymerization is a well-studied process that leads to the formation of stable polymer latex particles [49-51]. The main components of an emulsion polymerization system are: water, monomer(s), surfactant(s) and water-soluble initiator. According to commonly accepted scheme [52, 53], emulsion polymerization proceeds over three distinct stages (Figure 1.6):

Stage 1. Radical species nucleate the polymerization of monomer either inside the micelles, forming initial seeds for particle growth. Monomer is found in the micelles, emulsion droplets and polymer-rich particles.

Stage 2. Begins when nucleation of new particles stops. From here onwards, the number of particles in the system remains stable; no non-nucleated micelles are present in the system; monomer can be found in the initial emulsion droplets and in growing polymer-monomer particles.

Stage 3. Final stage of process – no more emulsion droplets present in system. The size of the polymer particles remains stable as the rest of the monomer is polymerized within the polymer-monomer particles.

The mechanism of emulsion polymerization effectively limits the choice of monomers to only monomers with limited yet sufficient aqueous solubility. For more hydrophobic monomers, such polymerization route is hindered and consequently only a small fraction of long alkyl chain monomers can be included in the final polymer latex [63]. Negligible

aqueous solubility of highly hydrophobic monomers prevents the possibility of the monomer molecules to transfer into the growing polymer-monomer particles. However several attempts to increase monomer aqueous solubility have been made, utilizing water-miscible organic solvents or phase-transfer aids, enabling emulsion polymerization of otherwise water insoluble monomers [64, 65]. Such approaches, while viable, also require the use of either additional organic solvents or other chemicals, which is not appealing in terms of environmental impact [66].

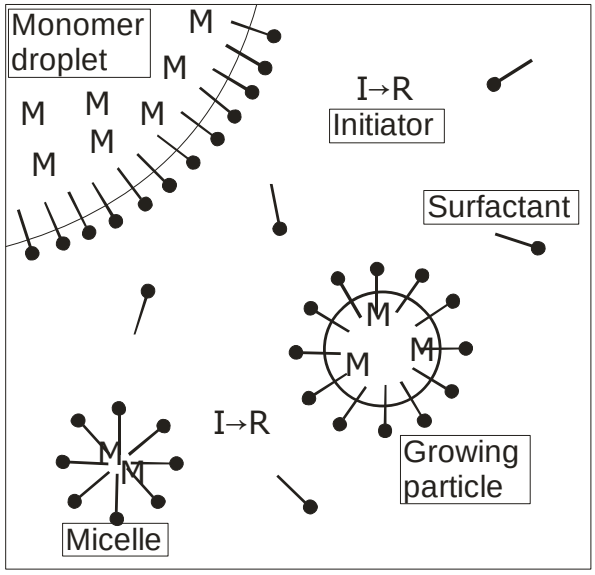

Figure 1.6. Simplified scheme of emulsion polymerization.

Emulsion polymerization is typically initiated using water-soluble initiators, however oil-soluble initiators have also been investigated, showing the possibility of emulsion polymerization process proceeding both in the presence of water and oil-soluble radical initiators [54, 55]. Additionally, macromolecular initiators were successfully employed in emulsions and have been shown to sustain the mode of classic emulsion polymerization [56-58]. It was shown that macroinitiators can be engineered to exhibit a high degree of surface activity (Figure 1.7). Such macroinitiators fall into a larger group of specialty initiators, called 'inisurfs' (initiator-surfactant), and were proven to play a dual role during the emulsion polymerization process: i) act as conventional surfactants – forming micelles

and providing colloidal stability to monomer droplets and polymer and polymer-monomer particles within system; ii) act as a source of free radicals – functional groups in inisurfs structure decompose yielding radicals and macroradicals of inisurfs. As a result, during the course of polymerization, the inisurfs are covalently grafted to the resulting latex particle surface, providing an additional *in-situ* functionalization of the latex particle. Functionalization of particle surface *in-situ* by use of inisurfs provides a reliable means of producing high-performance nanomaterials with additional colloidal stability [59, 60] and reactivity [61, 62].

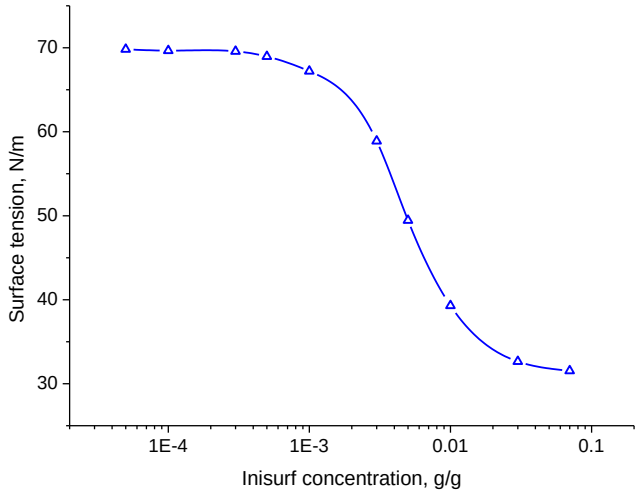

Figure 1.7. Typical isotherm of surface tension of polymer inisurf (PM-MA) aqueous solution [Chapter 3].

The use of inisurfs obviously allows for reducing the number of reagents in an emulsion polymerization, therefore reducing the extractable content of polymer latex product – two aspects that might lead to a lower environmental impact of produced polymer materials.

Another possibility to synthesize latex polymers out of hydrophobic monomers lies in the application of miniemulsion polymerization. Miniemulsion polymerization is a process of latex polymer particle formation, utilizing stable submicron-sized droplets as mini-reactor vessels – a special case of emulsion [67]. There is a fundamental difference between classic

emulsion polymerization and a miniemulsion polymerization, which allows for applications beyond the restrictions of emulsion system. No micelles are present in a miniemulsion system, thus polymerization occurs only within the droplets of monomer (oil phase), which effectively leads to the formation of latex particles of approximately same dimension and number as initial droplets and identical polymer composition [68].

Miniemulsion polymerization is relatively new, however most of the underlying principles are well-established [69, 70]. The formation of miniemulsion is achieved by shearing (typically via exposure to high power ultrasound) mixture of two immiscible liquids in the presence of one or more surfactants and co-surfactants (hydrophobic additives). In a miniemulsion system, coalescence and Ostwald ripening are suppressed due to the presence of the surfactants and co-surfactants. Hydrophobic additives increase hydrostatic pressure inside the droplets, thereby reducing the thermodynamic driving force of oil phase diffusion through the aqueous phase. Stable droplets with sizes between 50 and 1000 nm are obtained, depending on the shear force, type and concentration of surfactants. Miniemulsion-based processes are, therefore, particularly adapted for the production of polymeric nanomaterials [71-73].

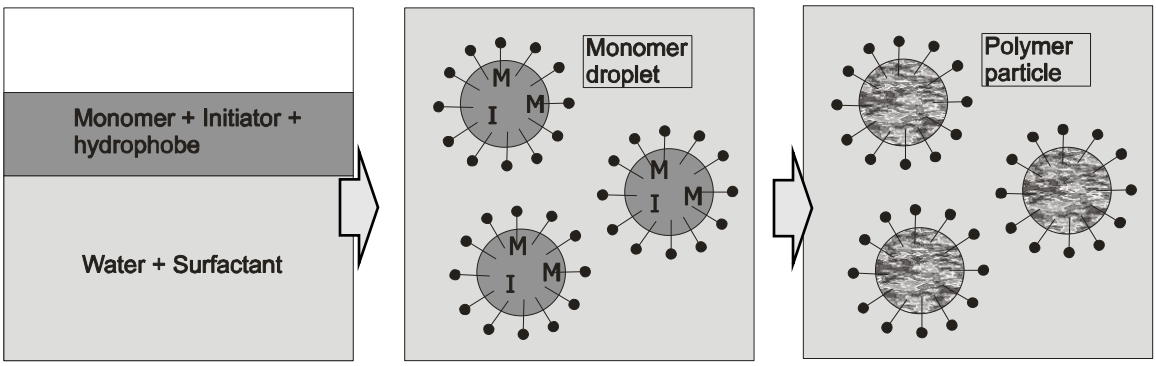

Figure 1.8. Simplified scheme of miniemulsion polymerization.

Miniemulsion polymerization proves to be a powerful tool for the development of new and advanced water-based polymers, especially if hydrophobic monomers are to be employed. Depending on the initial conditions, e.g. chemistry of polymerization reaction,

presence of significant amount of hydrophobic additive or incorporation of inorganic particles, miniemulsion polymerization can be used to synthesize complex morphology particles – hollow, sponge-like, core-shell, etc. [74-76].

The unique nature of miniemulsion polymerization lies mainly in the ability to incorporate either significantly hydrophobic cargo molecules to produce for example drug delivery carriers [77-79] or utilize water-insoluble monomers to yield otherwise unattainable latex polymer particles of homogenous composition [80-82].

Additionally, miniemulsion polymerization is a more eco-friendly route for the incorporation of hydrophobic monomers into latex polymers as it does not require the use of organic solvents or additional chemicals.

1.3. Polymer properties control via composition variations

Polymers already play a significant role in industrial processes and material development, introducing unique properties, otherwise unattainable. Amongst these properties are thermal, pH or solvent-driven property variations. Depending on the type of starting monomer, polymers will exhibit a range of properties, unique to its chemical and structural specialties, like elasticity, crystallinity, toughness, hydrophobicity, etc. Polymers based on a single monomer, i.e. homopolymers, represent the simplest case of polymer materials. In the case of homopolymers, properties of the final material can be tailored by selecting monomer and introducing changes into the structure of the homopolymer macromolecule – e.g. linear, branched, cross-linked. Another tool for polymer structure control is the degree of polymerization (number of monomer units comprising a single macromolecule) which determines overall length and molecular weight of macromolecules [53].

Homopolymers find their application in various industrial sectors, most prominent examples being commodity plastics – polyethylene, polypropylene, polyvinylchloride, polystyrene etc. These are easily manufactured and present properties sufficient for

application in as-is form, frequently without additives [83]. However, a large portion of industrial applications requires polymer materials to perform at levels not attainable by homopolymers. In such cases, it is necessary to combine the properties of different materials in final product. Such combination of properties can be achieved either by physical compounding – mixing of two or more homopolymers or by chemical compounding – synthesis of copolymers [84-86].

Copolymer macromolecules consist of units of two or more different monomer units. In addition to composition variation, copolymer properties can be tailored by the selection of monomers. In terms of composition variation and molecular architecture, copolymers can be classified as (Figure 1.9):

i) random copolymers (units of monomers are statistically distributed over the macromolecule);
ii) alternating copolymers (units of monomers alternate throughout macromolecule);
iii) block copolymers (units of monomers are arranged in blocks of several units);
iv) graft copolymers (units of one type of monomer form backbone of copolymer, while other type of monomer unit protrudes from the backbone in the form of grafted side chains);

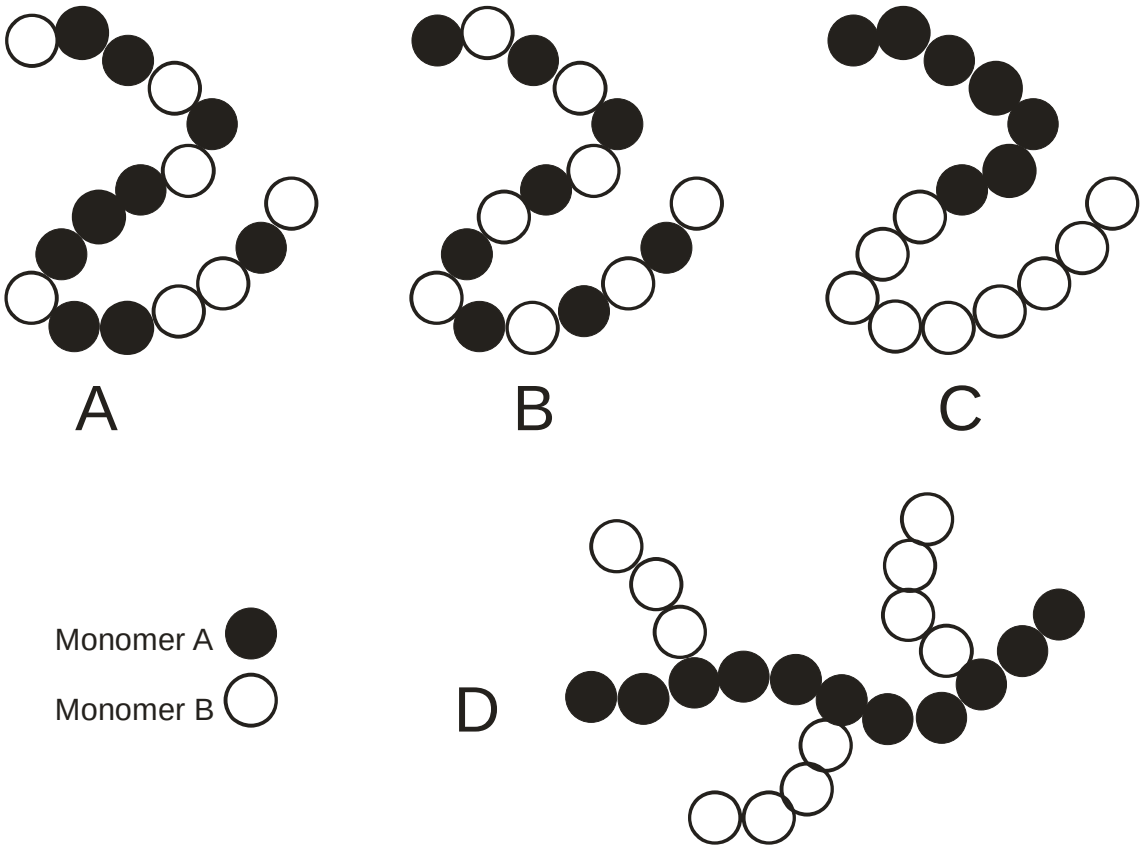

Figure 1.9. Schematic representation of different copolymer structures: A) random; B) alternating; C) block; D) graft.

Additionally, the chemical composition of the copolymer (types and number of constituting monomer units) plays an important role in determining the resulting material properties. For example, if the monomers that produce both rubbery and glassy homopolymers (at room temperature) are copolymerized, the resulting copolymer will present itself as a tough plastic, combining both rubbery and glassy features (extent of property expression depends on % composition) [87, 88].

It is possible to deliberately synthesize copolymers of specific composition in bulk or solvent-based processes, however, in waterborne systems (e.g. emulsion polymerization) synthesis of the same copolymers might be complicated. As was already discussed, depending on monomer hydrophobicity, the ability to polymerize via emulsion polymerization can be obscured. In the case of emulsion copolymerization, one should

consider not only the reactivity of the monomer pair, but also the differences in aqueous solubility of each monomer. In other words, it is not certain that the supply of monomer to the polymerization site (growing macroradical within polymer-monomer particle) will be consistent with the initial monomer feed, as one of the monomers may be more hydrophilic and, thus, more readily soluble in water [89-92]. In case of a miniemulsion system, each monomer droplet already has a pre-defined composition of monomers and the resulting copolymer particles are homogenous in composition.

All these considerations become very important when we start talking specifically about plant oil-based monomer utilization. As it was shown, most of monomers derived from plant oils inevitably exhibit high hydrophobic character, leaving limited number of approaches for their transformation into latex copolymers. However one of these approaches (miniemulsion polymerization) actually allows for control over the (co)polymer composition.

Copolymerization of plant oil derived monomers is a powerful tool that allows inclusion of large quantities of renewable matter into well-performing material, reducing polymer environmental impact. For instance, by copolymerizing soybean oil with divinyl benzene, it is possible to produce a library of polymer materials for composites with mechanical properties that vary greatly, depending on the copolymer composition and mode of copolymerization process (e.g. tensile modulus in 32-75 MPa range for cationic copolymerization and 0.03-1.12 GPa for thermally initiated free radical polymerization) [24]. Another example of advanced properties of renewable copolymers is a polymer surfactant based on 2-(vinyloxy)ethyl soyate [Chapter 2] [93]. A unique combination of the hydrophobic nature of oil-derived monomer with hydrophilic properties of poly(ethylene glycol) based monomer results in an amphiphilic copolymer, exhibiting high levels of surface activity, forming micellar aggregates, stabilizing colloidal dispersions, etc. Yet another example is the copolymerization of maleinized soy oil monoglycerides with styrene by free

radical polymerization, yielding a homogeneous rigid matrix that was successfully used in composite preparation [25]. In this case it was shown how copolymerization can be applied to the transformation of otherwise rubbery homopolymer into a rigid thermoset copolymer by the introduction of a high glass transition component – styrene.

In conclusion, the ability to develop plant oil-based monomers and convert them further into waterborne (latex) (co)polymers is a powerful tool in decreasing overall polymer material environmental impact. By far, mostly thermoset polymer materials were developed on the plant oil basis, leaving a huge thermoplastic segment of the polymer market open for new developments. Additionally, it is clear that advanced polymer materials offer positive environmental impact by reducing the usage of chemicals during polymer production and broadly employing water-based technologies.

This work reports on the several different approaches of polymer environmental impact reduction by following the general ideas outlined in the Introduction – development of new advanced (co)polymer, renewable plant oil based monomers and(co)polymers, and their application in industrial material development.

1.4. References

1. http://www.astm.org/Standards/paint-and-related-coating-standards.html (accessed 4/13/2015).
2. http://peak-oil.org/peak-oil-reference/peak-oil-data/oil-depletion/ (last accessed 4/13/2015).
3. Kopp R. J., Replacing Oil: Alternative Fuels and Technologies. *Resources* **2006,** Fall, 15-18.
4. Foreign Agricultural Service, Table 03: Major Vegetable Oils: World Supply and Distribution, http://apps.fas.usda.gov/ (accessed 4/13/2015).
5. William A. K., Soap compositions. US 3150097 A, **1961.**
6. Orville V. M., Plastic drying oil coating. US 2246452 A, **1941.**

7. Belgacem M. N., Gandini A., *Monomers, Polymers and Composites from Renewable Resources*, Elsevier: Amsterdam, **2008**.

8. Lu Y., Larock R. C., Novel Polymeric Materials from Vegetable Oils and Vinyl Monomers: Preparation, Properties and Applications. *Chem. Sus. Chem*. **2009,** 2, 136.

9. Zwilgmeyer F., Alkyd resins US1975246 A, Oct 2, **1934**.

10. Zambiazi R. C., Przybylski R., Zambiazi M. W., Mendonca C. B., Fatty acid composition of vegetable oils and fats. Ed.: Ceppa B., Curitiba **2007,** 25 (1), 111-120.

11. Kostik V., Memeti S., Bauer B., Fatty acid composition of edible oils and fats. *J. of Hygienic Eng. And Design,* **2013,** 4, 98-102.

12. Hamm W., Trends in edible oil fractionation. *Trends in Food Sci. and Tech.,* **1995,** 6 (4), 121-126.

13. O'Brien R. D., Farr W. E., Wan P. J., Introduction to Fats and Oils Technology, Second Edition, *AOCS Press*: Champaign, IL, US, **2000.**

14. Fang J. M, Fowler P. A, Tomkinson J., Hill C. A. S, An investigation of the use of recovered vegetable oil for the preparation of starch thermoplastics. *Carbohydrate Polymers,* **2002,** 50 (4), 429-434.

15. Jose J., Pourfallah G., Merkley D., Li S., Bouzidi L., Leao A. L., Narine S. S., Thermoplastic polyesters and Co-polyesters derived from vegetable oil: synthesis and optimization of melt polycondensation for medium and long chain poly(ω-hydroxyfatty acid)s and their ester derivatives. *Polym. Chem.,* **2014,** 5, 3203-3213.

16. Philipp C., Eschig S., Waterborne polyurethane wood coatings based on rapeseed fatty acid methyl esters. Prog. in Org. Coat., 20132

17. Shah M.Y., Ahmad S., Waterborne vegetable oil epoxy coatings: Preparation and characterization, *Prog. Org. Coat.,* **2012,** 75, 248–252.

18. Rakoff H., Thomas F. L., Gast L. E., Reversibility of yellowing phenomenon in linseed-based paints. *J. of Coat. Tech.,* **1979,** 649 (51), 25-28.

19. Simpson L.A., Yellowing of alkyd paint films. *Journal of the oil and colour chemists' association,* **1981,** 64 (12), 490-498.

20. Wang R., Schuman T. P., Vegetable oil-derived epoxy monomers and polymer blends: A comparative study with review. *eXPRESS Polymer Letters*, **2013,** 7, (3) 272–292.

21. Rahim N. F. A., Watanabe K., Ariffin H., Ando Y., Hassan M. A., Shirai Y., Synthesis of Biobased Monomer from Vegetable Oil Fatty Acids and Design of Functionalized Greener Polyester. *Chemistry Letters*, **2014,** 43 (9), 1517-1519.

22. Miao S., Zhang S., Su Z., Wang P., A Novel Vegetable Oil–Lactate Hybrid Monomer for Synthesis of High-Tg Polyurethanes. *J. of Pol. Sci. Part A: Pol. Chem.,* **2009,** 48 (1), 243-250.

23. Badami R. C., Patil K. B., Structure and occurrence of unusual fatty acids in minor seed oils. *Prog. in Lipid Res.* **1980,** (19) 3-4, 119-153.

24. Li F., Perrenoud A., Larock R. C., Thermophysical and mechanical properties of novel polymers prepared by the cationic copolymerization of fish oils, styrene and divinylbenzene. *Polymer* **2001,** 42, 10133–10145.

25. Li F., Larock R. C., Synthesis, properties and potential applications of novel thermosetting biopolymers from soybean and other natural oils. In *Natural Fibers, Biopolymers, and Biocomposites*; Mohanty A. K., Misra M., Drzal L. T., CRC Press, online only.

26. Khot S. N., Lascala J. J., Can E., Morye S. S., Williams G. I., Palmese G. R., Development and application of triglyceride-based polymers and composites. *J. Appl. Polym. Sci*. **2001,** 82(3), 703–23.

27. Nelson T. J.; Bultema L., Eidenschink N., Webster D. C., Biobased High Functionality Polyols and Their Use in 1K Polyurethane Coatings. *J. of Ren. Mat.* **2013,** 2 141-153.

28. Chisholm B. J., Bezbaruah A., Kalita H., Functionalized amphiphilic plant-based polymers. WO 2013173734 A1, US20130320255, Nov 21, **2013**.

29. Hazer B., Demirel S. I., Borcakli M., Eroglu M. S., Cakmak M., Burak E., Free radical cross-linking of unsaturated bacterial polyesters obtained from soybean oily acids. *Polym. Bull*. **2001,** 46, 389–394.

30. Alam M., Akram D., Sharminc E., Zafar F., Ahmad S., Vegetable oil based eco-friendly coating materials: A review article. *Arab. J. of Chem.* **2014,** 7 (4), 469-479.

31. Wills P. E., Alkyd Resin Technology. Formulating Techniques and Allied Calculations. Interscience Manual 8 *J. Am. Chem. Soc*., **1963,** 85 (3), 369-369.

32. Wicks Z. W. Jr., Alkyd resins. In *Encyclopedia Of Polymer Science and Technology*; Wiley Online Library, published online **2007**.

33. Patton T. C., Alkyd resin technology, formulating techniques and allied calculations. *Interscience*: New York **1962**.

34. Clauwaert E., Cobalt-Based Catalytic Dryer for Polymer Coatings. US 20120041133 A1, **2009.**

35. Nabuurs T., Baijards R. A., German A.L., Alkyd-acrylic hybrid systems for use as binders in waterborne paints. *Prog. in Org. Coat.,* **1996,** 27 (1-4), 163-172.

36. Shoaf G. L., Stockl R. R., Alkyd/Acrylic Hybrid Latexes with Enhanced Oxidative Curing. *Pol. Reac. Eng.,* **2003,** 11 (3), 319-334.

37. Harris R. R., Pollack W. J., Polyurethane-modified alkyd resin. US4116902 A, **1977.**

38. Pourreau D. B., Smyth S. E., High solids alkyds resins with improved properties based on styrene allyl alcohol resinous polyols. *Proceedings of 81st Annual Meeting of the Federation of Societies for Coatings Technology*, Philadelphia, PA, November 12-14, **2004.**

39. Clark M. D., Helmer B. J., Acrylic modified waterborne alkyd dispersions. US6242528 B1, Aug 12, **1998**.

40. Akbarinezhad E., Ebrahimi M., Kassiriha S.M., Khorasani M., Synthesis and evaluation of water-reducible acrylic–alkyd resins with high hydrolytic stability. *Prog. in Org. Coat.* **2009,** 65 (2), 217-221.

41. Cochran E. W., Williams R. C., Hernandez N., Cascione A. A., Thermoplastic rubbers via atom transfer radical polymerization of acrylated epoxidized soybean oil. *US Patent App.* US 20130184383 A1, **2013.**

42. Mohammed I. A., Jaffar Al-Mulla E. A., Abdul Kadar N. K., Ibrahim M., Structure-Property Studies of Thermoplastic and Thermosetting Polyurethanes Using Palm and Soya Oils-Based Polyols, *J. of Oleo Sci.,* **2013,** 62 (12), 1059-1072.

43. Wang Z., Yuan L., Trenor N. M., Vlaminck L. S. Billiet, Sarkar A., Du Prez F. E., Stefik M., Tang C., Sustainable thermoplastic elastomers derived from plant oil and their "click-coupling" via TAD chemistry. *Green Chemistry,* **2015,** (online only, DOI: 10.1039/C5GC00822K).

44. Meier M. A. R., Metzger J. O., Schubert U. S., Plant oil renewable resources as green alternatives in polymer science. *Chem. Soc. Rev.* **2007,** 36, 1788-1802.

45. Sharma V., Kundu P. P., Addition polymers from natural oils—A review. *Prog. Polym. Sci*. **2006,** 31, 983-1008.

46. Lin H.-R., Solution polymerization of acrylamide using potassium persulfate as an initiator: kinetic studies, temperature and pH dependence. *European Pol. J.,* **2001,** 37 (7), 1507-1510.

47. Arshady R., Suspension, emulsion, and dispersion polymerization: A methodological survey. *Col. and Pol. Sci.,* **1992,** 270 (8), 717-732.

48. Lau W., Emulsion polymerization of hydrophobic monomers. *Macromolecular Symposia Special Issue: Free radical Polymerization: Kinetics and Mechanism*, **2002,** 182 (1), 283-289.

49. Harkins W. D., A General Theory of the Mechanism of Emulsion Polymerization. *J. Am. Chem. Soc.* **1947,** 69 (6), 1428-1444.

50. Smith W. V., Ewart R. H., Kinetics of Emulsion Polymerization. *J. Chem. Phys.* **1948,** 16, 592.

51. J. Ugelstad, F. K. Hansen, Kinetics and Mechanism of Emulsion Polymerization. *Rubber Chem. and Tech.* **1976,** 49 (3), 536-609.

52. R. Arshday, Suspension, emulsion, and dispersion polymerization: A methodological survey. *Col. and Pol. Sci.* **1992,** 270 (8), 717-732.

53. G. Odian, Principles of Polymerization. 4th Edition, *John Wiley and Sons, Inc*.: Hoboken, New Jersey, USA, **2004**.

54. Asua J. M., Rodriguez V. S., Sudol E. D., El-Aasser M. S., The free radical distribution in emulsion polymerization using oil-soluble initiators. *J. of Pol. Sci. Part A: Pol. Chem.* **1989,** 27 (11), 569-3587.

55. Nomura M., Fujita K., Kinetics and mechanism of emulsion polymerization initiated by oil-soluble initiators, 1. The average number of radicals per particle. *Die Makromolekulare Chemie, Rapid Comm.* **1989,** 10 (11), 581-587.

56. Guyot A., Tauer K., Reactive Surfactants in Emulsion Polymerization. *Adv. in Pol. Sci.* **1994,** 111, 45-64.

57. Voronov S., Tokarev V., Oduola K., Lastukhin Yu., Polyperoxide surfactants for interface modification and compatibilization of polymer colloidal systems. *J. Appl. Polym. Sci.* **2000,** 76, 1217-1227.

58. Ivanchev S., Pavljuchenko V., Burdina N., Elementary reactions of the emulsion polymerization of styrene with the localization of radical formation acts at the interface. *J. Pol. Sci. Part A: Polym. Chem.* **1987,** 25 (1), 47-62.

59. Guyot A., Advances in reactive surfactants. *Adv. in Col. and Int. Sci.,* **2004,** 108-109, 3-22.

60. Abele S., Gauthier C., Graillat C., Guyot A., Films from styrene–butyl acrylate lattices using maleic or succinic surfactants: mechanical properties, water rebound and grafting of the surfactants. *Polymer,* **2000,** 41, 1147–1155.

61. Bognolo G., Polymerizable surfactants. In Chemistry and Technology of Surfactants. Ed.: Farn R. J., *Blackwell Publishing*: Oxford, UK. **2006.**

62. Pich A., Richter S., Adler H.-J., Datsyuk V., Voronov S., Functionalization of Latex Particles by using Polymeric Inisurfs. *Macromol. Symp.,* **2001,** 164, 11-24.

63. Barnett G. W., Process for producing an exterior latex paint having improved chalk adhesion. By The Glidden Company, US5202378 A, **1993.**

54. Švec F., What is real mechanism of polymer-supported phase-transfer catalysis. *Pure & Appl. Chem*., **1988,** 60 (3), 377-386.

65. Leyrer R. J., Mächtle W., Emulsion polymerization of hydrophobic monomers like stearyl acrylate with cyclodextrin as a phase transfer agent. *Macro. Chem. and Phys.* **2000,** 201 (12), 1235-1243.

66. Long T. E., Hunt M. O., Solvent-Free Polymerizations and Processes: Recent Trends in the Minimization of Conventional Organic Solvents. *ACS Symposium Series*; American Chemical Society: Washington, DC, **1999.**

67. Asua J. M., Miniemulsion polymerization. *Prog. in Pol. Sci.,* **2002,** 27 (7), 1283–1346.

68. Antonietti M., Landfester K., Polyreactions in miniemulsions. *Prog. in Pol. Sci.,* **2002,** 27 (4), 689–757.

69. Ugelstad J., El-Aasser M. S., Vanderhoff J. W., Emulsion polymerization: Initiation of polymerization in monomer droplets. *J. of Pol. Sci.: Pol. Lett. Ed.* **1973,** 11 (8), 503-513.

70. Bourgeat-Lami E., Farzi G. A., David L., Putaux J.-L., McKenna T. F. L., Silica Encapsulation by Miniemulsion Polymerization: Distribution and Localization of the Silica Particles in Droplets and Latex Particles. *Langmuir*. **2012,** 28 (14), 6021–6031.

71. Landfester K., Bechthold N., Tiarks F., Antonietti M., Formulation and Stability Mechanisms of Polymerizable Miniemulsions. *Macromolecules*, **1999,** 32 (16), 5222–5228.

72. van Herk A. M., Landfester K., Hybrid Latex Particles: Preparation with (Mini)emulsion Polymerization. *Advances in Polymer Science,* Springer-Verlag: Berlin Heidelberg, Germany, **2010.**

73. Tronc F., Li M., Lu J., Winnik M. A., Kaul B. L., Graciet J.-C., Fluorescent Polymer Particles by Emulsion and Miniemulsion Polymerization. *J. of Pol. Sci. Part A: Pol. Chem.,* **2003,** 41 (6), 766-778.

74. M. van Herk A., Landfester K., Hybrid Latex Particles: Preparation with (Mini)emulsion Polymerization. *Springer*, USA, **2010,** 185-236.

75. Landfester K., Rothe R., Antonietti M., Convenient Synthesis of Fluorinated Latexes and Core−Shell Structures by Miniemulsion Polymerization. *Macromolecules*, **2002,** 35 (5), 1658–1662.

76. Alfrey T. Jr., Price C. C., Relative reactivities in vinyl copolymerization. *J. of Polym. Sci.,* **1947,** 2 (1), 101-106.

77. Musyanovych A., Landfester K., Biodegradable Polyester Based Nanoparticle Formation by Miniemulsion Technique. *Material Matters,* **2012,** 7 (3), 30-34.

78. Landfester K., Mailänder V., Nanocapsules with specific targeting and release properties using miniemulsion polymerization. *Expert Opinion on Drug Delivery,* **2013,** 10 (5), 593-609.

79. Shi Ai-min, Li D., Wang Li-jun, Li Bing-zheng, Adhikari B., Preparation of starch-based nanoparticles through high-pressure homogenization and miniemulsion cross-linking: Influence of various process parameters on particle size and stability. *Carbohydrate Polymers*, **2011,** 83 (4), 1604-1610.

80. Landfester K., Rothe R., Antonietti M., Convenient Synthesis of Fluorinated Latexes and Core−Shell Structures by Miniemulsion Polymerization. *Macromolecules*, **2002,** 35 (5), 1658-1662.

81. Zhang S.-W., Zhou S.-X., Weng Y.-M., Wu L.-M., Synthesis of SiO_2/Polystyrene Nanocomposite Particles via Miniemulsion Polymerization. *Langmuir*, **2005,** 21 (6), 2124–2128.

82. Takasu M., Kawaguchi H., Preparation of colored latex with polyurea shell by miniemulsion polymerization. *Col. and Pol. Sci.,* **2005,** 283 (7), 805-811.

83. Gent A. N., Major industrial polymers. *Encyclopedia Britannica*, online edition: http://www.britannica.com/EBchecked/topic/468698/major-industrial-polymers/76436/Polypropylene-PP (last accessed 4/13/2015)

84. Kenney J. F., Properties of block versus random copolymers. Pol. Eng. and Sci., **1968,** 8 (3), 216-226.

85. White J. L., Bumm S. H., Polymer Blend Compounding and Processing, Encyclopedia of Polymer Blends: Volume 2: Processing, First Edition. Ed.: Isayev A. I., *Wiley-VCH*: Verlag GmbH, **2011.**

86. Utracki L. A., Introduction to polymer blends, in Polymer Blends Handbook, Kluwer Academic Publishers: Dordrecht, Netherlands, **2002.**

87. Gordon M., Taylor J. S., Ideal copolymers and the second-order transitions of synthetic rubbers. I. non-crystalline copolymers. *J. of App. Chem.,* **1952,** 2 (9), 493–500.

88. Wood L. A., Glass transition temperatures of copolymers. *J. of Pol. Sci.,* **1958,** 28 (117), 319-330.

89. Gugliotta L. M., Arzamendi G., Asua J. M., Choice of monomer partition model in mathematical modeling of emulsion copolymerization systems. *J. of App. Pol. Sci.,* **1995,** 55 (7), 1017-1039.

90. Armitage P. D., De La Cal J. C., Asua J. M., Improved methods for solving monomer partitioning in emulsion copolymer systems. J. of App. Pol. Sci., **1994,** 51 (12), 1985-1990.

91. Schoonbrood H. A. S., Thijssen H. A., Brouns H. M. G., Peters M., German A. L., Semi-continuous emulsion copolymerization to obtain styrene–methyl acrylate copolymers with predetermined chemical composition distributions. *J. of App. Pol. Sci.,* **1993,** 49 (11), 2029-2040.

92. Arzamendi G., Asua J. M., Monomer addition policies for copolymer composition control in semi-continuous emulsion copolymerization. *J. of App. Pol. Sci.,* **1989,** 38 (11), 2019-2036.

93. Chisholm B. J., Bezbaruah A., Kalita H., Vegetable oil-based polymers for nanoparticle surface modification. US patent application US 20130320255 A1, published Dec 5, **2013**.

CHAPTER 2. RESEARCH SCOPE

It is crucial to understand that, in today's world of emerging advanced materials, environmental impact of new technologies, as well as already well-established products, is of utmost importance. Environmental safety is as crucial as performance/price ratio for new materials. Talking specifically about polymer materials, vast research efforts are dedicated to enhancing material biodegradability, sustainability, manufacturing process improvements etc. In context of polymer materials environmental impact, the extensive use of organic solvents, monomers and other chemicals during production process reflects major concerns. It starts to become an industrial standard – to eliminate solvents from polymer materials production routines, reduce number of chemicals, reactions and material usage, increase biobased content and generally move towards "green synthesis" concept (use of renewable and/or reclaimed resources throughout whole production process). Another aspect of polymer material's environmental impact lies in vast generation of waste worldwide – issue that calls for biodegradable and sustainable material development, as well.

Synthesis of waterborne polymer materials (WPM) is one of the most straightforward ways to address issue with organic solvents, by substituting them during process with water. There are a number of polymerization techniques to produce WPMs, including emulsion, suspension, miniemulsion polymerization processes. They all result in ready-to-use materials (polymer latex for adhesives, paints, coatings etc.), which require little or no post-purification, solvent recycling or disposal. In addition, emulsion and miniemulsion processes utilize free radical polymerization and provide control over composition and molecular weight of produced (co)polymers. WPM fabrication routes allow for fine adjustment of material properties to fit requirements posed by different industrial applications.

Another approach to reduce polymer material's environmental impact lies in utilization of renewable sources for monomer/polymer production. In fact, entirely biobased

polymer materials that outperform petroleum-based counterparts are yet to be developed. However, by diligently developing biobased monomers and polymers and finding application niches, they have potential for replacing (at least partially) petroleum-based polymer materials in many industrial applications.

Plant oils recently became one the most promising and abundant source in synthesis of biobased polymer materials. However, monomers synthesized from plant oils often exhibit highly hydrophobic properties that makes it difficult to incorporate them in WPM manufacturing processes [Chapter 1].

Main goal of this work was to develop novel advanced polymer materials with lower environmental impact, including new biobased polymer materials with properties and performance not sacrificed by the presence of renewable content, and demonstrate their feasibility in industrial applications.

For this purpose, new polymer ingredient, which combines features of both initiator and surfactant (the inisurf), to be applied in conventional emulsion polymerization was developed and discussed in Chapter 3. Substituting initiator and surfactant improves shelf-life (colloidal stability) and enables post-polymerization functionalization of latex particles. It was demonstrated that modified latex particles can be used as reactive filler for commercial WPMs [Chapter 3] and as building blocks for micron-sized colloidosome capsules (delivery or storage vehicles) [Chapter 4].

Another focus of this work was on a development of biobased polymer materials, using plant oils as a raw source. A variety of biobased polymer materials was developed, based on triglycerides of soybean oil, sebacic (from castor oil) and caprylic (coconut, palm kernel oils) fatty acids, using conventional polymerization routes.

Using conventional polymerization routes three different approaches to biobased polymer materials were developed. Specifically, this work describes synthesis and properties of:

1) Surface active soybean-based polymer surfactants (SBPS), which can be considered as a safer replacement for low molecular weight surfactants (e.g. sodium dodecyl sulfate) in the solubilization of poorly soluble ingredients in cosmetics [Chapter 5]. SBPSs are based on vinyl ether soyate and vinyl ether polyethylene glycol derivatives. It was shown that the presence of SBPS improves cleaning, foaming and conditioning of model shampoo formulations [Chapter 6];

2) Fabrication of biobased thermoresponsive polymer latexes for fragrance protection and controlled release in consumer cosmetic formulations [Chapter 7]. Latexes were synthesized on the basis of derivatives of stearic, caprylic and sebacic (plant oil origin) fatty acids;

3) Renewable monomer based on soybean oil (SBA), which could advantageously replace petroleum-based monomers in free radical polymerization production of, in particular, polymer latexes, adhesives and other polymer materials that utilize acrylic monomers [Chapter 8].

Finally, Chapter 9 contains overall conclusion drawn from work presented in this thesis disquisition, capitalizing on achievements and scientific progress in the field of reducing environmental impact of polymer materials, as provided by this work results.

CHAPTER 3. REINFORCING LATEX COATINGS WITH REACTIVE LATEX PARTICLES[1]

3.1. Abstract

A new approach to the cross-linking and filling synthetic latex coatings has been developed. Peroxidized monodisperse polystyrene latex particles have been used as a cross-linker and, simultaneously, as a filler of polymer coatings based on acrylic and styrene-butadiene latexes. The synthesis of reactive (peroxidized) latex particles was carried out using the emulsion polymerization of styrene in the presence of the polymer inisurf, the initiator-surfactant, a copolymer of a peroxide monomer, N-[(*tert*-butylperoxy)methyl] acrylamide with maleic anhydride. The reactive latex particles were employed to crosslink polymer coatings from synthetic acrylic and styrene-butadiene latexes.

The hardness and solvent resistance of the coatings based on both latexes increase with an increasing amount of the reactive latex filler in the formulation. The cross-linked coatings, based on styrene-butadiene exhibited better characteristics in terms of hardness and solvent stability. The properties of latex-cross-linked coatings depend on reaction temperature and the amount of the cross-linker, peroxidized reactive polystyrene latex particles.

3.2. Introduction

The properties of polymer colloid systems, such as latexes and latex composites (filled and reinforced plastics, paints, varnishes etc.), are often governed by system

---

[1]Based on manuscript published in *Progress in Organic Coatings*, **2014**, 77 (12, B), 2123-2132.

The material in this chapter was co-authored by Andriy Popadyuk and Ihor Tarnavchyk, Nadiya Popadyuk, Ananiy Kohut, Volodymyr Samaryk, Stanislav Voronov, Andriy Voronov. Andriy Popadyuk had primary responsibility for synthetic work, analytical measurements and data interpretation. Andriy Popadyuk was the primary developer of the conclusions that are advanced here. Andriy Popadyuk also drafted and revised all versions of this chapter.

heterogeneity and depend on properties of the interface (polymer adsorption, interfacial reactions, interfacial layer formation etc.) [1-2]. Environmentally friendly waterborne coatings are widely prepared from acrylic and styrene-butadiene polymer latexes [3-4]. Besides, the acrylic latexes are used in the textile and paper industry, coatings for wood, manufacturing artificial leather, where they provide high weather resistance, UV- and thermal stability, water, oil, and salt resistance. While acrylic latexes dominate the market, coatings from acrylic latexes lack the hardness, toughness and resistance to acids, bases and solvents, required for many industrial applications [5-6].

Number of cross-linkers and cross-linking technologies have been developed in order to improve properties and performance of latex-based coatings. The typical cross-linkers are polycarbodiimides [7-8], polyaziridines [9-10], polyoxazolines [11-12], epoxides [13-17], melamine-formaldehyde resins [18-21] etc. Prior to formation of a three-dimensional polymer network, the latex particles should be modified by incorporating functional groups into the polymer structure for further cross-linking. Despite the number of existing technologies, the development of the resultant latex coatings still remains challenging with a need of special cross-linkers [5].

Formation of a polymer latex network can be also approached by using peroxide cross-linkers that generate free radicals at elevated temperatures and initiate free radical reactions [22]. The application of reactive (peroxidized) latex particles as a filler enhances the mechanical properties of the coatings, and imparts specific properties, towards potential reducing the coatings price. For example, the use of high-styrene resin latex particles as a filler increases the film stiffness (especially at low stress), decreases the elongation at rupture, and improves tensile strength [23].

In this study, we foresee that monodisperse latex particles (for example, from polystyrene) with a controlled number of peroxide groups on the surface can be used simultaneously as cross-linker and filler, in latex coatings. Such peroxidized, reactive,

particles can be synthesized using emulsion polymerization of styrene in the presence of polymer inisurf (initiator-surfactant), generating free radicals [24]. Unlike traditional emulsifiers, the inisurf can be, thus, covalently grafted onto the surface of the particles during polymerization.

Recently, polyperoxide inisurfs have been synthesized in our group using peroxide monomers with a ditertiary peroxide group [25-26]. Developing a polymer initiator-surfactant with primary-tertiary peroxide groups enables free radicals generation at lower temperature. For this purpose, N-[(*tert*-butylperoxy)methyl]acrylamide peroxide monomer (PM), has been recently synthesized.

The main goal of this study was to develop a new approach for cross-linking latex polymer coatings using peroxidized polystyrene latex particles as cross-linker. In contrast to the reported cross-linking methods primarily based on condensation reactions, we propose to form three-dimensional polymer coating structures using free radical mechanism.

Achieving this goal involves the following stages: (i) synthesis of the PM, N-[(*tert*-butylperoxy)methyl]acrylamide, (ii) synthesis of the polyperoxide inisurf, a copolymer of PM with maleic anhydride (PM-MA), (iii) formation of peroxidized monodisperse polystyrene latex particles using emulsion polymerization of styrene in the presence of PM-MA, and (iv) formation of cross-linked coatings using the peroxidized polystyrene latex particles simultaneously as filler and cross-linker.

3.3. Experimental part

3.3.1. Materials

N-(Hydroxymethyl)acrylamide (HMAA) (TCI America, Portland, OR) was used as received. *Tert*-butyl hydroperoxide (TBHP) (Alfa Aesar, Ward Hill, MA) was dried over magnesium sulfate. Maleic anhydride (MA) (99%) (VWR, Radnor, PA) was purified by recrystallization from anhydrous benzene and sublimation in vacuum. Azobisisobutyronitrile (AIBN) (Sigma–Aldrich, St. Louis, MO) was purified by recrystallization from methanol.

Styrene monomer (St) (99%) (Sigma–Aldrich, St. Louis, MO) was distilled under vacuum to remove inhibitor and stored in a refrigerator. Cyclohexanone (Sigma–Aldrich, St. Louis, MO) was distilled. Pyrene (Sigma–Aldrich, St. Louis, MO) was used as received. Other solvents, analytical grade or better, were used as received. Deionized water was used for the synthesis and purification of the latex particles (MilliQ, 18 MΩ).

3.3.2. Syntheses

3.3.2.1. N-(tert-butylperoxymethyl)acrylamide (PM).

A solution of *tert*-butyl hydroperoxide (10.8 g, 0.12 mol) in diethyl ether (30 mL) was added dropwise to a solution of N-(hydroxymethyl)acrylamide (10.1 g, 0.1 mol) in diethyl ether (25 mL) at 5-7 °C. The mixture was stirred and a solution of H_2SO_4 (2.94 g, 0.03 mol) in diethyl ether (20 mL) was added dropwise at 14-16°C for 1 h. After stirring for an additional 3 h at 22-25 °C, the organic phase was separated, washed in series with water, 5% aq Na_2CO_3, and water until pH 7, dried over $MgSO_4$ for 12 h, and evaporated under reduced pressure to afford N-(*tert*-butylperoxymethyl)acrylamide at 98% purity as a colorless transparent liquid (15.5 g, yield 82%).

3.3.2.2. Poly[N-(tert-butylperoxymethyl)acrylamide-co-maleic anhydride], (PM-MA).

N-[(*tert*-Butylperoxy)methyl]acrylamide (0.8 M), maleic anhydride (1.2 M) and AIBN (0.012–0.06 M) were dissolved in acetone. The reaction mixture was purged with argon at room temperature for 30 min. The copolymerization was carried out under an argon blanket at 60 °C for 4–24 h until a total monomer conversion of 65–70% was reached. Small samples of the reaction mixture were taken to monitor the progress of the copolymerization reaction using a potentiometric titration. The resulting copolymer was isolated by precipitation in hexane and purified by multiple reprecipitations. The purified polymer was dried under reduced pressure at room temperature until a constant weight was obtained. The resulting copolymer, containing 63–75 mol % peroxide monomer units, was soluble in acetone, toluene and water in the presence of sodium hydroxide.

3.3.3. Characterization of PM-MA

3.3.3.1. Instrumental techniques

FTIR spectra were recorded using a Nicolet 8700 (Thermo Scientific) spectrometer with a resolution of 4 cm^{-1}.

^{1}H and ^{13}C NMR spectra were recorded at 400 MHz on a JEOL ECA 400 MHz NMR spectrometer.

The molecular weight of the PM-MA was determined by gel permeation chromatography (GPC) using a Waters Corporation modular chromatograph consisting of a Waters 515 HPLC pump, a Waters 2410 Refractive Index detector and a set of two 10 lm PL-gel mixed-B columns, the column temperature was set at 40 °C. Tetrahydrofuran was used as the carrier solvent.

3.3.3.2. PM-MA composition

To determine the PM-MA composition by ^{1}H NMR spectroscopy, the PM content was quantified through the determination of *tert*-butyl hydrogens present in the spectrum. For this purpose, phthalic anhydride was applied as an internal standard:

$$W = \frac{M_{PM} \cdot S_t \cdot 4 \cdot m_{PA}}{M_{PA} \cdot S_p \cdot 4 \cdot m_{comonomer}} \qquad F_{PM} = \frac{W/M_{PM}}{W/M_{PM} + (1-W)/M_{MA}} \tag{3.1}$$

where W is the weight fraction of the PM units in the copolymer, F_{PM} is the molar fraction of PM units in the copolymer, M_{PM} is the molar mass of the PM monomer (173 g/mol), M_{PA} is the molar mass of phthalic anhydride (148.1 g/ mol), M_{MA} is the molar mass of maleic anhydride (98 g/mol), m_{pa} is the mass of the internal standard (phthalic anhydride) (g), $m_{copolymer}$ is the mass of the copolymer sample (g), S_t is the integral of the *tert*-butyl hydrogens, and S_p is the integral of the phthalic anhydride hydrogens.

3.3.3.3. Potentiometric titration

A potentiometric titration (back titration using 0.1 N HCl as a titrant) was used to calculate the content of carboxylic groups in an aqueous solution of PM–MA with hydrolyzed

anhydride fragments. The molar fraction of maleic anhydride in the copolymer was determined using the following equation:

$$F_{MA} = M_{PM} / (\frac{2 \cdot 1000 \cdot m_{sample}}{\Delta V \cdot N} - M_{MA} + M_{PM}) \quad (3.2)$$

where F_{MA} is the molar fraction of MA fragments in the copolymer, M_{MA} is the molar mass of MA (98 g/mol), M_{PM} is the molar mass of PM (173 g/mol), m_{sample} is the mass of the titrated sample (g), N is the normality of the HCl titrant (here 0.1 mol eq/L) and ΔV is the volume of titrant between the two inflection points on the potentiometric curve (in mL of titrant).

3.3.3.4. Dilatometry

The course of the copolymerization was studied in dilatometers (15 mL, 20 cm of graded capillary tubing, grading accuracy 0.1 mL) as reaction vessels and in cyclohexanone as a solvent. The monomer reactivity ratios of PM and MA in the copolymerization reaction were determined using approaches developed by Skeist [27] and Feinmann-Ross [28].

3.3.3.5. Thermal analysis

Thermal analysis of the decomposition of the peroxide groups of PM–MA and peroxidized latex particles was carried out using thermogravimetry in a TA Instruments Q500. Samples were subjected to an underlying heating rate of 10 °C/min. The specimen was heated to 400 °C.

3.3.3.6. Critical micelle concentration determination

The critical micelle concentration of PM–MA in aqueous solution was measured using a previously reported solubilization of fluorescent probe (pyrene) method [29]. The spectra were taken using a Fluoromax-3 fluorescence spectrometer (Jobin Yvon Horiba) with a 90° geometry and a slit opening of 0.5 nm. For the fluorescence excitation spectra, λ_{em} = 390 nm was chosen. Spectra were accumulated with an integration time of 0.5 nm/s.

3.3.4. Methods

3.3.4.1. Formation of peroxidized polystyrene latex

A 10 wt. % emulsion of styrene in an aqueous solution of PM–MA (1–7.5 wt. % per styrene) was prepared at pH 9.5 by magnetic stirring at 1200 rpm for 30 min. The emulsion was purged with argon under constant stirring for 20 min and subsequently placed in an oil bath heated to 85 °C. The polymerization was conducted for 4 h under constant stirring (conversion up to 95%). At the end of the reaction, the latex was cooled and placed into a 5 mL dialysis bag (50 kDa molecular cutoff) and submerged into a 2000 mL beaker filled with distilled water adjusted to pH 9.5 using NaOH. At intervals of 24 h, the water in the beaker was replaced to ensure a constant high concentration gradient to improve the dialysis process. After 14 days, the latex was removed from the dialysis bag and stored at 4 °C.

3.3.4.2. Size distribution measurements

Size distribution measurements were performed in aqueous dispersions using Malvern Zetasizer Nano-ZS90 at 25 °C. The final numbers represent an average of a minimum of 5 individual measurements.

3.3.4.3. Imaging of latex

Digital images of latex particles were obtained using JEOL JSM-6490LV scanning electron microscope.

3.3.4.4. Reinforced latex formulation

Two commercial samples of latexes were used – acrylic HG-56 (Maincote, Rohm and Haas) (AL) [52.9 wt. % dry solids] and styrene-butadiene DL-215 (Encor, Arkema) (SB) [49.3 wt. % dry solids]. Reinforced formulations were prepared by addition of aqueous dispersion of peroxidized polystyrene latex to commercial samples. Five formulations were prepared for SB latex (0, 1, 10, 30 and 50 wt. % added peroxidized latex) and four for AL latex (0, 1, 10, and 30 wt. % added peroxidized latex). In typical formulation for 50 wt. % added peroxidized latex, 10 g of SB latex (4.93 g dry solids) was mixed with 14.8 g of

peroxidized latex (2.465 g dry solids). Obtained composition was conditioned under light stirring for 24 h.

3.3.4.5. Coating preparation

Latex formulations were cast on aluminum 2024T3 alloy test panels using drawdown bar with initial film thickness set to 5 mil. Prior casting, panels were washed with aqueous soap solution (10 % w/v sodium dodecyl sulfate), dried and wiped with hexane-soaked lint-free wipes, then dried again. After casting, each panel was placed in oven set to either 90 °C or 120 °C for 12 h. After curing, panels were removed from oven and allowed to cool down and condition for another 24 h.

3.3.4.6. Coating hardness measurements by pendulum damping test (König)

Hardness measurements were followed after ASTM D 4366-95. Test panel was placed on panel table inside pendulum apparatus, whereas pendulum was gently brought onto surface of panel coating. Pendulum was deflected to 6°, released and simultaneously stopwatch was started. Time for the amplitude to decrease from 6° to 3° was measured, which is the König hardness. Each sample was run in three areas on the panel.

3.3.4.7. Assessment of solvent resistance of coatings

Procedure was followed as described in ASTM D 5402-93 with slight variation. Clean, undamaged patch of coating surface of at least 150 mm was selected on each test panel. Folded cotton pad was saturated with methyl-ethyl ketone to dripping-wet condition. This pad was secured on 200 g weight which was used to produce equally-heaved rubs. Each forward and back motion was counted as one double-rub, performed at a rate of 1 Hz. Number of double rubs coating could resist before losing gloss in testing area is reproduced.

3.3.4.8. Resistance of coatings to the effect of rapid deformation (impact)

Impact resistance of coatings was estimated as described in ASTM D 2794-93. 12.7 mm indenter was secured on weight cylinder that is freely moving inside 1 m long guide. Sample panel was secured flat on a base support. Weight cylinder was raised above surface

of test panel and dropped onto the surface in 25 mm incremental steps starting from lowest known non-failure height. After each indentation surface of sample was inspected for cracks or delamination regions developed. Once latter were observed, indentation tests were run on similar heights for the same sample 5 times for reproducibility reasons. Tests were run both in intrusion and extrusion fashions and inch-pound values at the failure end point are presented.

3.3.4.9. Film hardness by pencil test

Procedure was followed after ASTM D 3363-05. Test panel was placed firmly on flat surface. Pencils, held firmly at 45°, were pushed away from operator in 6.5 mm strokes. The process is started from hard pencils and moving down the hardness scale until pencil no longer is able to cut or gouge into coating surface. Hardness of such pencil is recorded as pencil hardness value for tested coating.

3.4. Results and discussion

3.4.1. Synthesis of a peroxide monomer, N-[(tert-butylperoxy)methyl] acrylamide

The synthesis of the peroxide monomer has been carried out via the interaction of N-(hydroxymethyl)acrylamide with *tert*-butyl hydroperoxide (Scheme 3.1).

The yield of the PM did not exceed 10% when water was used as a reacrion medium. N-[(Acrylamino)methyl]acrylamide and N-{[(acryloylamino)methoxy]methyl}acrylamide were formed as by-products under the reaction conditions (initial concentration of HMAA 10%, HMAA : TBHP ratio from 1:1 to 1:1.7, and TBHP : H_2SO_4 ratio from 1:0.01 to 1:0.4). Thus, an aqueous medium cannot be used for the synthesis of N-[(*tert*-butylperoxy)methyl]acrylamide because of a low yield and complicated isolation technique.

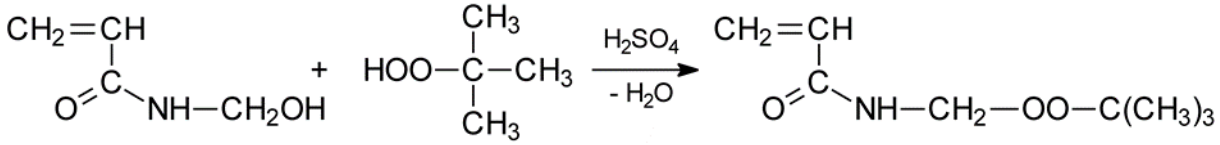

Scheme 3.1. Synthesis of the peroxide monomer N-[(*tert*-butylperoxy)methyl] acrylamide.

Diethyl ether has been found out to be the most suitable reaction medium for high-yield synthesis of N-[(*tert*-butylperoxy)methyl]acrylamide. The yield depends considerably on the initial concentration of the reactants and the ratio of H_2SO_4 (catalyst) to HMAA. The HMAA concentration of 0.135-0.138 g/mL and the molar ratio of reactants (HMAA : TBHP : H_2SO_4 as 1:1.2:0.3) result in the highest monomer yield (80-82%). With the increasing excess of TBHP in the reaction mixture, the monomer yield does not enhance, whereas when a greater amount of the catalyst is used, the reaction selectivity has been reduced. The chemical structure and properties of N-[(*tert*-butylperoxy)methyl]acrylamide have been confirmed by FTIR-, ^{1}H NMR- and ^{13}C NMR-spectroscopy as well as refractometry. The physico-chemical characteristics of the peroxide monomer are summarized in Table 3.1.

Table 3.1. Physico-chemical characteristics of N-[(*tert*-butylperoxy)methyl] acrylamide.

Parameter	Value
Refractive index, n_D^{20}	1.4512
Molar mass (calculated)	173.2 g/mol
Molar mass (found by differential cryoscopy)	168.3 g/mol
Active oxygen content (found by gas-liquid chromatography)	9.52%
Density, d^{20}	0.991
Molar refractivity (found using the Lorentz–Lorenz equation)	46.15
Molar refractivity (calculated)	45.91

The following absorption bands have been found in the FTIR-spectrum of N-[(*tert*-butylperoxy)methyl]acrylamide (Figure 3.1): intense absorption bands at 3300, 1670, and 1540 cm^{-1} correspond to the valence and deformation oscillations of subsituted amide groups, a band at 1630 cm^{-1}, indicating the presence of carbon-carbon double bonds C=C,

and an adsorption band at 880 cm^{-1}, which belongs to valence oscillations of peroxide groups.

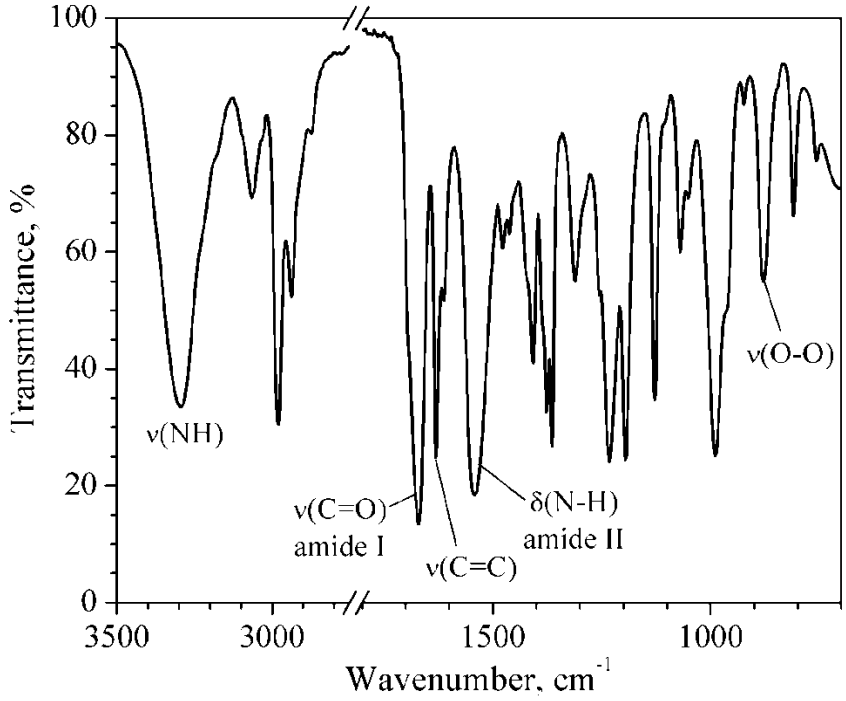

Figure 3.1. FTIR-spectrum of the peroxide monomer N-[(*tert*-butylperoxy)methyl] acrylamide.

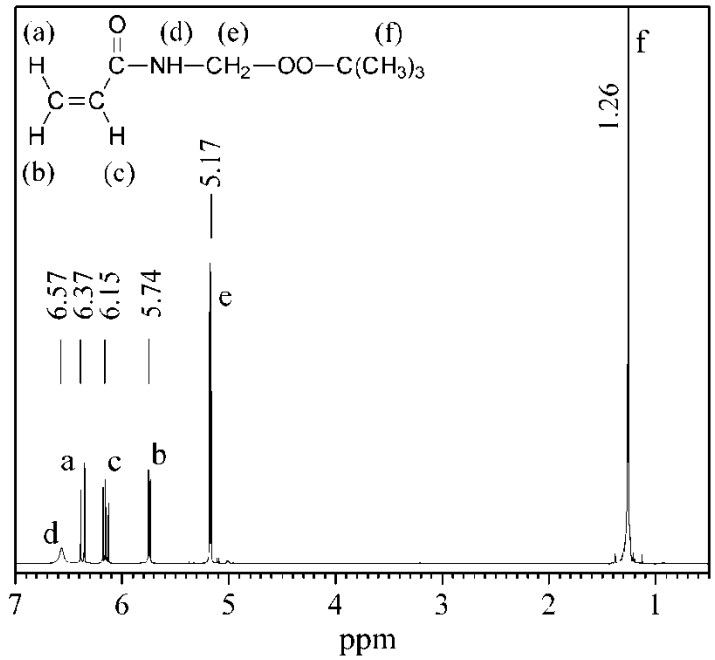

Figure 3.2. ^{1}H NMR-spectrum of the peroxide monomer N-[(*tert*-butylperoxy)methyl]acrylamide.

The following signals have been observed in the ^{1}H NMR-spectrum of the peroxide monomer: 1.26, 5.17, 5.74, 6.15, 6.37 and 6.57 ppm. The chemical shifts of each proton along with their integral values are given in Table 3.2.

Table 3.2. Chemical shifts and integration values in the ^{1}H NMR-spectrum of N-[(*tert*-butylperoxy)methyl]acrylamide.

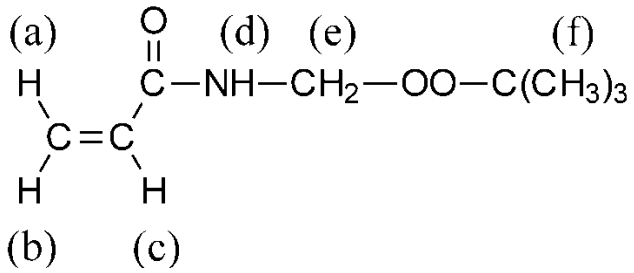

Signal	Chemical shift, ppm	Integration value
f	1.26	8.98
e	5.17	2.00
b	5.74	1.03
c	6.15	0.92
a	6.37	1.02
d	6.57	1.00

The ^{13}C NMR spectrum of the peroxide monomer with chemical shifts at 26.27, 73.55, 80.75, 127.69, 130.53, and 165.72 ppm attributed to the corresponding carbon atoms in the N-[(*tert*-butylperoxy)methyl]acrylamide molecule is shown in Figure 3.3.

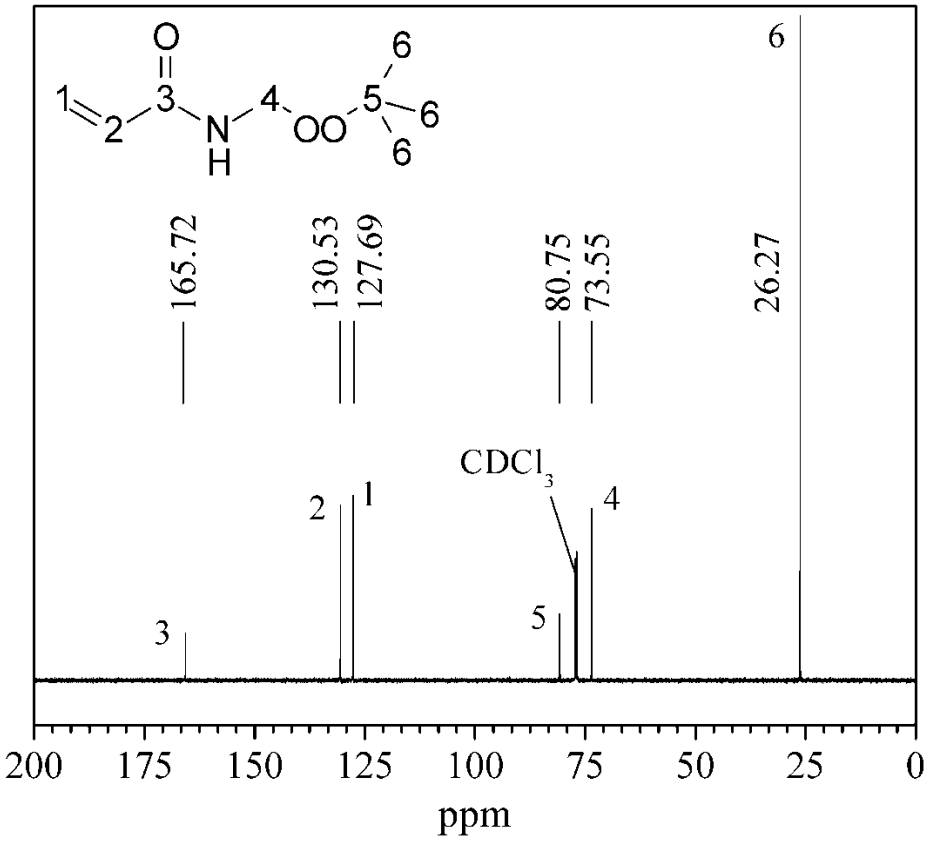

Figure 3.3. ^{13}C NMR-spectrum of the peroxide monomer N-[(*tert*-butylperoxy)methyl]acrylamide.

The good agreement of found and calculated molecular refraction values (Table 3.1) confirms the structure of the synthesized monomer. Peaks with chemical shifts at 5.74, 6.15, 6.37 ppm (^1H NMR-spectroscopy) and 127.69, 130.53 ppm (^{13}C NMR-spectroscopy) along with an adsorption band at 1630 cm^{-1} (FTIR-spectroscopy) indicate the presence of a carbon-carbon double bond in the peroxide monomer molecule. A chemical shift at 6.57 ppm (^1H NMR) and adsorption bands at 3300, 1670, 1540 cm^{-1} (FTIR) imply a secondary amide group whereas an absorption band at 880 cm^{-1} (FTIR) confirms the presence of a peroxide group. As show a peak with a chemical shift at 1.26 ppm and an integration value of 8.98 (methyl groups in a *tert*-butyl moiety), a peak at 5.17 ppm with an integration value of 2.00 (methylene group) (^1H NMR) as well as peaks at 80.75, 26.27 ppm (*tert*-butyl

group) and 73.55 ppm (methylene group) (^{13}C NMR), the peroxide group is a primary-tertiary one.

3.4.2. Copolymerization of the peroxide monomer N-[(tert-butylperoxy)methyl]acrylamide with maleic anhydride

For the development of a new polymer initiator-surfactant capable of generating free radicals at 120-160 °C, radical coplymerization of the peroxide monomer, N-[(*tert*-butylperoxy)methyl]acrylamide, with maleic anhydride has been carried out (Scheme 3.2) to yield functional polyperoxide (FPP) containing anhydride groups. This multifunctional polymer enables the localization of reactive groups at the interface in various colloidal systems, such as emulsions, latexes and polymer composites. The FPP macromolecules can be ionized through a hydrolysis reaction of the anhydride groups, resulting in the formation of water-soluble macroinitiator. The FPP synthesized in this work is an amphiphilic copolymer. The incorporation of both hydrophilic and hydrophobic moieties into the copolymer structure provides surface activity to the FPP macromolecules. At the same time, the peroxide groups of the PM units are capable of generating radicals and macroradicals through decomposition at elevated temperatures or in redox initiating systems.

Obviously, the ratio of peroxide-containing units to maleic anhydride units in the PM–MA copolymer, the molecular weight and the polydispersity index determine both the reactivity and surface activity of the peroxide copolymer during the emulsion polymerization. It is important to control the copolymer chemical composition during the synthesis of PM–MA, in particular, the content of the peroxide-containing units in the macromolecules. In this regard, an extensive study on the free radical copolymerization of PM and maleic anhydride was carried out to determine the extent of the reaction and the monomer reactivity ratios in the copolymerization.

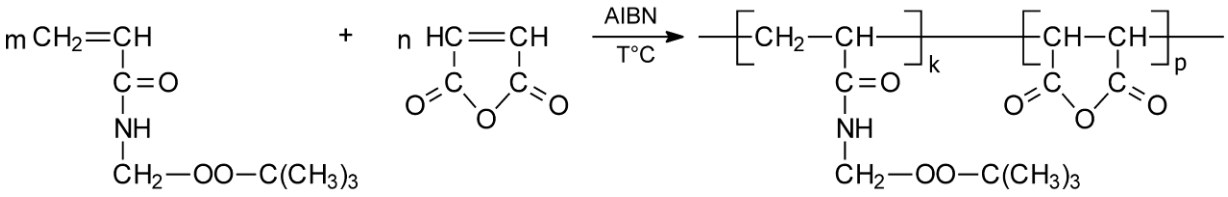

Scheme 3.2. Copolymerization of N-[(*tert*-butylperoxy)methyl]acrylamide and maleic anhydride.

To choose the initial monomer feed ratio in the copolymerization study, the reactivity ratios of PM and MA were first calculated using the Q–e values for the peroxide monomer (Q = 0.17, e = 0.13) [30] and maleic anhydride (Q = 0.89, e = 3.69) [28]. The theoretical values obtained, r_1 = 0.974 and r_2 = 0.011, indicate a high reactivity of the peroxide monomer in the addition reactions to a growing FPP macro radical. Thus, the copolymerization kinetic study was carried out at an initial PM:MA ratio of 1:1.5, and the total monomer concentration was chosen to be 2 mol/L.

The kinetic plots for the monomer consumption rate in the copolymerization reaction initiated by different AIBN concentrations are shown in Figure 3.4. The initiator reaction order can be determined by the tangent of the slope angle of the logarithmic plot in Figure 3.5. The obtained value of 0.95 indicates that the bimolecular termination reaction occurs mostly through disproportionation reactions.

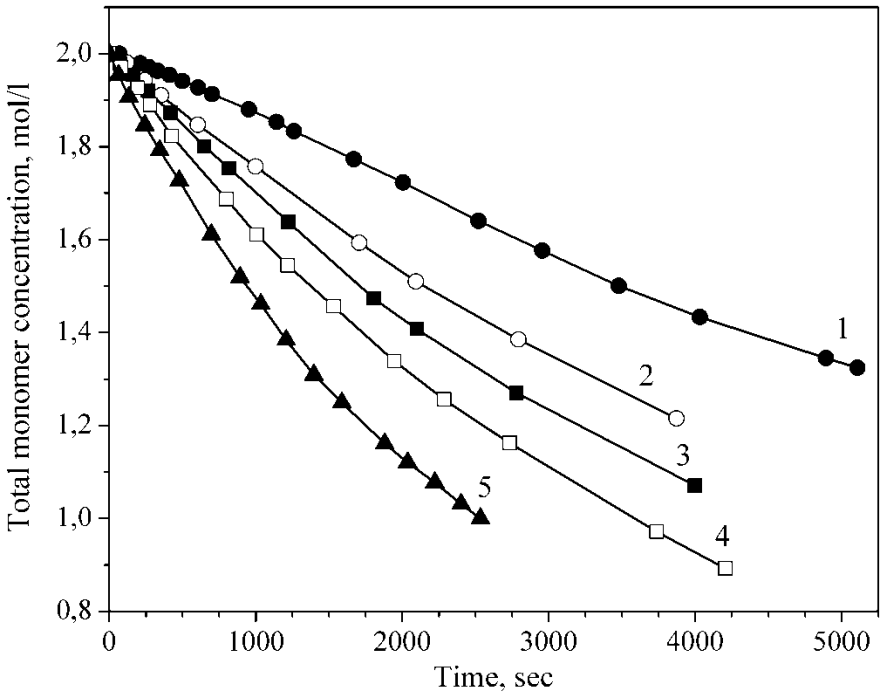

Figure 3.4. Kinetic plots of the consumption of comonomers in the copolymerization of PM and MA at various initial AIBN concentrations (1–0.012 M, 2–0.018 M, 3–0.024 M, 4–0.036 M, 5–0.06 M).

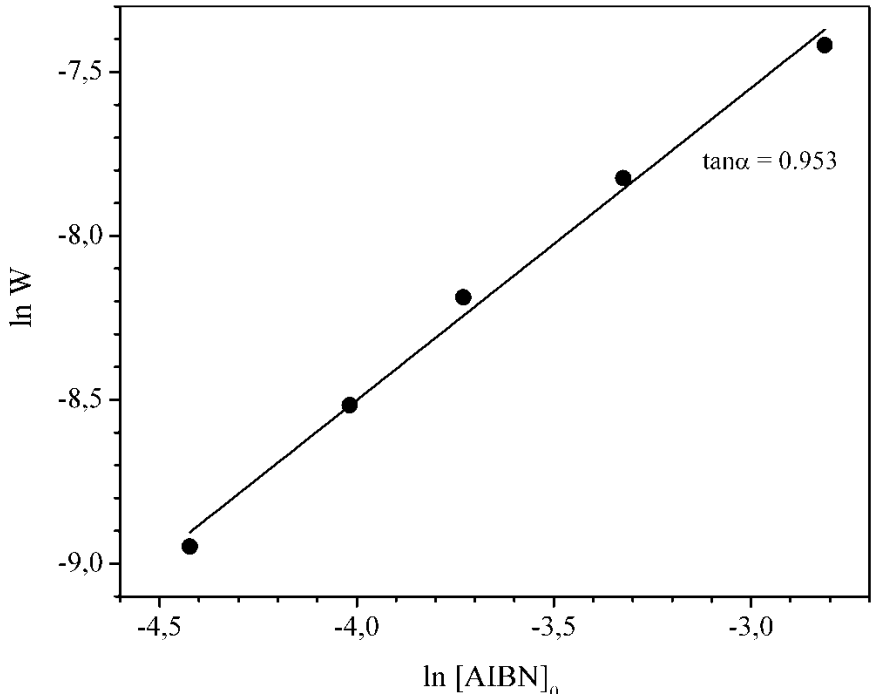

Figure 3.5. The logarithmic plot for the initial rate of the monomers' consumption vs. the AIBN concentration.

The integrated form of the copolymerization equation is the most useful way to determine the instantaneous copolymer composition as a function of conversion for the given comonomer feed ratio [28], and the Skeist method [27] can be applied to follow the drift in the composition of both the comonomer feed ratio and the resulting copolymer during the copolymerization. Analyzing the initial and residual monomer amounts, one can relate the degree of conversion to the change in the feed composition using the integrated form of the Skeist equation.

We employed this approach to determine the experimental monomer reactivity ratios for MA (r_2) and PM (r_1) based on the monomer conversion (determined by a potentiometric titration):

$$1-\frac{M}{M_0}=1-\left(\frac{f_1}{f_{1(0)}}\right)^{\alpha}\left(\frac{f_2}{f_{2(0)}}\right)^{\beta}\left(\frac{f_{1(0)}-\delta}{f_1-\delta}\right) \tag{3.3}$$

where f_1 is the PM mole fraction in the comonomer mixture, f_2 is the MA mole fraction in the comonomer mixture, $f_{1(0)}$ and $f_{2(0)}$ are the initial mole fractions in the comonomer feed and $f_1 = 1 - f_2$.

$$\alpha=\frac{r_2}{1-r_2} \quad \beta=\frac{r_1}{1-r_1} \quad \gamma=\frac{1-r_1\cdot r_2}{(1-r_1)(1-r_2)} \qquad \delta=\frac{1-r_2}{2-r_1-r_2} \tag{3.4}$$

The calculated experimental PM and MA reactivity ratios are shown in Table 3.3. At the same time, using the differential form of the Mayo-Lewis copolymerization equation (Feinmann and Ross's approach [28]), similar values were obtained for both r_1 and r_2. The observed coincidence of the monomers' reactivity data shows that the radical copolymerization of PM and MA can be described by classical copolymerization equations at a low and high monomer conversion and that the composition of the resulting copolymer can be controlled. The r_1 and r_2 values obtained from the Q–e scheme (r_1 = 0.974 and r_2 =

0.011) are in a good agreement with the values obtained experimentally (r_1 = 1.71 and r_2 = 0.06).

Table 3.3. Monomer reactivity ratios for copolymerization of PM and MA.

Comonomer	Monomer reactivity ratios (Skeist)		Monomer reactivity ratios (Feinmann-Ross)	
	r_1	r_2	r_1	r_2
PM (1)	1.71±0.2	-	1.65±0.2	-
MA (2)	-	0.06±0.02	-	0.31±0.05

Using the experimentally determined r_1 and r_2 for both monomers, the expected variation in the resulting copolymer composition can be plotted as a function of the initial comonomer feed composition (Figure 3.6), based on the Mayo-Lewis equation:

$$F_1 = \frac{r_1 f_1 + f_2}{r_1 f_1 + 2 f_2} \tag{3.5}$$

where F_1 is the PM mole fraction in the polymer.

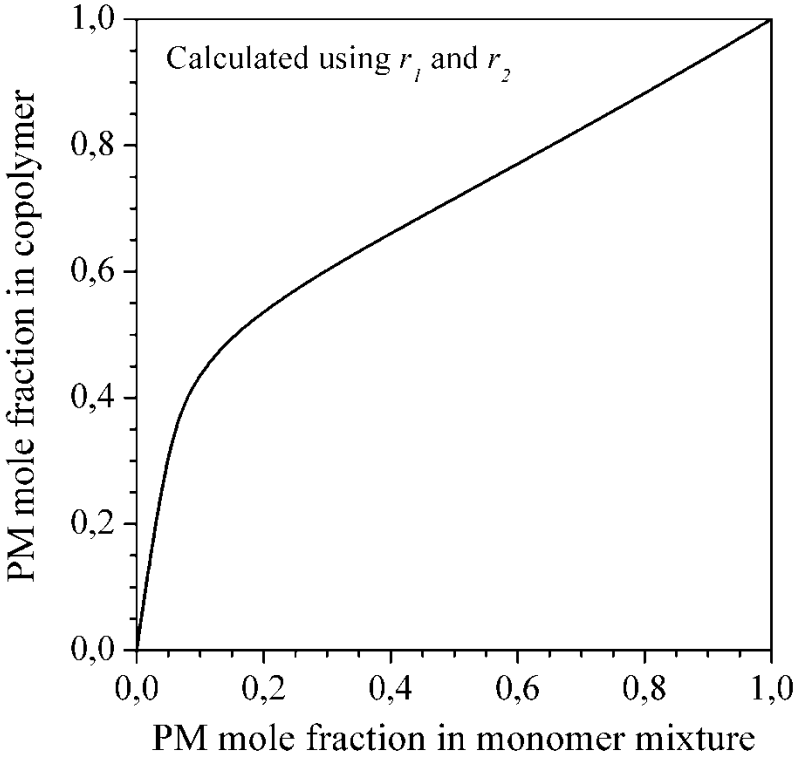

Figure 3.6. Calculated PM content in the copolymer vs. the PM content in the initial feed mixture.

To experimentally determine the copolymer composition drift throughout the course of the copolymerization, the effect of conversion on the instantaneous PM fraction (F_1) and the average PM fraction (F_{1av}) in the copolymer were estimated using the kinetic study carried out at an initial PM content $f_{(1)0}$ = 0.4 in the comonomer feed mixture. Figure 3.7 shows the change in the peroxide monomer content in the feed monomer mixture (f_1) and the resulting copolymer (F_1) with total monomer conversion.

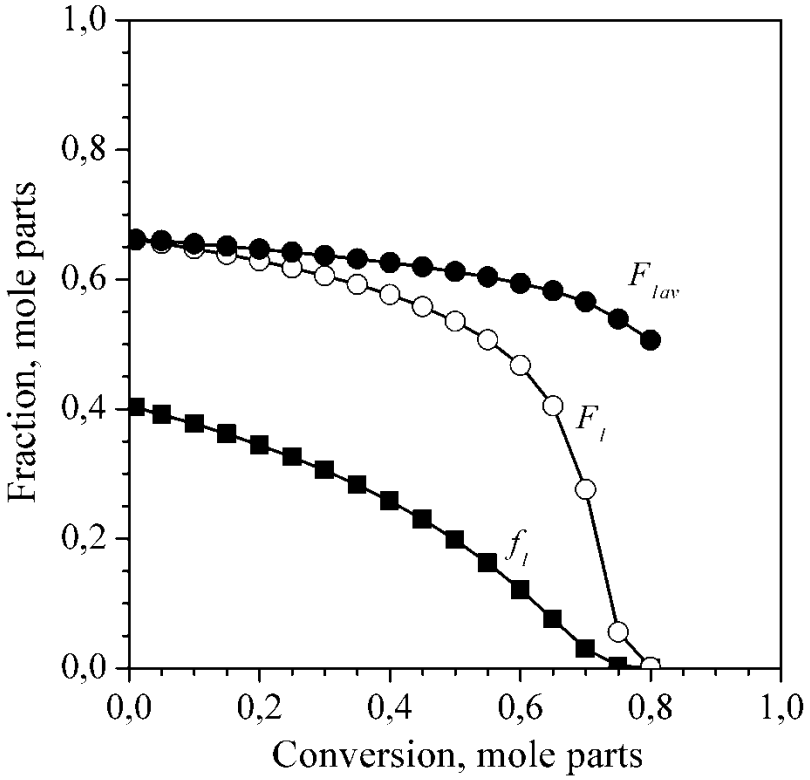

Figure 3.7. Experimental change of the PM content in the feed mixture and the PM–MA copolymer by changing the total monomer conversion (f_1, instantaneous PM content in the feed mixture, F_1, instantaneous peroxide monomer content in the copolymer, F_{1av}, average PM content in the copolymer).

During the course of the copolymerization, the comonomer feed mixture becomes enriched with maleic anhydride, thus confirming the higher reactivity of peroxide monomer. However, increasing total conversion does not significantly change the average peroxide monomer fraction F_{1av} in the resulting PM–MA copolymer. Most of the peroxide monomer becomes consumed at a total conversion exceeding 60%, and afterward, this experimental fact leads to the compositional drift in the resulting copolymer. It is, however, evident that if the total monomer conversion is below 50–55%, the experimental kinetic data observed for $f_{(1)0} = 0.4$ are in fairly strong agreement with the calculated PM content in the copolymer composition plotted vs. PM content in the initial feed mixture in Figure 3.6.

It can be concluded that to synthesize the PM–MA copolymer with a controlled variation of average peroxide monomer fractions, the total monomer conversion during the copolymerization should not exceed the values mentioned above.

Based on the copolymerization study, the synthetic route presented in Scheme 3.2 was followed to synthesize the PM–MA copolymer (M_n = 8500 g/mol, PDI = 1.68). The chemical structure of the copolymer was confirmed using ^{1}H NMR and FTIR spectroscopy. The ^{1}H NMR spectrum (Figure 3.8) contains peaks confirming the presence of both monomers in the copolymer chemical structure – the signals at 1.18, 2.30, 3.35 and 5.03 ppm correspond to the C–CH_3, C–CH_2–C, C–CH–C and N–CH_2–OO– protons, respectively.

FTIR spectroscopy (Figure 3.9) confirms the presence of functional groups from both MA and PM in the copolymer structure. Characteristic bands at 887 and 868 cm^{-1} correspond to the peroxide O–O, the signals at 930 and 1238 cm^{-1} are caused by the anhydride (5-membered ring) C–O–C, the bands at 1533 and 3350 cm^{-1} are attributed to the amide N–H, the anhydride C=O stretch appears at 1800 and 1849 cm^{-1}, the peak at 1675 cm^{-1} corresponds to the amide C=O groups.

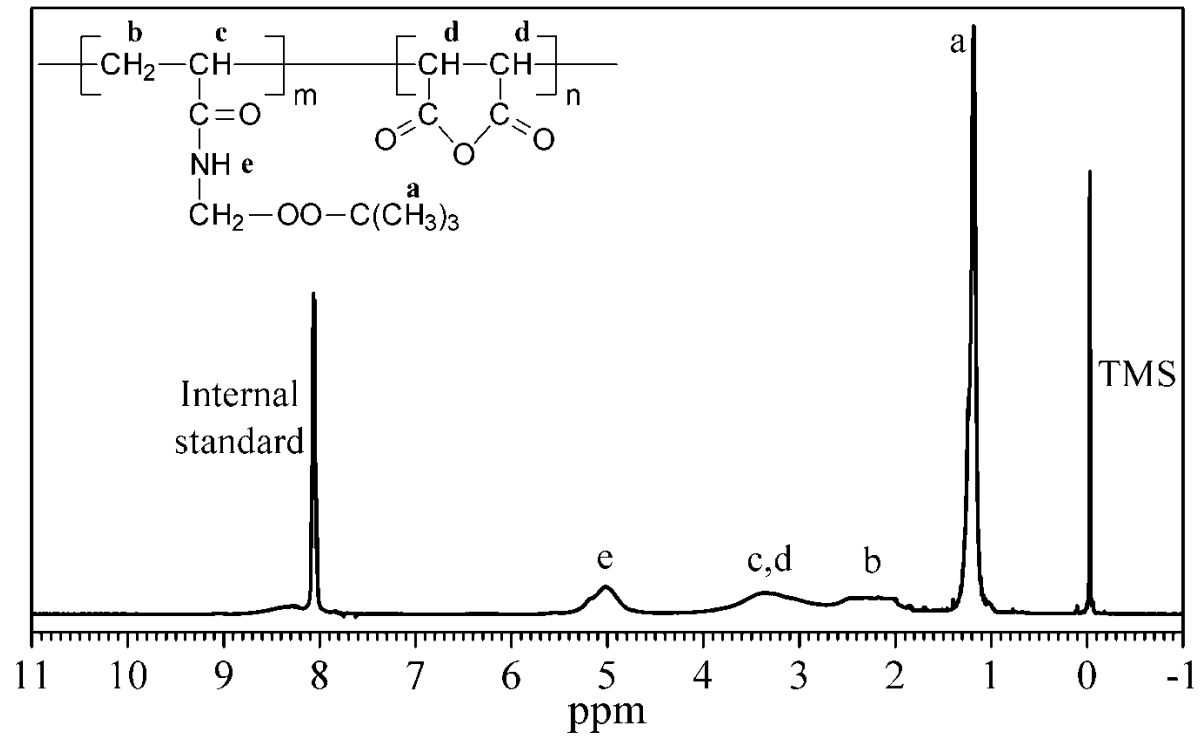

Figure 3.8. ^{1}H NMR spectrum of the PM–MA copolymer.

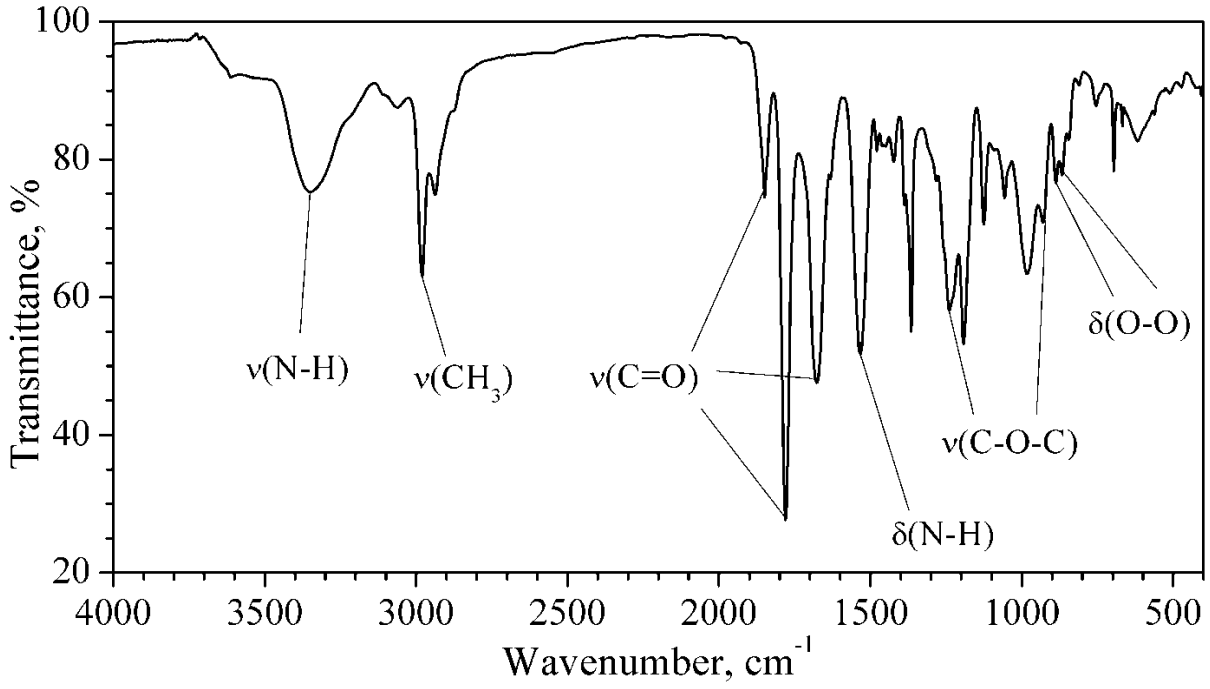

Figure 3.9. FTIR spectrum of the PM–MA copolymer.

The synthesized PM–MA copolymer is soluble in water due to the hydrolysis of the maleic anhydride groups to give carboxylic groups and their further ionization by increasing pH. To confirm the copolymer surface activity and formation of micelles in aqueous solution, the solubilization of a fluorescent probe [31], pyrene, as a function of PM–MA concentration in water was determined, and surface tension measurements were performed. From the latter (data not shown), it was observed that the surface tension of the PM–MA aqueous solution decreases to 30 mN/m when the copolymer concentration in water increases, confirming that the macromolecules of the synthesized copolymer are surface active.

To determine the critical micelle concentration of PM–MA using solubilization experiments, pyrene excitation spectra were monitored in the wavelength range of 300–360 nm. A red shift of the fluorescence excitation spectra from 333 to 336.5 nm with an increasing copolymer concentration in aqueous solution indicates the formation of micelles and the solubilization of pyrene, which migrates from water to the micellar environment of PM–MA (Figure 3.10).

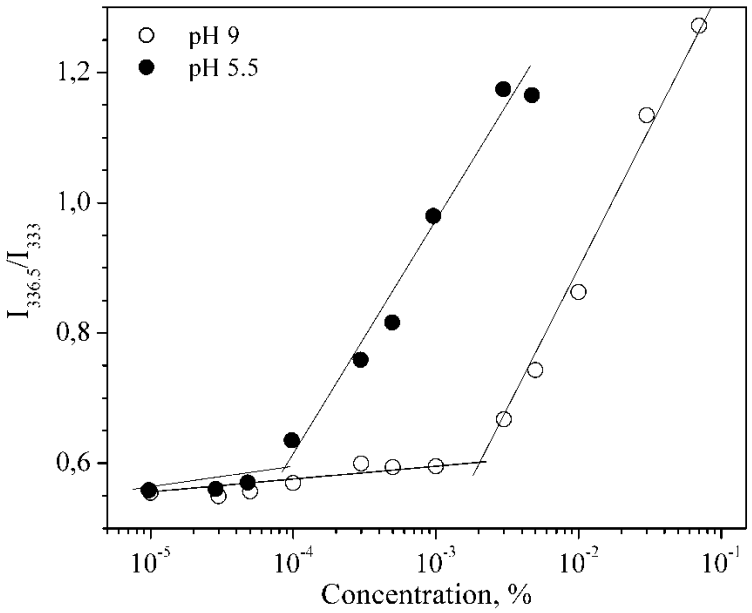

Figure 3.10. The intensity ratio, $I_{336.5}/I_{333.5}$, of the excitation spectra of pyrene in the copolymer aqueous solutions vs. the copolymer concentration.

The sharp increase in the intensity ratio corresponds to the critical micelle concentration of the copolymer for each pH. The PM–MA copolymer shows higher surface activity at a lower pH. The critical micelle concentration increases with increased pH from 1.2×10^{-5} mol/L (0.1 mg/L) at pH 5.5 to 2.3×10^{-3} mol/L (20 mg/L) at pH 9, indicating that PM–MA is more hydrophilic at higher pH due to the higher degree of ionization of the carboxylic groups in the copolymer.

To determine the copolymer composition by quantifying the carboxylic group content in the PM–MA, we employed a back potentiometric titration on the PM–MA copolymer dissolved in aqueous alkali solution. The titration plot shows two inflection points (Figure 3.11). The first inflection point indicates the neutralization of excess alkali, whereas the second inflection point corresponds to the pH where two carboxylic groups are formed (pH 3) [32, 33]. The volume of titrant between the two inflection points, ΔV, can be used to calculate the amount of carboxylic groups in the PM–MA copolymer. Using the calculated amount of carboxylic groups, the composition of the peroxide copolymer has been determined. The synthesized PM–MA copolymer (initial comonomer feed [PM] = 0.8 M, [MA] = 1.2 M) contains 0.33 mol parts of maleic anhydride and 0.67 mol parts of peroxide monomer.

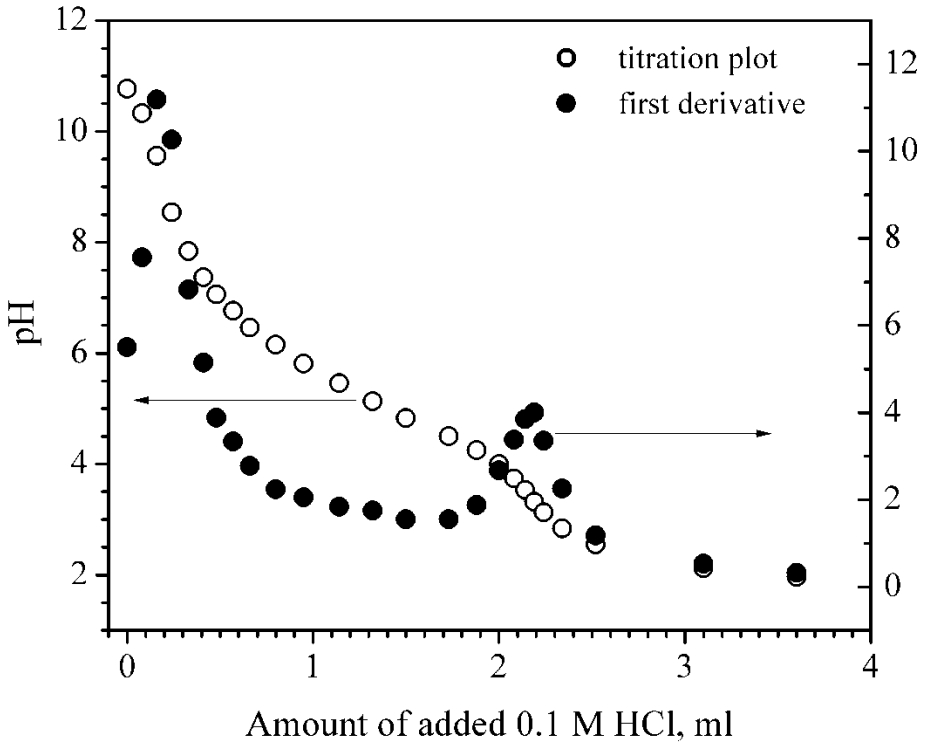

Figure 3.11. Titration plot and first derivative of PM–MA in aqueous solution.

This result is in a good agreement with the copolymer composition obtained from analyzing the ^{1}H NMR spectrum and determining the composition of PM–MA by assessing the ratio of tret-butyl and phthalic anhydride protons.

The capability of the peroxide groups in the PM–MA copolymer to undergo thermal decomposition was demonstrated using thermogravimetric analysis. Figure 3.12 indicates that the PM–MA samples undergo weight loss at 130–210°C. The recorded weight loss is due to the decomposition of the primary-tertiary peroxide groups in the PM units of the copolymer.

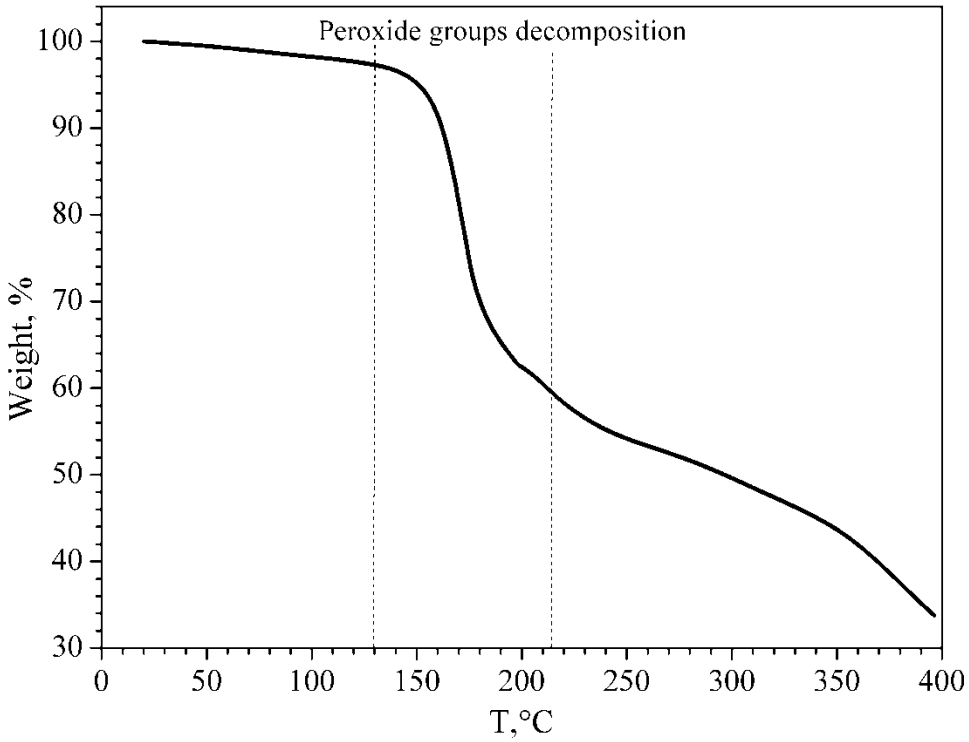

Figure 3.12. TGA analysis of PM–MA.

3.4.3. Synthesis of surface functionalized latex particles by emulsion polymerization using PM–MA

Varying concentrations of the synthesized PM–MA copolymer were used in a series of emulsion polymerizations of styrene at pH 9.5. Our expectation was that the PM–MA would act as an inisurf during the polymerization process, initiating polymerization by generating free radicals at elevated temperatures, and ensuring micelle formation and stabilization of growing polymer particles.

The obtained data show that polystyrene latexes with a narrow unimodal size distribution were synthesized at varying concentrations of PM–MA by styrene emulsion polymerization (Table 3.4). One can see that the increasing concentration of peroxide copolymer results in a slight decrease in the particle size. The polydispersity index indicates that the size distribution is narrow for all four polymerization experimental conditions. Analysis of the ζ-potential measurements for latexes synthesized at various concentrations

of the peroxide copolymer showed that the synthesized latex particles have a negative charge due to the presence of carboxylic groups on the surface.

Table 3.4. Physico-chemical characteristics of latex particles synthesized using varying concentrations of PM-MA in emulsion polymerization of styrene at pH 9.5.

Initial [PM-MA], %*, (-OO-, mmol/g)	[PM-MA] localized at the latex particle surface, % **	D_h, nm	PDI	ζ-potential, mV	-OO- localized at the surface, mmol/g **/***
1.0 (0.05)	0.73	196	0.050	-58 ± 2.1	0.04/0.01
2.5 (0.13)	1.76	162	0.015	-57 ± 1.9	0.09/0.07
5.0 (0.27)	3.99	146	0.041	-54 ± 2.0	0.21/0.19
7.5 (0.40)	6.21	155	0.033	-54 ± 1.8	0.32/0.29

*in reaction feed, per styrene monomer
**using potentiometric titration (as no decomposition occurs)
***using TGA analysis (considering decomposition)

Knowing the PM–MA composition from the copolymerization study described above, we were able to calculate the maximum amount of the peroxide copolymer that localizes on the latex particles during the emulsion polymerization and the amount of peroxide groups on the particles, assuming that no decomposition of the peroxide groups occurs.

For this purpose, each latex sample after dialysis was titrated using 0.1 N HCl to obtain the content of carboxylic groups on the surface and calculate the amount of localized peroxide copolymer and the concentration of –OO–** groups.

$$[PM\text{-}MA]_{localized}\,(\%) = (\Delta V \cdot N \cdot M \cdot 100)\,/(m_{sample} \cdot \omega_{sample} \cdot 1000 \cdot 2 \cdot F_{MA}) \quad (3.6)$$

where m_{sample} and ω_{sample} are the masses of the latex sample and its solid residue, respectively, F_{MA} is the mole fraction of maleic anhydride units in the copolymer, N is the

normality of the HCl titrant (here 0.1 mol eq/L), ΔV is the volume of titrant in mL, and M is the average repeat unit molecular weight, calculated using the following equation:

$$M = F_{MA} \cdot M_{MA} + (1 - F_{MA}) \cdot M_{PM} \quad (3.7)$$

The obtained data follow the concentration of the copolymer and demonstrate that most of the employed PM–MA was found on the latex particle surface after polymerization (Table 3.4).

Having confirmed the immobilization of the peroxide copolymer on the latex particles, our next goal was to evaluate how much polyperoxide was consumed during the free radical initiation of the emulsion polymerization and the formation of the polystyrene latex particles. For this purpose, a thermal analysis was performed on the polystyrene latex particles synthesized at each experimental copolymer concentration.

Figure 3.13 shows the TGA of the surface functionalized polystyrene particles synthesized at different copolymer concentrations and the DSC data for the latex sample obtained at 7.5 wt. % PM–MA. The results confirm that the resulting amount of reactive peroxide groups on the latex particle surface depends on the initial concentration of the peroxide copolymer in the polymerization and increases with increasing PM–MA concentration. The thermolysis of the peroxide groups is an exothermic reaction, generating maximum heat at 177°C.

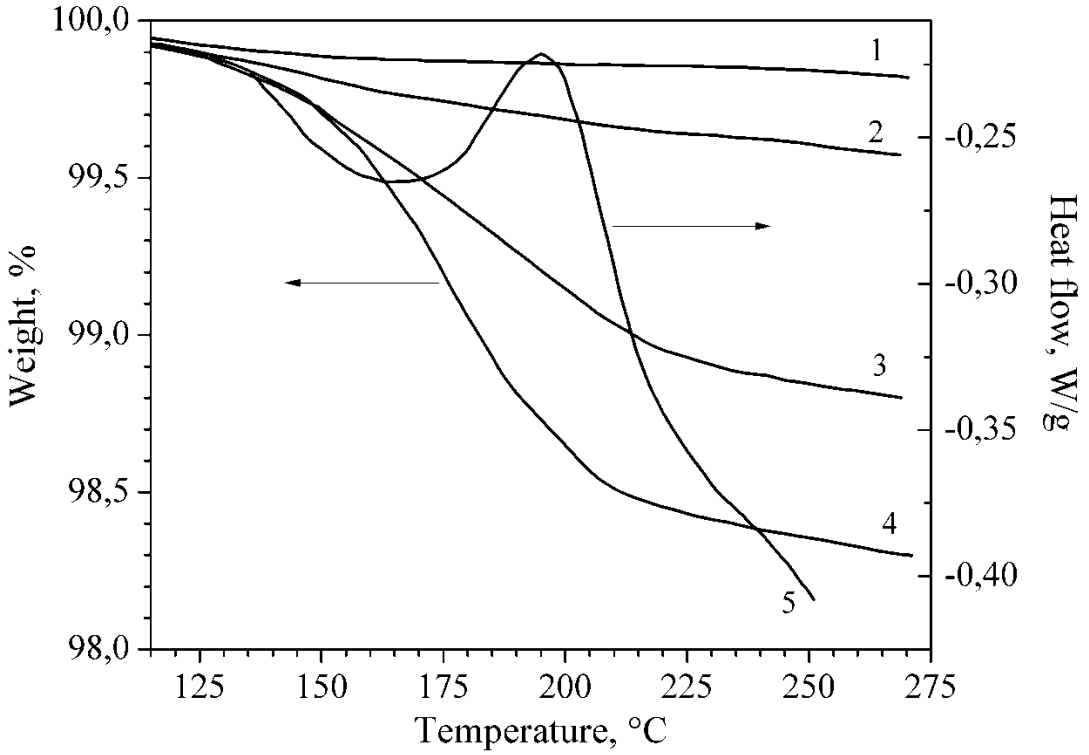

Figure 3.13. TGA (1–4) and DSC (5) of surface functionalized polystyrene latex particles (1–1, 2–2.5, 3–5, 4, 5–7.5 wt. % of peroxide copolymer).

To evaluate how much polyperoxide was consumed in the free radical initiation of the emulsion polymerization and the formation of the polystyrene latex particles, the amount of localized peroxide groups was calculated using the TGA data in the following equation:

$$\text{-OO-}^{***}_{localized}\ (mmol/g) = ((\delta_{latex}/\delta_{PM\text{-}MA})/M)\cdot(1\text{-}F_{MA})\cdot 10^3 \qquad (3.8)$$

where δ_{latex} and δ_{PM-MA} are the weight losses for the dry latex sample and PM–MA in the range of 130–210°C, respectively, as recorded from the TGA and M is the average repeat unit molecular weight.

The data in Table 3.4 show that a similar amount of peroxide groups, 0.02–0.03 mmol/g, (the difference between –OO–** and –OO–*** values) was consumed to initiate the polymerization in all four experiments. The latter fact provides an opportunity to not only localize the reactive peroxide groups on the latex particles' surface during polymerization

but also to control the amount of these groups, which are available for further modification, such as the formation of core–shell particle morphology.

As shown in Figure 3.14, the SEM analysis of the reactive latex particles supports the general observations of the DLS study, the synthesized polystyrene particles are monodisperse with a spherical morphology. The average particle size for the sample synthesized at a peroxide copolymer concentration of 7.5% per styrene monomer is approximately 150 nm, which is in strong agreement with the DLS data (Figure 4.15).

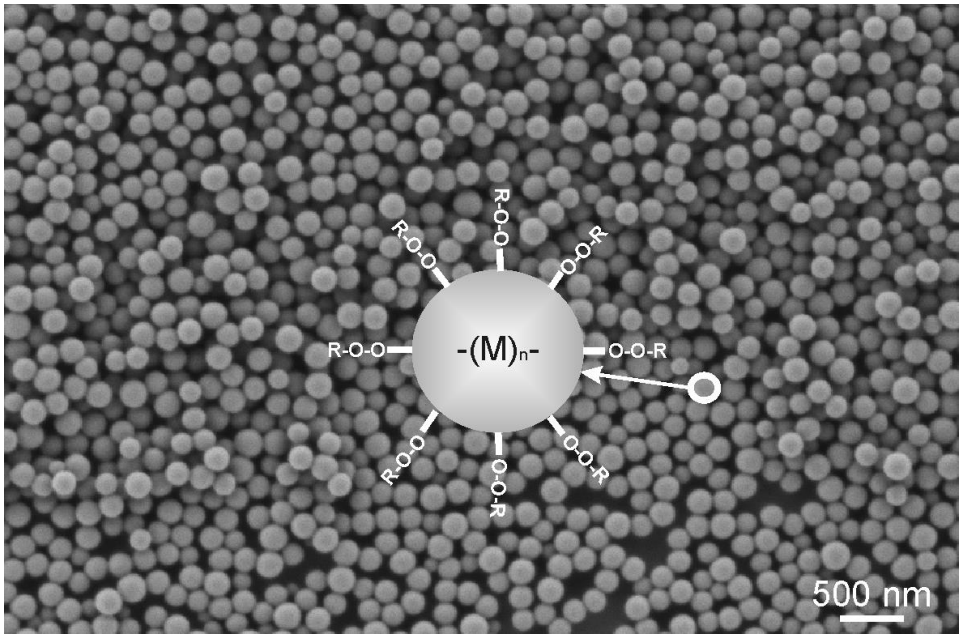

Figure 3.14. SEM image of a surface functionalized polystyrene latex particle, synthesized by emulsion polymerization using 7.5 wt. % PM–MA per styrene monomer.

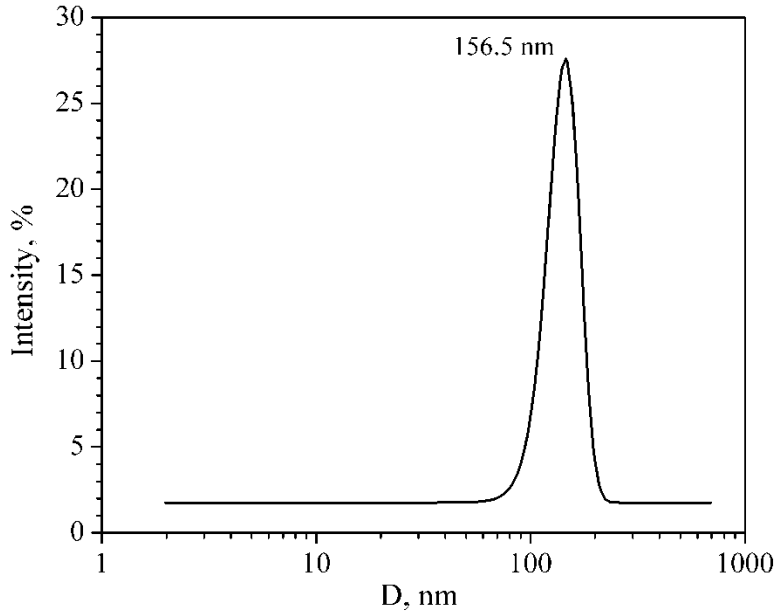

Figure 3.15. Size distribution (DLS) of a surface functionalized polystyrene latex particles, synthesized by emulsion polymerization using 7.5 wt. % PM–MA per styrene monomer.

3.4.4. Cross-linking and filling of synthetic latex coatings with peroxidized monodisperse polystyrene latex particles

The properties of latex coatings cross-linked using the peroxidized polystyrene particles is shown in Tables 3.5 and 3.6. Addition of 1 and 10 wt. % of the peroxidized latex to the acrylic latex results in increasing coating hardness (as determined by the pendulum damping test) in the range: AL-00 < AL-01 < AL-10 (110 sec < 114 sec < 126 sec).

Table 3.5. Properties of acrylic latex based reinforced coatings.

Property	AL-00	AL-01	AL-10
Content of peroxidized latex, wt. %*	0	1	10
Pencil hardness (gouge)	B	HB	H
König hardness, sec	110 ± 5	114 ± 5	126 ± 6
Impact resistance (intrusion/extrusion), in.-lb.	>176 / 136 ± 8	>176 / 120 ± 8	158 / 24 ± 4
MEK, # of double rubs	0 ± 1	2 ± 1	8 ± 3
Thickness, $x10^{-6}$ m	16 ± 2	13 ± 2	13 ± 3

* calculated on the basis of AL latex dry solids.

Table 3.6. Properties of styrene-butadiene based reinforced coatings.

Property	SB-00	SB-00-120	SB-01	SB-10	SB-30	SB-30-120	SB-50	SB-50-120
Curing temperature, °C	90	120	90	90	90	120	90	120
Content of modified latex, wt. %*	0	0	1	10	30	30	50	50
Pencil hardness (gouge)	HB	H	H	2H	3H /4H	6H	4H	5H
König hardness, sec	176 ± 3	180 ± 3	203 ± 3	211 ± 2	230 ± 4	212±10	227 ± 5	208±12
Impact resistance (intrusion/extrusion), in.-lb.	80 / 40 ± 8	80 / 32 ± 4	72 / 32 ± 4	72 / 24 ± 4	60 / 24 ± 8	60 / 20 ± 4	68 / 20 ± 8	72 / 16 ± 4
MEK, # of double rubs	24 ± 2	25 ± 2	41 ± 4	48 ± 3	60 ± 5	66 ± 5	36 ± 4	40 ± 5
Thickness, $x10^{-6}$ m	17 ± 2	18 ± 2	22 ± 3	18 ± 2	17 ± 2	25 ± 5	23 ± 3	25± 6

* calculated on the basis of SB latex dry solids.

These data are in a good agreement with the results of the film hardness by pencil test: B < HB < H. Similarly, solvent resistance of the coatings increases with increasing content of peroxidized latex. Methyl ethyl ketone is known to dissolve polystyrene. Since the solvent resistance increases with increasing content of peroxidized latex in the coating formulation, it could be concluded that the revealed peculiarities can be explained by the formation of cross-linked polymer coatings using the peroxidized latex particles. It is confirmed by the impact resistance (intrusion/extrusion) measurements. The values of impact resistance indicate the formation of cross-linked structures with different cross-link densities depending on the content of peroxidized latex.

There is an essential difference between the data on coatings from styrene-butadiene latexes in comparison to acrylic latexes, obviously caused by presence of the unsaturated butadiene fragments enabling free radical reactions of cross-linking. With an increasing content of the peroxidized polystyrene latex particles, König hardness changes in range SB-00 < SB-01 < SB-10 < SB-30 ≈ SB-50 (176 < 203 < 211 < 230 ≈ 227) (Table 3.6). With an increase of the polystyrene particles content from 30% to 50%, hardness does not change. The similar results have been observed using pencil hardness (gouge) technique: HB < H < 2H < 3H/4H ≈ 4H. By curing at 120°C, the coating shows König hardness of 6H.

The obtained indicate radical mechanism of the cross-linking the reinforced composites. Noteworthy, solvent resistance of the coatings increases from 24 double rubs for SB-00 to 60 of double rubs for SB-30. The impact resistance of coatings is determined by their chemical nature, namely the presence of unsaturated polystyrene units. It is clearly seen from Table 6, that the increase in content of the polystyrene particles to 50% and in temperature to 120°C do not affect the coating hardness and its solvent resistance.

3.5. Conclusions

A new approach to the cross-linking and filling synthetic latex coatings has been developed. Peroxidized monodisperse polystyrene latex particles have been used as a cross-linker and, simultaneously, as a filler of polymer coatings based on acrylic and styrene-butadiene latexes. The synthesis of peroxidized latex particles was carried out using the emulsion polymerization of styrene in the presence of the polymer inisurf, the initiator-surfactant, a copolymer of a peroxide monomer, N-[(*tert*-butylperoxy)methyl]acrylamide, with maleic anhydride. The peroxidized latex particles were employed to crosslink polymer coatings from synthetic acrylic and styrene-butadiene latexes.

The hardness and solvent resistance of the coatings based on both latexes increase with an increasing amount of the peroxidized latex filler in the formulation. The cross-linked coatings, based on styrene-butadiene exhibited better characteristics in terms of hardness

and solvent stability. The properties of latex-cross-linked coatings depend on reaction temperature and the amount of the cross-linker, peroxidized polystyrene latex particles.

3.6. References

1. Daniels E. S., Sudol E. D., El-Aasser M. S., Polymer colloids: science and technology of latex systems. *Am. Chem. Soc.* **2002,** 413.

2. Pomogailo A., Kestelman V., Metallopolymer Nanocomposites. Springer-Verlag: Berlin, **2005**.

3. Johnson T. L., ultra-low viscosity oxazolidine and aldimine-based reactive diluents for high-solids polyurethane coatings. *J. Coat. Technol.* **1995,** 67 (849), 41-47.

4. Paints, Coatings and Solvents, 2nd Edition. Eds. Freitag W., Stoye D., **2008**.

5. Wu S., Soucek M. D., Cross-linking of acrylic latex coatings with cycloaliphatic diepoxide. *Polymer* **2000,** 41, 2017–2028.

6. Huang Y., Jones F. N., Synthesis of crosslinkable acrylic latexes by emulsion polymerization in the presence of etherified melamine-formaldehyde (MF) resins. *Prog. Org. Coat.* **1996,** 28, 133-141.

7. Brown W., Polycarbodiimides in coatings technology. *Surf. Coat. Int*. **1995,** 6, 218-238.

8. Williams A., Carbodiimide chemistry: recent advances. *Chem. Rev*. **1981,** 81, 589-636.

9. Moles P., Acrylic latex cross-linking with aziridines. *Polym. Paint Color J.* **1991,** 181 (267), 4279-4283.

10. Pollano G., Cross-linking with Aziridines. Polym. Matr. *Sci. Eng.* **1997,** 77, 380-383.

11. Moor G., Zhu D.-W., Clark G., Aziridinesin coating technology. *Surf. Coat. Int.* **1995,** 9, 376-379.

12. Nippon Shokubai Products Information Bulletin: Novel Waterborne Cross-linkers, https://www.shokubai.co.jp/en/products/functionality/epocros.html, (last accessed 4/13/2015)

13. Geurts J. M., Jacobs P. E., Muijs J., Molecular mass control in methacrylic copolymer latexes containing glycidyl methacrylate. *J. Appl. Polym. Sci.* **1996,** 61 (1), 9-19.

14. B. Klumperman, J. Geuert, *Polym. Mater. Sci. Eng*. **1997,** 76, 177-182.

15. D. R. Eslinger, *J. Coat. Technol.* **1995,** 67 (850), 45-47.

16. D. Yu, S. Liu, *Gaodeng Xuexiao Huaxue Xuebao 1993,* 14(5), 725-726.

17. (a) Simpson D. A., Singer D. L., Dowbenko R., Blackburn W. P., Kania C. M. Color plus clear coatings employing polyepoxides and polyacid curing agents in the clear coat, US Patent 4681811, July 21, **1987**; (b) Yen-Jer S., Epoxy modified core-shell lattices, US Patent 5177122, June 14, **1993** and (c) McMonigal S. U., Singer D. L., Simpson D. A., Klanica J. A., Mayo M. A. One package stable etch resistant coating process, WO Patent 1992019660, October 30, **1992**.

18. Santer J. O., Etherified amino resins: synthesis and reactions in surface coatings applications. *Prog. Org. Coat*. **1984,** 12 (4), 309-320.

19. Bauer D. R., Melamine/formaldehyde cross-linkers: characterization, network formation and crosslink degradation. *Prog. Org. Coat.* **1986,** 14 (3), 193-218.

20. Ferrell P. E., Gummeson J. J., Hill L. W., *J. Coat. Technol*. **1995,** 67 (851), 63-71.

21. Essenfeld A., Wu K.-J., *Polym. Mater. Sci. Eng*. **1997,** 77, 385.

22. Natural rubber science and technology, Ed. A.D. Roberts, *Oxford University Press*, **1988,** 1136.

23. Erkova L. N., Chechik O. S., Lateksy. in Russian. Khimiya: Leningrad, Russia, **1983,** 224.

24. Voronov S., Tokarev V., Petrovska G., Heterofunctional Polyperoxides. Theoretical Basis of Their Synthesis and Application in Compounds, *Lviv Polytechnic State University*: Lviv, Ukraine, **1994,** 86.

25. Voronov S. A., Varvarenko S. M., Peroxide-containing Macromolecules at Interface. *Lviv Polytechnic State University*: Lviv, Ukraine, **2011,** 312.

25. Guyot A., Tauer K., Reactive surfactants in emulsion polymerization, *Adv. Polym. Sci*. **1994,** 111, 43-65.

26. Hourston, D.J. Williams, G.D. Satguru, R. Padget, J.C. Pears, D.Influence of the degree of neutralization, the ionic moiety, and the counterion on water-dispersible polyurethanes. *J. App. Pol. Sci.,* **1996**, 66, 89-105

27. Skeist I., Copolymerization mechanism. *J. Am. Chem. Soc.* **1946**, 68, 1781–1784.

28. Odian G., Principles of Polymerization, *Wiley*: New York, **1981**, 730.

29. Kohut A., Sieburg L., Vasylyev S., Kudina O., Hevus I., Stafslien S., Daniels J., Kislenko V., Voronov A., in Amphiphiles: Molecular Assembly and Applications, Ed.: Nagarajan R., *ACS Symposium Series 1070*, American Chemical Society: Washington, DC, **2011**, 205–224.

30. Samaryk V., Tarnavchyk I., Voronov A., Varvarenko S., Nosova N., Kohut A., Voronov S., *Macromolecules,* **2009**, 42, 6495–6500.

31. Hevus I., Kohut A., Voronov A., *Polym. Chem*., **2011**, 2, 2767–2770.

32. Kawaguchi S., Kitano T., Ito K., Minakata A., *Macromolecules,* **1991**, 24, 6335–6339.

33. Kitano T., Kawaguchi S., Anazawa N., Minakata A., *Macromolecules,* **1987**, 20, 2498–2506.

CHAPTER 4. SYNTHESIS OF COLLOIDOSOMES FROM PEROXIDIZED LATEX PARTICLES

4.1. Abstract

A new approach to synthesizing colloidosomes (micro-capsules with a shell from colloidal particles) was developed on the basis of Pickering emulsions (emulsion stabilized exclusively by colloidal particles), prepared from functionalized (peroxidized) polymer latexes. Soft template synthetic technique was employed, where free radical polymerization is used to convert droplets of Pickering emulsion into colloidosomes. Peroxidized latex particles were used to ensure formation and colloidal stability of Pickering emulsion during polymerization. The latex particles were developed with the use of inisurf (initiator-surfactant), amphiphilic polyperoxide copolymer (PM-MA). The inisurf was applied as both initiator and surfactant during emulsion polymerization. The polymerization results in latex particles with controllable amount of functional (peroxide and anhydride, both derived from PM-MA molecules) groups at the particle surface. It was demonstrated that structure of synthesized (using latex particles) colloidosomes depends on amount of functional groups and pH during synthesis. Size and morphology of colloidosomes can be thus controlled by latex particle surface hydrophilic-lipophilic balance (HLB).

4.2. Introduction

It is difficult to underestimate the importance of colloidal systems in current polymer technology development. Constant efforts are being made in the field of emulsion/suspension/miniemulsion polymerization techniques. Such processes use templates from liquid droplets stabilized by molecular surfactants (that eventually contaminate final product) to produce tailored solid nanomaterials.

Over last decade, considerable attention was focused on the surfactant-free systems [1], as they provide an opportunity to reduce environmental impact of polymer materials.

More specifically, great attention was drawn to Pickering emulsions, stable colloidal system of two immiscible liquids, whereas one is dispersed in the other with the help of solid particles [2], [3], [4]. The phenomena of particle surface activity was first described by Pickering and Ramsden [5], [6]. Several decades later, Velev [7], [8] proposed mechanism of self-assembly of colloidal particles at the liquid-liquid interphase. It was established that Pickering emulsion exhibits superior kinetic and thermodynamic stability when compared to conventional emulsions. Stabilization mechanism of colloidal particles is based on reducing of interphasial tension, similar to molecular surfactants. However, compared to surfactant molecules, colloidal particles are significantly larger and that imparts specifics to emulsification process and stability profile [9], [10]. Using Pickering emulsions opens a broad area of opportunities for not only improving of existing colloidal systems, but also for development of new composite polymer materials [11].

Colloidal structures, obtained as a result of fully or partially solidifying droplets of Pickering emulsion are generally denoted as colloidosomes (Scheme 4.1). To date, literature reports on synthesis of various types of colloidosomes, in particular, 'hairy' [12], 'sensitive' [13, 14], 'carbon nanotubosomes' [15]. Formation of covalently cross-linked colloidosomes via free radical and condensation polymerization mechanisms are reported [16-18], as well as possibility to fabricate core-shell and capsule-like colloidosome morphologies [17]. Because of ability to finely tune colloidosome properties (density of particle packing at the surface, shell thickness and its porosity, core type, composition etc.), such structures can be engineered to efficiently encapsulate (absorb) and deliver (release) various cargos in a controllable fashion [19]. Reports show that colloidosomes indeed can be employed as an effective encapsulation device, serving purpose of delivery (e.g. drug delivery) or protection of components in various fields of food, coating and cosmetic industries [20–23].

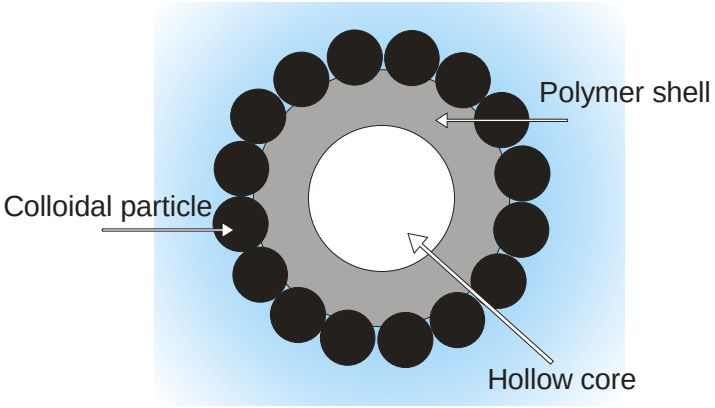

Scheme 4.1. Schematic representation of hollow colloidosome.

In this study surface-functionalized latex particles (described in Chapter 3) were utilized in synthesis of colloidosomes. Latex particles were synthesized using inisurf (amphiphilic polyperoxide copolymer). Presence of carboxyl and peroxide functional groups (both derived from inisurf molecules) on the particles surface can provide: i) tuneable hydrophilic-lipophilic balance of the surface, sustaining requirements of Pickering emulsion mechanism for synthesis of colloidosomes [7]; ii) initiation of free radical reactions, grafting and cross-linking within Pickering emulsion droplets; iii) possibility of further functionalization of colloidosomes in post-polymerization reactions (targeting ligands, protective layers etc.) [24].

It was shown that functional groups on particle surface play crucial role in stability of Pickering emulsion (by controlling hydrophilic-lipophilic balance) and determine success in colloidosomes synthesis. By utilizing peroxide functional groups of latex particles, colloidosomes can be further modified to obtain covalently cross-linked shell and hollow (liquid) core.

4.3. Materials

Styrene (St), divinylbenzene (DVB) (Sigma-Aldrich, St. Louis, MO), hexadecane (HD) (Alfa Aesar, Ward Hill, MA), 2,2'-azobis-isobutyronitrile (AIBN) (Aldrich, St. Louis, MO). Amphiphilic copolymer poly[N-(t-butyl-peroxymethyl) acrylamide]-co-maleic anhydride

(inisurf, PM-MA) was synthesized as described in Chapter 3 [25]. All monomers were purified by vacuum distillation, other reagents and water (MiliQ, 18 MΩ) were used as received.

4.4. Methods

4.4.1. Peroxidized latex synthesis

Emulsion polymerization was carried out in order to synthesize peroxidized latex particles following procedure described in Chapter 3 [p. 36]. Briefly, A 10 wt. % emulsion of styrene in an aqueous solution of PM–MA (1 wt. % per styrene) was prepared at pH 7.5 by magnetic stirring at 1200 rpm for 30 min. The emulsion was purged with argon under constant stirring for 20 min and subsequently placed in an oil bath heated to 85 °C. The polymerization was conducted for 4 h under constant stirring (conversion up to 95%). At the end of the reaction, the latex was cooled and placed into a 5 mL dialysis bag (50 kDa molecular cut-off). The bag was submerged into a 2000 mL beaker filled with distilled water adjusted to pH 9.5 using NaOH. At intervals of 24 h, the water in the beaker was replaced to ensure a constant high concentration gradient to improve the dialysis process. After 14 days, the latex was removed from the dialysis bag and stored at 4 °C.

Resulting polymer was then either i) stored in at 4 °C or ii) precipitated by freeze-thaw cycle and washed repeatedly with 0.1 N NaOH and hexane to remove any non-reacted material. Resulting polymer was collected, dried at room temperature and stored at 4 °C to be used for further analysis.

4.4.2. Dynamic light scattering and zeta-potential measurements

Size distribution measurements were performed in dilute aqueous dispersions of latex particles using Malvern Zetasizer Nano-ZS90 at 25 °C. The final numbers represent an average of a minimum of 5 individual measurements.

4.4.3. Potentiometric titration

A potentiometric titration (back titration using 0.1 N HCl as a titrant) was used to calculate the amount of carboxyl groups (originated from PM-MA) on the surface of latex particles.

4.4.4. Peroxide content evaluation

Thermal analysis of the decomposition of the peroxide groups at the surface of peroxidized particles was carried out using thermogravimetry using a TA Instruments Q500. Samples were subjected to an underlying heating rate of 10 °C/min. The specimen was heated to 400 °C in presence of air. Sample size of 15 mg.

4.4.5. Colloidosomes synthesis

Pickering emulsions were formed by mixing 28 g of aqueous phase, containing 0.3÷1 wt. % peroxidized latex particles, with 2 g of oil phase, consisting of HD, St, DVB and 0.06 g AIBN initiator. Mixtures of oil and aqueous phases were homogenized at 10,000 rpm in pulsating regime (1 pulse consisting of 60 sec homogenizing + 20 sec rest time) for 8 min, using T25 Ultra-Turrax homogenizer (IKA, USA). Obtained Pickering emulsions were transferred into round bottom flask, purged with Ag for 20 min and subsequently polymerized at 80 °C for 24h. After polymerization, colloidosomes were isolated from dispersion, thoroughly washed with acetone/ethanol (1:1) mixture and stored either under H_2O or HD layer, or in dry state.

4.4.6. Colloidosomes imaging

Digital images of latex particles were obtained using JEOL JSM-6490LV scanning electron microscopy.

4.5. Results and discussion

The main goal of this work was to develop a fabrication route for colloidosomes synthesis on the basis of Pickering emulsions stabilized with peroxidized latex particles. To achieve this goal, two objectives were detailed i) to investigate how presence of hydrophilic

functional groups on latex particle surface impacts Pickering emulsion stability and ii) to synthesize colloidosomes using peroxidized latexes.

4.5.1. Synthesis and characterization of peroxidized latexes

Amphiphilic PM-MA copolymer (inisurf) was employed in emulsion polymerization to synthesize peroxidized latex particles (Chapter 3). In order to provide surface activity and ability to stabilize Pickering emulsion, the latex particles need to exhibit amphiphilic behaviour – i.e. to combine hydrophilic and hydrophobic functional groups at the surface. In case of peroxidized latexes, hydrophilic properties are provided by hydrolysed maleic anhydride groups (carboxyl) in PM-MA (Figure 4.1), whereas non-polar PM fragments of the copolymer macromolecules and polystyrene (core material of latex) provide hydrophobic properties to the particle's surface.

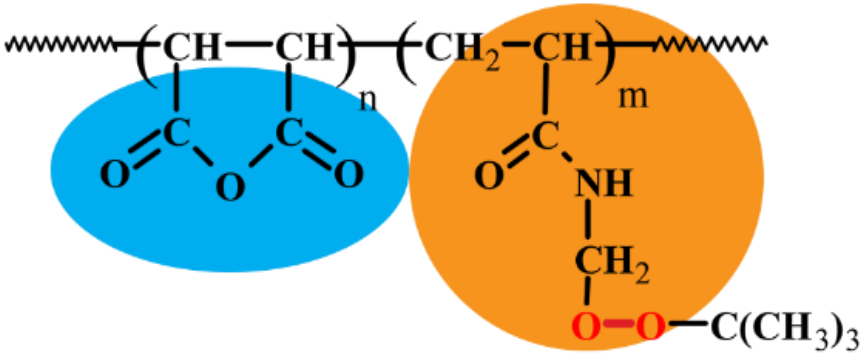

Figure 4.1. PM-MA copolymer structure (blue and orange represent hydrophilic and hydrophobic functional groups of PM-MA).

In order to investigate the ability to control the amount of carboxyl groups on the surface of latex particles, and thus particle's surface activity, series of latexes were synthesized at pH 5.5, 7.5 and 9.5 using various PM-MA concentrations (0.3, 1, 2.5, 5 and 7.5 wt. % based on monomer weight). Figure 4.2. A represents size variations of the obtained peroxidized latex particles as a function of pH and initial PM-MA concentration. In general, size of latex particles decreases with increasing inisurf concentration and by decreasing pH. Higher concentration of PM-MA (acting as a surfactant) obviously results in

formation of larger number of micelles (nucleating sites for the particle growth in emulsion polymerization), thus, greater number of smaller particles is formed. HLB value of inisurf macromolecules depends on pH of solution (degree of deprotonation of PM-MA carboxyl groups). At higher pH, inisurf macromolecules are more hydrophilic, thus more of them are required to form a micelle (vice versa for lower pH). Consequently, the pH changes total number of micelles in polymerization and results in variations in latex particle number and size (Figure 4.2 A).

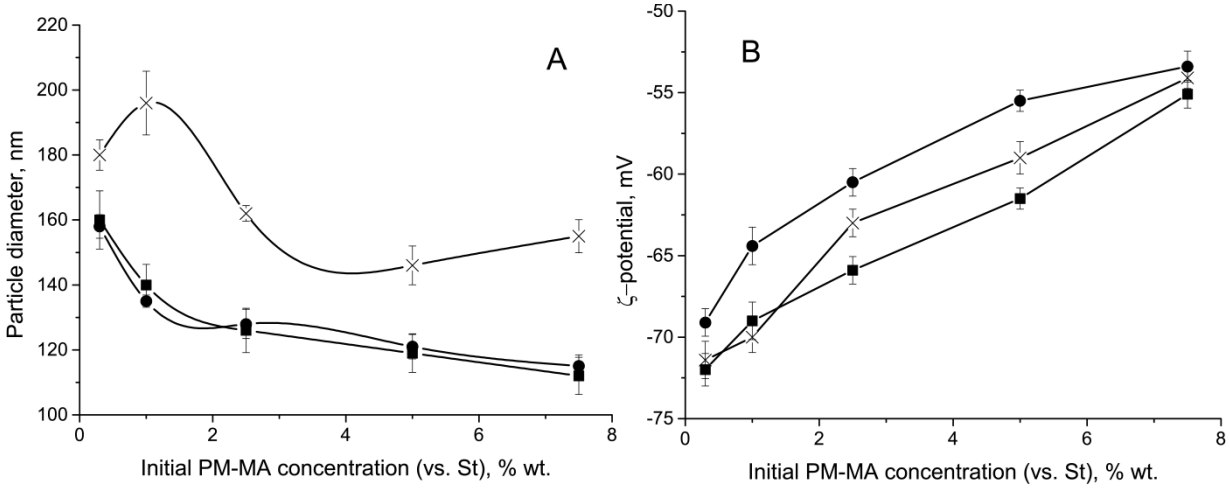

Figure 4.2. Size variations (A) and ζ-potential values (B) of peroxidized latex samples with various PM-MA content, synthesized at: ■ pH 5.5; ● pH 7.5; × pH 9.5.

It was confirmed (Chapter 3), that inisurf macromolecules undergo covalent attachment (grafting) to latex particle surface during polymerization. Potentiometric titration of peroxidized latex was performed in order to determine absolute number of carboxyl functional groups present on the surface (Figure 4.3).

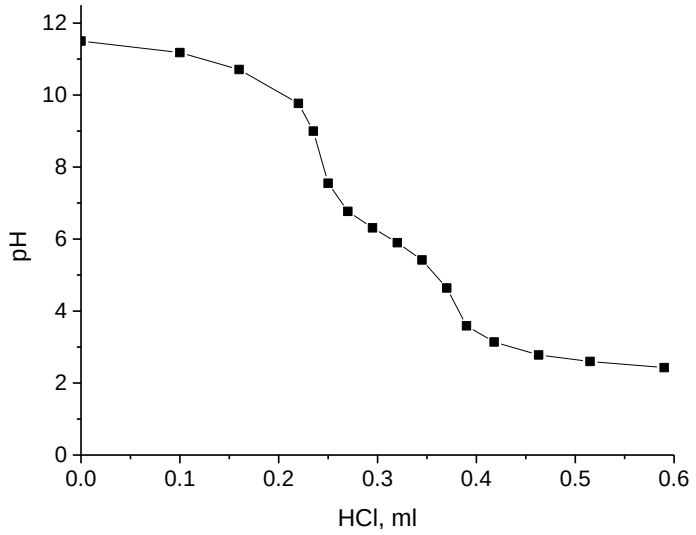

Figure 4.3. Potentiometric titration plot of peroxidized latex (synthesized at pH 7.5 and with 1 wt. % PM-MA based on monomer weight).

The obtained data reveal that only 60-80 % of carboxyl groups from grafted inisurf macromolecules are indeed located on the latex particle's surface, thus part of anhydride groups are localized in particle core and may not undergo hydrolysis. Figure 4.2 B shows zeta potential measurements of peroxidized latexes, providing information on overall effect of inisurf concentration and pH on particle's charge. The data show that amount of carboxyl groups on the surface of latex particles linearly depends on concentration of inisurf (Figure 4.4 B). However, density of the functional groups on the surface differs with inisurf concentration, possibly due to changes in latex particle size (Figure 4.4 A). We believe that changes of zeta potential with respect to pH during synthesis can be explained by the fact that part of MA groups are not accessible for hydrolysis, as it was determined by potentiometric titration.

To summarize, it was observed that increasing inisurf concentration results in significantly smaller particle size and greater amount of carboxyl groups on the surface. Even though more carboxyl groups are present on the surface of latex particles, zeta potential value decreases by increasing inisurf concentration. Size of latex particles is

determined by pH, while it impacts number of carboxyl groups on the surface of particles as well.

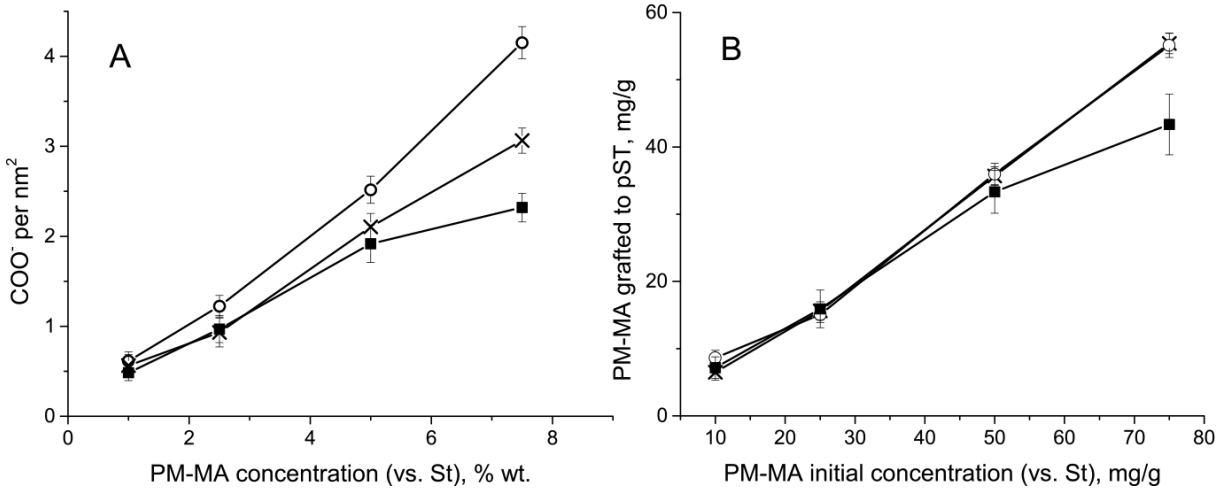

Figure 4.4. Amount of carboxyl groups (A) and PM-MA copolymer (B) on peroxidized latex particles, synthesized at: ■ pH 5.5; ○ pH 7.5; × pH 9.5.

As a result, a controllable amount of carboxyl groups on the surface of peroxidized latex particles (hydrophilic groups) allows to control particle surface HLB. As the next step, the colloidosome synthesis was attempted, using peroxidized latex particles.

4.5.2. Colloidosome preparation

This study utilized 'soft template' synthesis approach, where liquid droplets of Pickering emulsion serve as templates for colloidosomes formation [7]. Pickering emulsion was composed of oil phase from monomer mixture, initiator and hydrophobic solvent (HD) that was emulsified in aqueous phase, where peroxidized latex particles, exclusively acting as a surface active ingredient, were located. Once Pickering emulsion is formed, it was heated to initiate the free radical polymerization inside each oil droplet, yielding hollow (HD filled) colloidosomes (Figure 4.5).

Formation and stability of Pickering emulsion depend on the latex particles surface activity (surface HLB), therefore an ability to control the HLB of particle surface is crucial. To confirm that peroxidized latex particles can be used in Pickering emulsion formation for colloidosomes synthesis, series of Pickering emulsions were prepared.

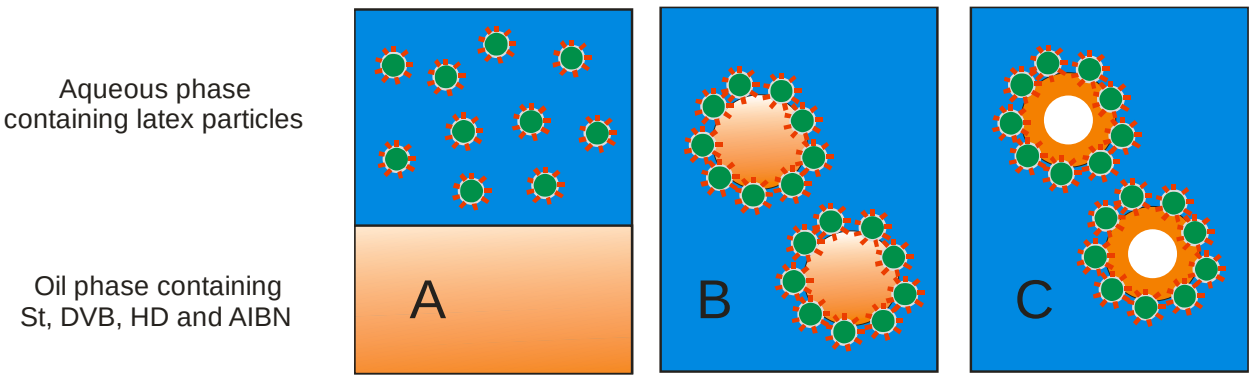

Figure 4.5. Schematic of the colloidosomes synthesis: A) aqueous and oil phases before homogenization; B) Pickering emulsion droplets after homogenization; C) colloidosomes after polymerization (polymeric shell covered with grafted peroxidized latex particles and solvent-filled hollow interior).

For the synthesis of colloidosomes, latex synthesized at pH 7.5 in the presence of 1 wt. % (based on monomer weight) inisurf was chosen. It was our assumption that such latex, while having small number of carboxyl groups, exhibits sufficient surface activity to stabilize Pickering emulsion.

First, formation and long-term stability of formulated Pickering emulsion were studied as a function of pH. Stability of a series of Pickering emulsions, prepared at different pH was studied (Figure 4.6). It was found that there is an optimal pH range, where superior Pickering emulsion stability can be achieved (Figure 4.7). Notably, at pH < 3 and pH > 9, no emulsion formation was observed which can be explained by either absence (pH < 3) or excessive amount (pH > 9) of ionized carboxyl groups on latex particle's surface, causing particle coagulation due to detrimental HLB change of inisurf macromolecules acting as particle stabilizers.

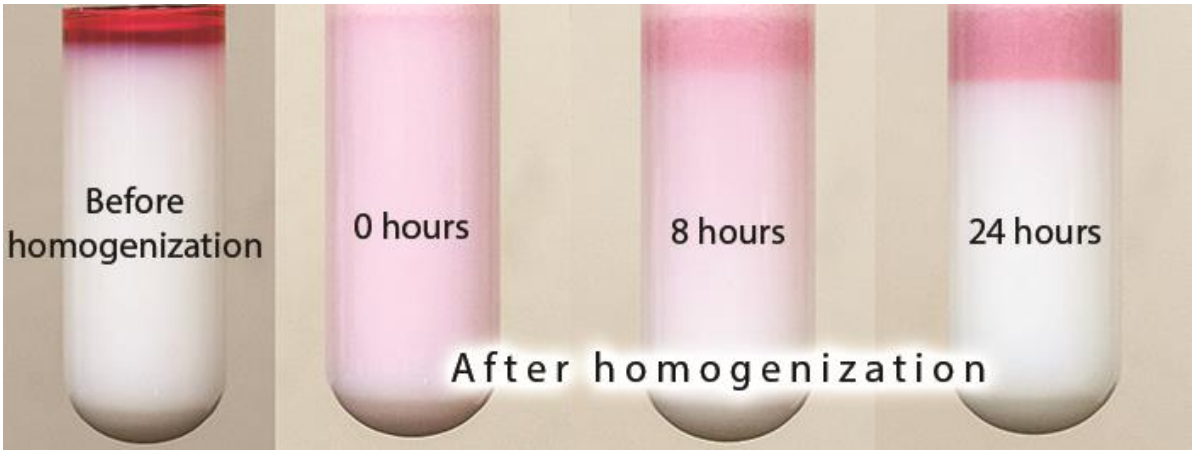

Figure 4.6. Stability of Pickering emulsions over time (pH 4.5; oil phase contains 0.01% Nile Red dye for imaging purposes).

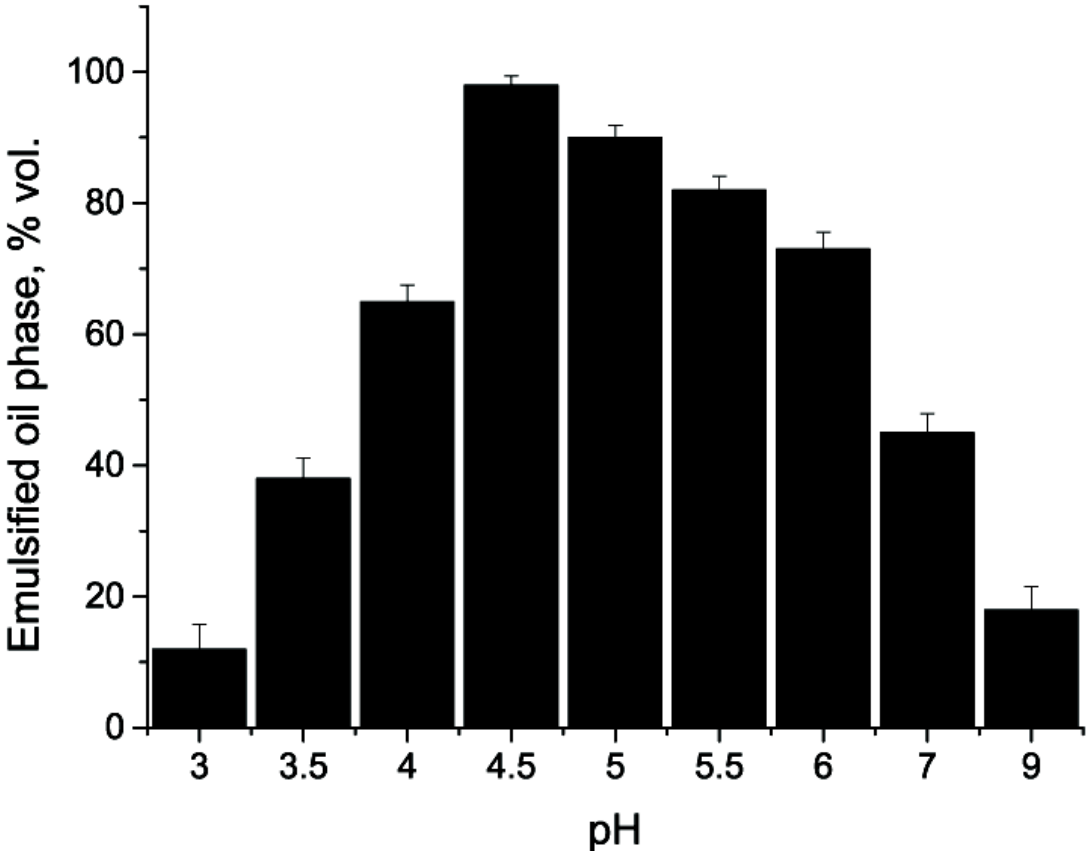

Figure 4.7. Fraction of oil phase remaining in emulsified form for Pickering emulsions prepared at various pH (recorded after 24 h rest period).

Immediately after formation, Pickering emulsion 'creams' by floating emulsified oil phase on top of excessive aqueous phase (Figure 4.6). This effect can be explained by different density of aqueous and oil phases (large size prevents droplet suspending). At this

point, formulation quality can be assessed by inspecting aqueous phase for the presence of excessive latex particles. Opalescence and turbidity would signify inefficient use of latex particles. By adjusting pH, shear rate and concentration of latex particles, it is possible to form clear (particle-free) aqueous phase, indicating that all particles are used in stabilization of droplets.

After formulating Pickering emulsion, polymerization was conducted to yield hollow colloidosomes, decorated with peroxidized latex particles. Table 4.1 shows information on properties of the synthesized colloidosomes.

Table 4.1. Colloidosomes synthesis conditions and properties.

Sample	**pH**	**Oil phase composition, wt. %**				**Colloidosomes dimensions**	
		St	DVB	HD	AIBN	D, μm	Shell, μm
CS1	7.5	28	12	57	3	10±8	1.7±0.4
CS2	3.5	28	12	57	3	10±4	1.3±0.3
CS3	4.5	28	12	57	3	15±3	1.5±0.4
CS4	4.5	14	6	77	3	10±2	0.8±0.2

The obtained results indicate that several morphological characteristics of colloidosomes can be controlled by variations in oil phase composition (e.g. monomers/HD ratio) and pH of aqueous phase. At the same time, the size of colloidosomes can be adjusted by pH of aqueous phase and homogenization parameters (pulse length, sonication intensity), whereas shell thickness depends on total initial concentration of monomers.

SEM measurements show several different colloidosomes morphologies can be synthesized using peroxidized latex particles (Figure 4.8).

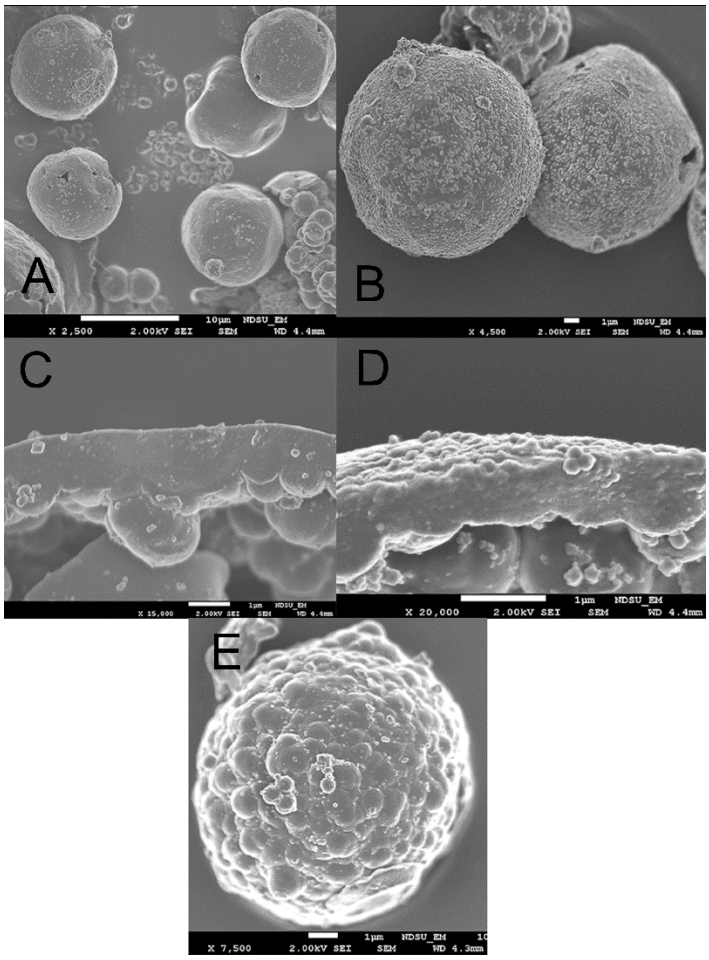

Figure 4.8. SEM photographs of colloidosomes: CS2 (A), CS3 (B), shell of CS3 (C) shell of CS4 (D), CS1 (E).

Although the surface charge of latex particles is essential for electrostatic stabilization of droplets in Pickering emulsion, it can also be disruptive if it is too large. Notably, the colloidosomes prepared at pH 7.5, unlike other samples, did not feature smooth surface, covered with grafted latex particles. Their outer surface shows signs of phase separation during synthesis and obvious lack of latex particles due to possibly excessive particle charge at pH 7.5.

4.6. Conclusion

Peroxidized latex particles with variable amount of carboxyl functional groups were successfully employed in formation of colloidosomes using Pickering emulsion polymerization approach. It was shown that by controlling surface HLB of latex particles

(number of carboxyl and peroxide groups on the surface) colloidosomes with several different morphologies can be synthesized. It was also found, that the surface charge of the particles is essential for stability of the droplets in Pickering emulsion and for colloidosomes formation. Proposed technique allows for fabrication of carrier capsules without contamination with surfactants that can potentially leach out during application.

4.7. References

1. Sakai T., Surfactant-free emulsions. *Curr. Op. in Coll. & Int. Sci.,* **2008,** 13 (4), 228-235.

2. Binks B. P., Particles as surfactants. *Curr. Op. in Coll. Int. Sci.*, **2002,** 7, 21-41.

3. Rossier-Miranda F. J., Schroen C. G. P. H., Boom R.M., Colloidosomes: Versatile microcapsules in perspective. *Coll. and Surf.*, **2009,** 343, 43-49.

4. Saraf S., Rathi R., Kaur C. C. D., Saraf S., Colloidosomes and Advanced Vesicular System in Drug Delivery. *Asia J. of Sci. Res.*, **2001,** 4 (1), 1-15.

5. Pickering S. U., Emulsions. *J. of Chem. Soc.*, **1907,** 91, 2001-2021.

6. Ramsden W., *Proceedings of Royal Society*, **1903,** 72, 156-164.

7. Velev O. D., Furusawa K., Nagayama K., Assembly of latex particles by using emulsion droplets as templates. 1. Microstructured hollow spheres. *Langmuir*, **1996,** 12, 2385-2391.

8. Velev O. D., Furusawa K., Nagayama K., Assembly of latex particles by using emulsion droplets as templates. 2. Ball-like and composite aggregates. *Langmuir*, **1996,** 12, 2385-2391.

9. Dismore A. D., Hsu M. F., Nicolaides M. G., Marquez M., Bausch A. R., Weitz D. A., Colloidosomes: selectively permeable capsules, composed of colloidal particles. *Science*, **2002,** 298, 1006-1009.

10. Taubman A. B., Koretskiy A. F., Stabilization of emulsions with solid surfactants and coagulative structure formation. *Achiev. of Col. Sci.*, Nauka: Moscow, USSR, **1976.**

11. Kim S.-H., Yi G.-R., Kim K. H., Yang S.-M., Photocurable Pickering emulsions for colloidal particles with structural complexity. *Langmuir*, **2008,** 24, 2365-2371.

12. Noble P. F., Cayre O. J., Alargova R. G., Velev O. D., Paunov V. N., Fabrication of 'Hairy' colloidosomes with shells of polymeric nanorods. *J. of Am. Chem. Soc.*, **2004,** 126, 8092-8093.

13. Lawrence D. B., Cali T., Hu Z., Marquez M., Dinsmore A. D., Temperature-responsive semipermeable capsules composed of colloidal microgel spheres. *Langmuir*, **2007,** 23, 295-298.

14. Kim J.-W., Frenandes-Nieves A., Dan N., Utada A. S., Marquez M., Weitz D. A., Colloidal assembly route for responsive colloidosomes with tunable permeability. *Nano Letters,* **2007,** 7, 2876-2880.

15. Panhuis M., Paunov V. N., Assembling carbon nanotubosomes using an emulsion-inversion technique. Chem. Comm., **2005,** 13, 1726-1728.

16. Yin D., Zhang Q., Zhang H., Yin C., Fabrication of covalently-bonded polystyrene/SiO_2 composites by Pickering emulsion polymerization. *J. of Pol. Res.,* **2010,** 17, 689-696.

17. Chen T., Colver P. J., Bon S. A. F., Organic-inorganic hybrid hollow spheres prepared from TiO_2-stabilized Pickering emulsion polymerization. *Adv. Mat.,* **2007,** 19, 2286-2289.

18. Thompson K. L., Arnes S. P., Howse J. R., Ebbens S., Ahmad I., Zaidi J. H., York D. W., Burdis J. A., Covalently cross-linked colloidosomes. *Macromolecules*, **2010,** 43, 10466-10474.

19. San Miguel A., Scrimgeour J., Curtis J. E., Sven H., Smart colloidosomes with dissolution trigger, *Soft Matter*, **2010,** 14, 3136-3166.

20. Zhang K., Wu W., Guo K., Chen J.-F., Zhang P.-Y., Magnetic polymer enhanced hybrid capsules prepared from a novel Pickering emulsion polymerization and their application in controlled drug release. *Coll. and Surf. A*., **2009,** 349, 110-116.

21. Shilpi S., Jain A., Gupta Y., Jain S. K., Colloidosomes: an emerging vesicular system in drug delivery. *Crit. Rev. Ther. Drug. Carrier Syst.,* **2007,** 24 (4), 361-91.

22. Porta F., Kros A., Colloidosomes as Single Implantable Beads for the In Vivo Delivery of Hydrophobic Drugs. *Particle & Particle Sys. Char.,* **2013,** 30 (7), 606-613.

23. Zhao Y., Pan Y., Nitin N., Tikekar R. V., Enhanced stability of curcumin in colloidosomes stabilized by silica aggregates. *LWT - Food Science and Technology*, **2014,** 58 (2), 667-671.

24. Vyas S. P., Khar R. K., Targeted and Controlled Drug Delivery – Novel Carrier Systems. 1st Ed. *CBS Publisher: New* Delhi, **2002.**

25. Samaryk V., Tarnavchyk I., Voronov A., Varvarenko S., Nosova N., Kohut A., Voronov S., A New Acrylamide-Based Peroxide Monomer: Synthesis and Copolymerization with Octyl Methacrylate. *Macromolecules*, **2009,** 42 (17), 6495–6500.

CHAPTER 5. SOY-BASED SURFACE ACTIVE COPOLYMERS AS SAFER REPLACEMENT FOR LOW MOLECULAR WEIGHT SURFACTANTS[2]

5.1. Abstract

Environmentally friendly soybean-based polymeric surfactants (SBPS) were synthesized using cationic polymerization of a vinyl ether monomer derived from soybean and tri(ethylene glycol) ethyl vinyl ether. The ability of SBPS to form micelles that solubilize hydrophobic molecules has been shown. Micellar "capacity" (size of micellar interior) increased with increasing polymeric surfactant concentration and temperature. The obtained results provide evidence for potential use of SBPS as a safer replacement for low molecular weight surfactants in the solubilization of poorly soluble ingredients in cosmetics. The macromolecules developed can be used as both a surface active agent and an additive that enhances the surface activity of low molecular weight surfactants (for example, anionic sodium lauryl sulfate) in personal-care products.

5.2. Introduction

The amount of surfactants used in personal-care products in the United States is close to 800 million pounds and is valued at over $70 billion [1]. The personal-care market includes bubble baths, body washers, hand soaps and cleaners, shaving products, hair shampoos and oral-care products. In 90% of personal-care products that foam, sodium lauryl sulafate (SLS) and ammonium lauryl sulfate (ALS) surfactants are used [2]. SLS and

---

[2]Based on manuscript published in *ACS Sustainable Chem. Eng*., **2013**, 1 (1), 19–22. The material in this chapter was co-authored by Andriy Popadyuk, Samim Alam, Harjyoti Kalita, Olena Kudina, Bret J. Chisholm and Andriy Voronov. Andriy Popadyuk had primary responsibility for, analytical measurements and data interpretation. Andriy Popadyuk was the primary developer of the conclusions that are advanced here. Andriy Popadyuk also drafted and revised all versions of this chapter.

ALS are highly soluble in water at a wide range of pH and temperature, insensitive to water hardness and can generate copious amounts of foam [3]. However, being anionic surfactants that contain sulfate groups, they can pose acute health threats. Global consumer products companies now seek new alternative surfactant compositions to substitute for SLS and ALS across their product portfolio [1]. Having the same functional properties as SLS and ALS, the replacement composition should not contain sulfate, sulfonate or amine oxide groups, be non-ionic in aqueous solution, and unaffected by water hardness.

Additional desirable features include production of the novel surfactants from a renewable resource and the use of "green chemistry" for surfactant production [4]. To this end, natural product ingredients are an important trend in global cosmetics, making the development of new environmentally friendly natural product ingredients more prevalent in the personal-care area than in other segments of the surfactant market [5]. To this end, oleo-based surfactants have been commonly derived from plant oils (coconut and palm) or from animal fats [6-8]. In recent years, animal fat feedstocks have been targeted for replacement by vegetable oils, including growing utilization of soybean oil, that is about 30% of the 2007 world seed oil production [7]. In addition to food uses, the industrial oleochemicals business is investigating the use of high oleic soybean oils as a feedstock for the production of numerous products. These products not only have the ecological benefit of being biodegradable and derived from a renewable resource, but they also lend different and increased functionality. Independent testing has shown that new oils actually may perform better than petroleum-based products in some uses [9]. High oleic soybean oil is being tested and utilized in cosmetics and has become the predominant feedstock used in the production of surfactants where soybeans are used (another starting material to produce surfactants can be soy protein). Both soybean oil and soy protein are used as raw ingredients to produce surfactants [1].

Very commonly used in formulating personal-care products, polymeric surfactants form micelles by self-association of one or several macromolecules containing hydrophilic and hydrophobic sequences distributed along the macromolecular backbone [10-11]. Increasing environmental awareness and the utilization of renewable materials provide opportunities to use soybeans for the production of new polymeric materials, in particular for the synthesis of soybean-based polymeric surfactants [12-13]. To our knowledge, no soybean-based non-ionic polymeric surfactants have been reported for personal-care products.

In this study, we focus on developing novel environmentally friendly and efficient soybean-based polymeric surfactants (SBPS) for personal-care applications. The reported synthetic approach combines benefits from using a natural ingredient, soybean oil, as a starting material, with an ability of amphiphilic polymeric macromolecules to self-assemble into micelles at a specific concentration (critical micelle concentration, CMC) and solubilize hydrophobic molecules in the micellar interior.

5.3. Experimental section

5.3.1. Monomer synthesis

The synthesis of 2-(vinyloxy)ethyl soyate (2-VOES) has been described elsewhere [14]. Tri(ethylene glycol) ethyl vinyl ether (TEGEVE) was synthesized as follows: 16.5 g of di(ethylene glycol) monoethyl ether (99% purity from Sigma-Aldrich, St. Louis, MO), 8 g of sodium hydroxide, 60 ml of tetrahydrofuran, and 40 ml of de-ionized water were combined in a 500 ml, 3-neck, round-bottom flask using constant stirring to produce a homogeneous solution. The mixture was cooled to 0 °C and then 25.7 g of *p*-toluenesulfonyl chloride (99% purity from Sigma-Aldrich, St. Louis, MO) in 50 ml of tetrahydrofuran (THF) was added to the reaction mixture drop-wise using an addition funnel and the reaction was continued for 2 hours at 0 °C. The reaction mixture was then poured into 100 ml of ice cold water and the product extracted with methylene chloride. The organic layer was washed with water and

dried with anhydrous magnesium sulfate. The product, i.e. the tosylate of di(ethylene glycol) monoethyl ether (Ts-DEGMEE), was recovered after rotary evaporation of all the volatiles and dried under vacuum overnight. In the second step, 1.5 g of sodium hydride (95 % purity from Sigma-Aldrich, St. Louis, MO) and 75 ml of THF were dissolved in a 500 ml, 3-neck, round-bottom flask equipped with a nitrogen blanket. The solution was cooled at 0 °C and a solution of 4.77 g of ethylene glycol monovinyl ether (95 % purity, from TCI America, Portland, OR) in 30 ml THF was added drop wise. Next, a solution of 15 g of Ts-DEGMEE in 45 ml THF was added to the reaction mixture and the temperature was raised to 60 °C. After 24 hours, the reaction mixture was cooled to room temperature and diluted with 150 ml of diethyl ether. The organic layer was washed three times with 75 ml of water and dried with anhydrous magnesium sulfate. The product monomer, TEGEVE, was collected after rotary evaporation of all volatiles and dried under vacuum overnight. Successful synthesis of TEGEVE was confirmed by proton NMR: 6.4 ppm (q, 1H, OC**H**=C), 4. 0 - 4.2 ppm (m, 2H, C=C**H$_2$**), 3.4 – 3.8 ppm (m, 14H, OC**H$_2$**C**H$_2$**O, OC**H$_2$**C), 1.2 ppm (t, 3H, C**H$_3$**C).

5.3.2. Typical synthesis of SBPS

All glassware used for the polymerization was dried at 200 °C for 2 h. In addition, 2-VOES and TEGEVE were dried over $MgSO_4$ just prior to polymerization. Polymerizations were carried out in a glove box equipped with a cold-well. For copolymer 2-VOES-*ran*-TEG-2, 5.56 g of 2-VOES, 15.0 g of TEGEVE and 0.007 g of 1-isobutoxyethyl acetate initiator (synthesized as described by Aoshima and Higashimura [14]) were dissolved in 120 mL of toluene and the reaction mixture cooled to 0 °C. Next, a 2.40 mL of a 25 wt% solution of ethylaluminum sesquichloride in toluene was rapidly added to the reaction mixture to initiate polymerization. After 18 h, the polymerization was terminated by the addition of 120 mL of methanol. To purify the copolymer, the terminated reaction mixture was transferred to a 1 L separating funnel and 250 mL of dichloromethane added. The mixture was washed thrice with 100 mL of water and the polymer isolated by vacuum stripping

dichloromethane. To remove any unreacted 2-VOES, column chromatography was used with silica gel as the stationary phase and hexane as the mobile phase. Once the unreacted 2-VOES eluted from the column, the purified polymer was flushed from the column with methylene chloride and the polymer isolated by vacuum stripping the volatiles. For copolymer 2-VOES-*ran*-TEG-1, the same procedure was used with the exception that amount of 2-VOES utilized was 3.17 g.

5.3.3. Characterization of SBPS

The chemical structure of the 2-VOES-*ran*-TEG copolymers (Figure 5.1) was confirmed by ^{1}H NMR and FTIR spectroscopy (Figure 5.2 and 5.3). A ^{1}H NMR spectrum of one of the copolymers is depicted in Figure 5.2. The proton signals of the fatty acid moieties, triethylene glycol fragments, and polymer backbone are indicated in the ^{1}H NMR spectrum.

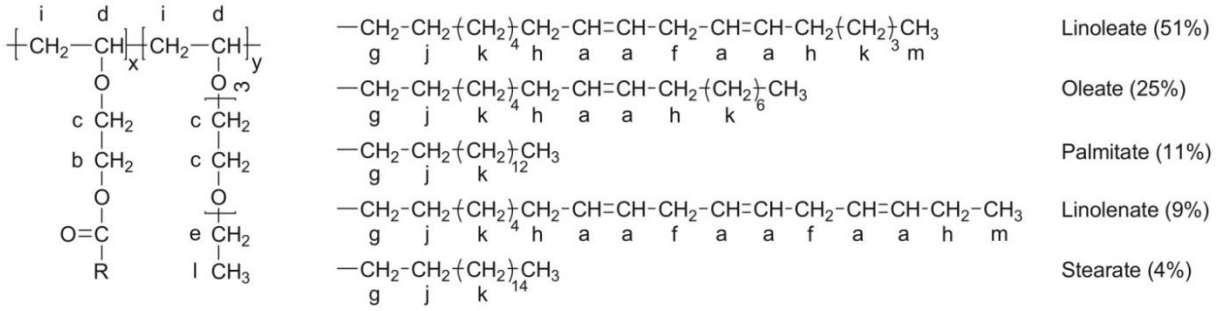

Figure 5.1. Chemical structure of 2-VOES-*ran*-TEG copolymers.

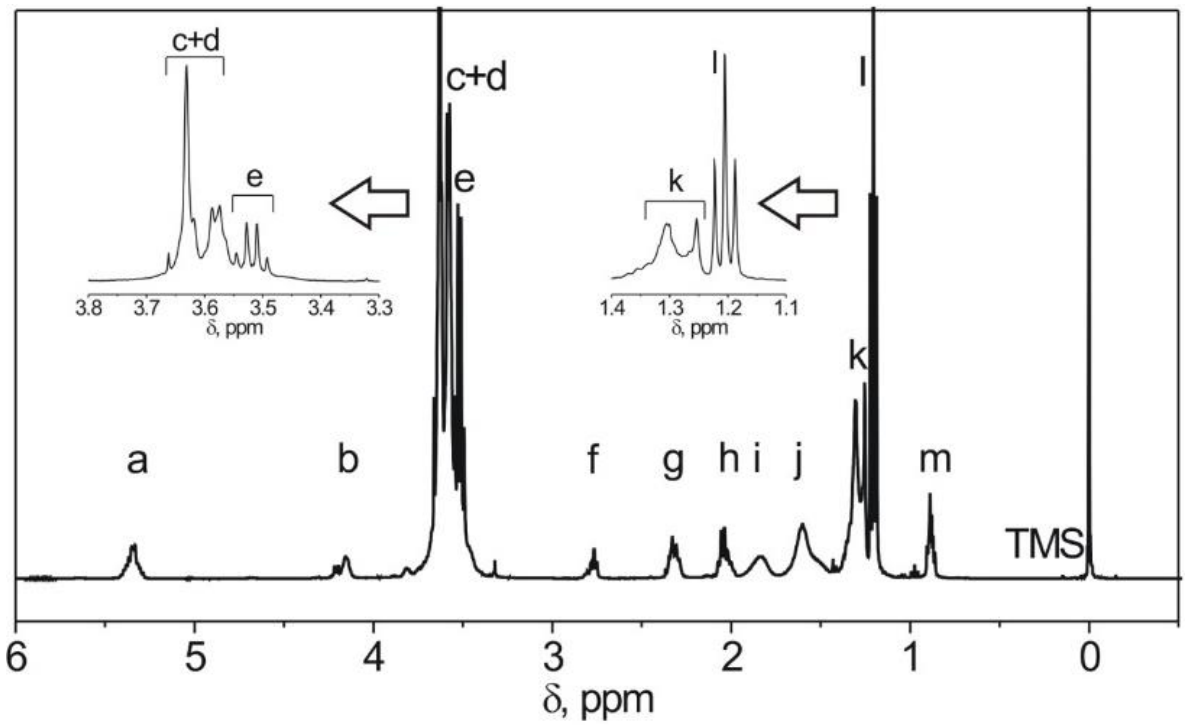

Figure 5.2. A representative ^{1}H NMR spectrum of a 2-VOES-*ran*-TEG copolymer.

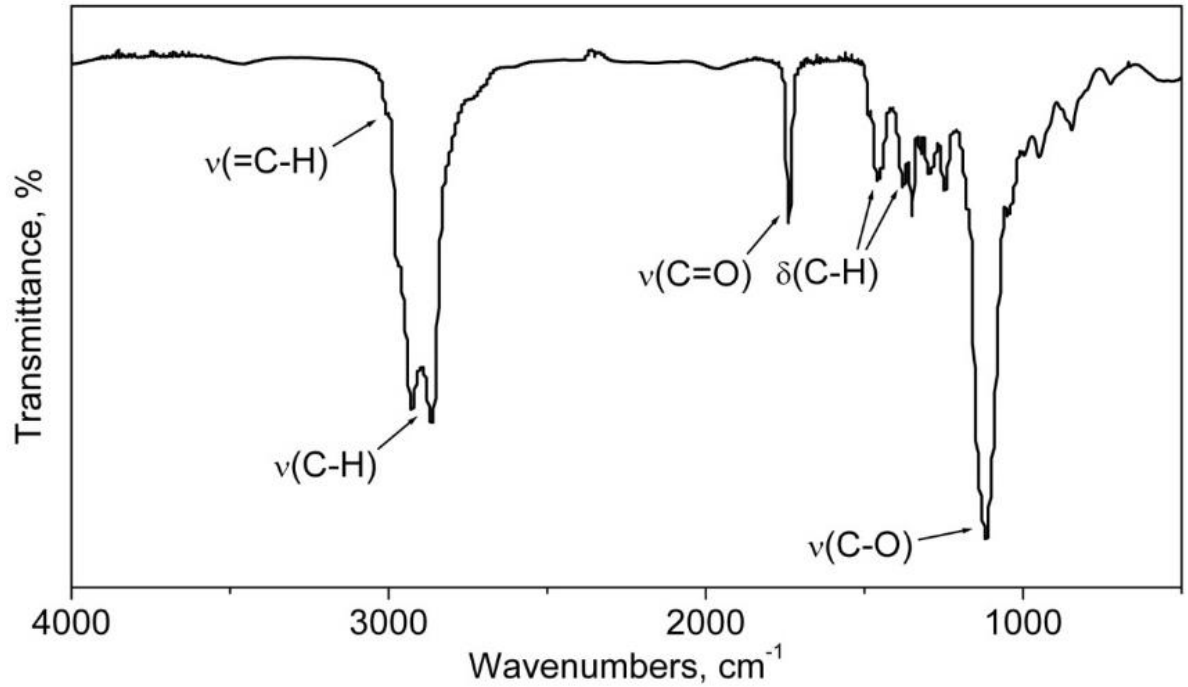

Figure 5.3. A representative FTIR spectrum of a 2-VOES-*ran*-TEG copolymer.

For the FTIR spectrum of a 2-VOES-*ran*-TEG copolymer (Figure 5.3), the intense adsorption band at 1112 cm^{-1} corresponds to C–O stretching vibrations, while the narrow band at 1733 cm^{-1} is attributed to the stretching vibrations of C=O bonds of ester fragments. The shoulder absorbance band at 3010 cm^{-1} is due to stretching vibrations of C–H bonds of the unsaturated fragments of VOES fatty acid moieties.

5.3.4. Study of SBPS critical micelle concentration

Critical micelle concentration of SBPS was measured using a pyrene fluorescent probe using a previously reported method to measure solubilization [15]. The spectra were taken using a Fluoromax-3 Fluorescence Spectrometer (Jobin Yvon Horiba, Japan) with 90° geometry and a slit opening of 0.5 nm. For fluorescence excitation spectra, λ_{em} = 390 nm was chosen. Spectra were accumulated with an integration time of 0.5 nm/s. Critical micelle concentration values were determined after fitting the semi-logarithmic plots of intensity ratio $I_{336.5}/I_{332.5}$ versus log concentration to the sigmoidal curve.

5.3.5. Solubilization of Nile Red by SBPS micelles

Micellar dyes were prepared by thin film method [16]. According to this method, 0.1 g of polymer and 0.5 mL of acetone solution of Nile red (1 mg/mL) were dissolved in 10 mL of acetone. The solvent was removed by rotary evaporation at 60°C for 1 hour to obtain a solid dye/SBPS matrix. Residual acetone remaining in the dye/SBPS matrix was evaporated overnight under vacuum. The resultant thin film was hydrated with 10 mL of Millipore water; the unincorporated dye aggregates were removed by filtration through 0.45 μm filters.

5.4. Results and discussion

The general chemical structure of the SBPSs produced is shown in Figure 5.4. The repeating unit possessing the ester group is derived from soybean oil by conducting a base-catalyzed transesterification of soybean oil with ethylene glycol vinyl ether to produce a vinyl ether possessing pendant groups containing the fatty acid esters of soybean oil. The

process for producing this vinyl ether monomer, 2-(vinyloxy)ethyl soyate (2-VOES), was developed recently by Chisholm et. al. [17]. In addition, a carbocationic polymerization process was developed for 2-VOES, which allowed for high molecular weight polymers to be produced without consuming any of the vinyl groups present in the fatty acid portion of the monomers [14].

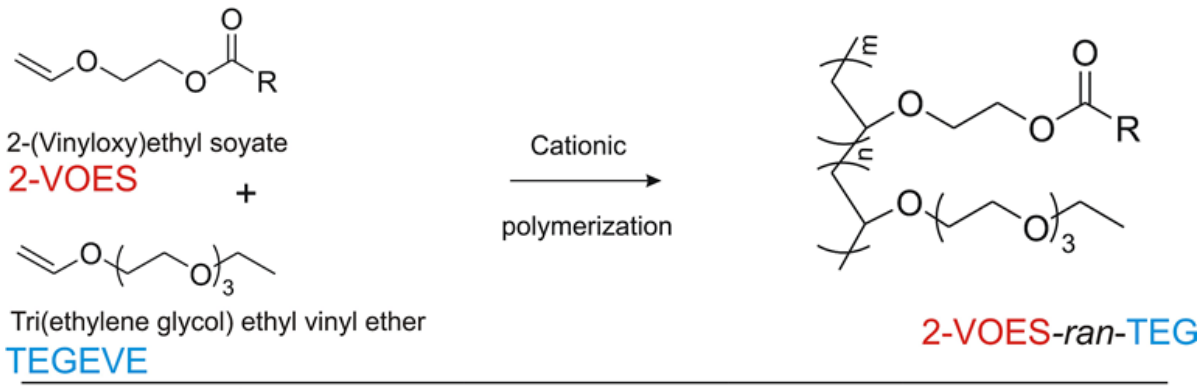

SBPS (soy-based monomer content, wt %)	M_n	PDI	CMC, mol/L
2-VOES-*ran*-TEG1 (16%)	11,500	1,48	$8{,}3 \times 10^{-7}$
2-VOES-*ran*-TEG2 (25%)	11,400	1,41	$3{,}8 \times 10^{-7}$

Figure 5.4. Synthesis and characteristics of SBPS (R – soybean oil fatty acid components).

In this work, cationic polymerization was used to synthesize two different SBPSs that differed with respect to the relative ratio of the two repeat units. For these random copolymers, the 2-VOES repeat units serve as hydrophobes while the other repeating unit, which possesses a triethylene glycol (TEG) pendant group, acts as a hydrophilic sequence in the amphiphilic SBPS macromolecules.

Figure 5.4 shows the chemical structures of the two poly(2-VOES-*ran*-TEG) copolymers used in this study. Molecular weight, polydispersity index, and critical micelle concentration of the SBPSs are shown in Table on Figure 5.4. The chemical structures of the copolymers were confirmed by ^{1}H NMR and FT-IR spectroscopy.

It is expected that SBPS macromolecules present in aqueous solution at concentrations far above critical micelle concentration will immediately form micelles, consisting of a hydrophobic interior and hydrophilic exterior (Figure 5.5, top).

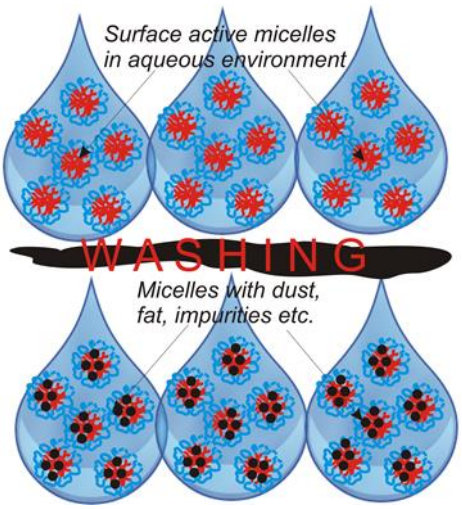

Figure 5.5. Schematic of SBPS aqueous solution cleaning the surface.

The hydrophilic exterior of SBPS micelles facilitates stability in water and the hydrophobic interior solubilizes hydrophobic dirt, oils, and other molecular debris. The size of the micellar interior and, thus, it's "capacity" for extracting the impurities, can be tuned by the length and number of 2-VOES fragments in SBPS macromolecules. Upon SBPS solution contact with a surface, the "dirt" will be extracted and accumulated into the interior of the micelles and removed from the surface (Figure 5.5, bottom) when the solution is rinsed.

Different surface activity for the synthesized SBPSs was targeted to achieve varying capacity of SBPS micelles in the solubilization of hydrophobic molecules ("dirt") in water. To confirm formation of SBPS micelles in aqueous solution, CMC values were measured using solubilization of pyrene, a well-known fluorescent probe for studying the association behavior of amphiphilic polymers [18-19]. Depending on the environment of the pyrene, a red shift of the absorption band with enhanced excitation intensity was observed due to the migration of the probe from the hydrophilic to the hydrophobic region of the polymer micelles. In our experiments, pyrene excitation spectra were monitored in the wavelength range of 300–360 nm. From the pyrene excitation spectra, the intensity ratios $I_{336.5}/I_{332.5}$ were plotted as a function of SBPS concentration (Figure 5.6).

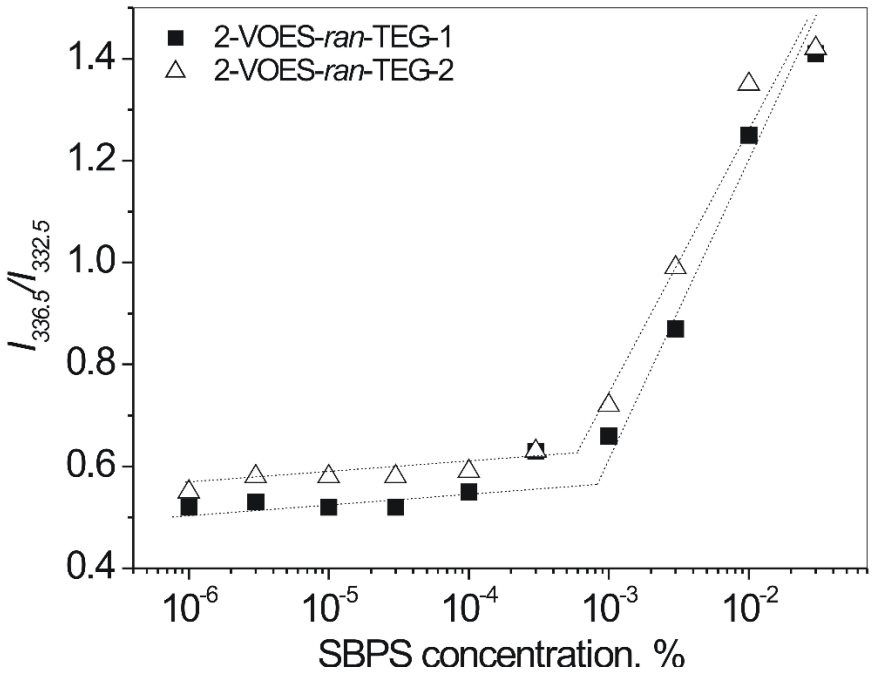

Figure 5.6. The intensity ratio $I_{336.5}$ / $I_{332.5}$ of the excitation spectra of pyrene in SBPS solutions vs. copolymer concentration.

A red shift of the fluorescence excitation spectra from 332.5 nm to 336.5 nm with an increasing SBPS concentration indicates the solubilization of pyrene within the micellar hydrophobic environment and the transfer of pyrene molecules from water to the polymer micelles. The sharp increase in the intensity ratio corresponds to the critical micelle concentration for each SBPS. The data indicate that both SBPS are surface active and form micelles. The CMC values correlate with the chemical structure of the SBPS.

Changing the ratio of hydrophilic to hydrophobic fragments in SBPS macromolecules results in a difference in recorded CMC values. The CMC increases with an increasing TEG repeat unit content in the reactive mixture from 3.8 x 10^{-7} mol/L (4.4 mg/L) for slightly more hydrophobic 2-VOES-*ran*-TEG-2 to 8.3 x 10^{-7} mol/L (9.5 mg/L) for 2-VOES-*ran*-TEG-1. In addition, the low CMC values for both SBPSs indicate that the micelles would provide good stability in solution even after strong dilution if required for preparation of special formulations.

In the next step, an ability of SBPS micelles to solubilize poorly water soluble hydrophobic materials in aqueous solutions was shown. Nile red (7-diethylamino-3,4-benzophenoxazine-2-one) is a lipophilic dye that is insoluble in water [20] and shows no absorption in optical spectroscopy measurements [21]. However, in the presence of a micellar solution of 2-VOES-*ran*-TEG-2 (1% w/v), the dye was immediately solubilized by SBPS micelles in water (Figure 5.7 A). The absorption intensity corresponding to the selected wavelength of 547 nm increases with an increasing SBPS concentration in water. This fact confirms that polymer micelles provide a microenvironment that is capable of sequestering hydrophobic molecules in water. In addition, the increasing absorption intensity recorded for solubilization carried at 37°C demonstrates that more lipophilic material has been polymer-sequestered from water at higher temperature.

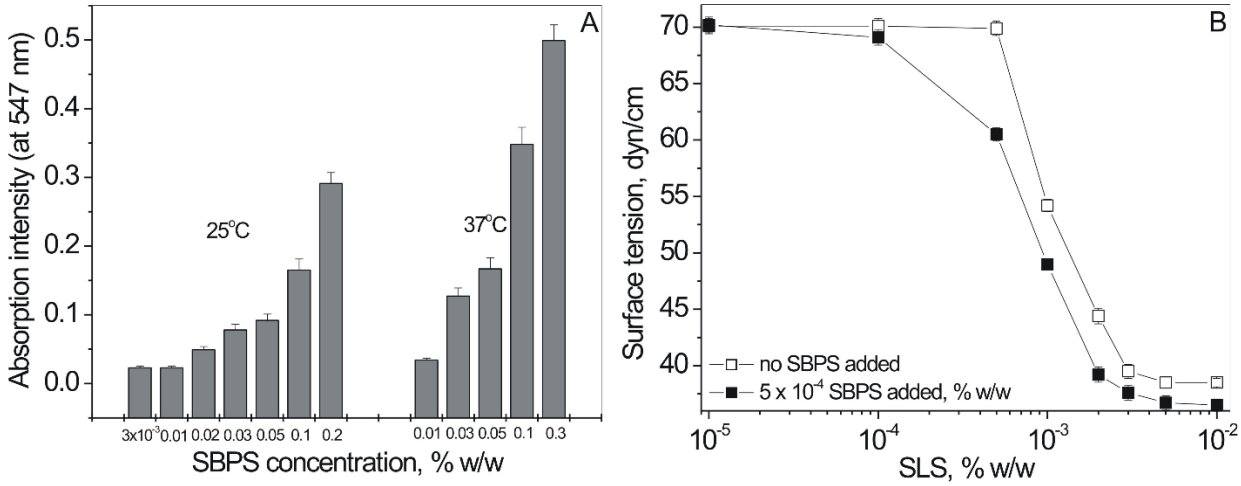

Figure 5.7. Solubilization of insoluble dye by SBPS macromolecules at 25°C and 37°C in aqueous solutions (A). Surface tension measurements of SBPS and SBPS/SLS mixture in aqueous solutions (B).

To study possible synergy of two surfactants, the low molecular weight anionic, SLS and the polymeric SBPS, the surface activity of SLS/SBPS mixtures was determined using surface tension measurements, The surface tension data showed that when a small concentration of SBPS (below CMC) is added to the SLS micellar solution (above CMC), the critical micelle concentration of the mixture shifts towards lower (in comparison to pure

SLS) values (Figure 5.7 B). A few general conclusions can be drawn from Figure 5.7 B. Firstly, there is an interaction between SLS and SBPS in aqueous solutions which indicates that surface activity of SLS can be changed by adding the SBPS already at low polymer concentration. Secondly, the critical micelle concentration of an SLS/SBPS mixture is lower than the CMC of SLS itself, showing that surface activity of SLS can be enhanced by adding the SBPS. Finally, the synergetic behavior of the surfactant mixture, SBPS and SLS, can potentially result in a decrease in the amount of SLS needed in formulations where this surfactant is used. Similar surface activity is, thus, possible by lowering the concentration of SLS when it is mixed with SBPS.

5.5. Conclusions

In summary, we report on novel, environmentally friendly soybean-based polymeric surfactants synthesized using cationic copolymerization of a monomer derived from soybean oil fatty acids and tri(ethylene glycol) ethyl vinyl ether. The ability of SBPSs to form micelles that further solubilize hydrophobic molecules has been demonstrated. Micellar "capacity" (size of micellar interior) increases with increasing polymeric surfactant concentration and temperature. The obtained results provide evidence for potential use of SBPSs as a safer replacement for low molecular weight surfactants in the solubilization of poorly soluble ingredients in cosmetics. The macromolecules can be used as both surface active agents and additives that enhance the surface activity of low molecular weight surfactants (for example, anionic sodium lauryl sulfate) in personal care products.

5.6. References

1. Rust D., Wildes S., Surfactants. A Market Opportunity Study Update. *Prepared for United Soybean Board*, **2009**.

2. Edward. F., Natural Skin Care Products Toxic Chemicals. http://www.ghchealth.com (accessed 4/26/2015).

3. Ho Tan Tai L., Nardello-Rataj V., Application of Personal Care Detergent Formulations. In *Handbook of Detergents*. Ed.: Uri Zoller, CRC press, 109-135, **2008**.

4. Hayes D. G., Kitamoto, D., Solaiman, D. K. J, Ashby, R. D., Biobased Surfactants and Detergents. Synthesis, Properties and Applications. AOCS Press, **2009**.

5. Biobased US. What are Biobased Products? **2007,** http://www.biobased.us/biobased.html (accessed 4/26/2015).

6. Santosa S. J., Palm Oil Boom In Indonesia: From Plantation to Downstream Products and Biodiesel. *Clean: Soil, Air, Water* 36, **2008,** 453-465.

7. Edser C., Is the Time Ripe for Methyl Ester Sulfonates? *Focus on Surf.* **2006,** (*Sept.*), 1-2.

8. McCoy M., Greener Cleansers. *Chem. Eng. News* **2008,** *86(3),* 15-23.

9. Butzen S., Schnebly S. High Oleic Soybean Crop Insights. **2007,** 17(17), 1-3.

10. Hamley I. W., Introduction to Soft Matter. Synthetic and Biological Self-Assembling Materials. *John Wiley and Sons, Inc*.: Hoboken, New Jersey, USA **2007**.

11. Somasundaran P., Chakraborty S., Deo P., Deo N., Somasundaran T., Contribution of Surfactants to Personal Care Products, in *Surfactants in Personal Care Products and decorative Cosmetics*; Rhein L. D., Schlossman M., O' Lenick A., Somasundaran P. CRC press, **2007,** 121-135.

12. Liu Z. S., Erhan S. Z. Soy-based thermosensitive hydrogels for controlled release systems. US 2007077298 A1, Soy-Based Thermosensitive Hydrogels for Controlled Release Systems US 20050930.

13. Biresaw G., Liu Z. S., Erhan S. Z., Investigation of the surface properties of polymeric soaps by ring-opening polymerization of epoxidized soybean oil. *J. Appl. Polym. Sci.* **2008,** 108, 1976-1985.

14. Aoshima S., Higashimura T., Living Cationic Polymerization of Vinyl Monomers by Organoaluminum Halides. 3. Living Polymerization of Isobutyl Vinyl Ether by

thyldichloroaluminum in the Presence of Ester Additives. *Macromolecules*, **1989**, 22 1009–1013.

15. Zhang X., Jackson J. K., Burt H. M. Development of amphiphilic diblock copolymers as micellar carriers of taxol. *Int. J. Pharm.* **1996,** 132, 195–206.

16. Kohut A., Sieburg L., Vasylyev S., Kudina O., Hevus I., Stafslien S., Daniels J., Kislenko V., Voronov A. In: *Amphiphiles: Molecular Assembly and Applications,* Nagarajan, R., Ed., ACS Symposium Series 1070, American Chemical Society: Washington, DC, **2011,** 205–224.

17. Alam S., Chisholm B. J., Coatings derived from novel, soybean oil-based polymers produced using carbocationic polymerization. *J. Coat. Technol. Res.* **2011,** 8 (6), 671-683.

18. Schmitz C., Mourran A., Keul H., Möller M. *Macromol. Chem. Phys.* **2008,** 209, 1859–1871.

19. Wilhelm M., Zhao C. L., Wang Y., Xu R., Winnik M. A., Mura J. L., Riess G., Croucher M. D. *Macromolecules* **1991,** 24, 1033–1040.

20. Deye J. F., Berger T. A. *Anal. Chem.* **1990,** 62*,* 615-622.

21. Hevus I., Kohut A., Voronov A. Interfacial micellar phase transfer using amphiphilic invertible polymers. *Pol. Chem.,* **2011,** 2, 2767-2770.

CHAPTER 6. EVALUATION OF SOY-BASED SURFACE ACTIVE COPOLYMERS AS SURFACTANT INGREDIENTS IN MODEL SHAMPOO FORMULATIONS[3]

6.1. Synopsis

Objective:

A new non-toxic soybean oil-based polymeric surfactant (SBPS) for personal-care products was developed and extensively characterized, including an evaluation of the polymeric surfactant performance in model shampoo formulations.

Methods:

In order to experimentally assure applicability of the soy-based macromolecules in shampoos, either in combination with common anionic surfactants (in this study, sodium lauryl sulfate, SLS) or as a single surface-active ingredient, the testing of SBPS physicochemical properties, performance and visual assessment of SBPS-based model shampoos was carried out.

Results:

The results obtained, including foaming and cleaning ability of model formulations, were compared to those with only SLS as a surfactant as well as to SLS-free shampoos. Overall, the results show that the presence of SBPS improves cleaning, foaming and conditioning of model formulations.

---

[3]Based on manuscript published in *International Journal of Cosmetic Science*, **2014,** 36 (6), 537-545.

The material in this chapter was co-authored by Andriy Popadyuk, Harjyoti Kalita, Bret J. Chisholm and Andriy Voronov. Andriy Popadyuk had primary responsibility for analytical measurements and data interpretation. Andriy Popadyuk was the primary developer of the conclusions that are advanced here. Andriy Popadyuk also drafted and revised all versions of this chapter.

Conclusion:

SBPS-based formulations meet major requirements of multifunctional shampoos - mild detergency, foaming, good conditioning, and aesthetic appeal, which are comparable to commercially available shampoos.

In addition, examination of SBPS/SLS mixtures in model shampoos showed that the presence of the SBPS enables the concentration of SLS to be significantly reduced without sacrificing shampoo performance.

6.2. Introduction

A hair shampoo is a surfactant solution with a number of different additives that cleanse the hair and scalp and enhance hair combability and appearance [1]. Surfactants are mainly responsible for cleaning, but can also provide other important benefits, such as formulation aesthetics, stability, and color, to shampoos [2]. There is extensive literature pertaining to different surfactant types, properties, and applications [3-9], including applications in cosmetics [10-11].

Surfactants usually have both hydrophobic and hydrophilic components in their chemical structure. They are effective cleaning agents because of the ability of the hydrophobic part of the molecules to interact with "dirt" (oil, sebum, etc.), while the hydrophilic fragments serve to suspend the surfactant and bound dirt in water. Depending on the nature of the hydrophilic portion of the molecule, the surfactants are classified as non-ionic (no charge), anionic (negatively charged), cationic (positively charged) and amphoteric (carry both charges once ionized) [1]. The majority of personal-care products, that foam, contain the anionic surfactants, sodium lauryl sulfate (SLS) and/or ammonium lauryl sulfate (ALS), as the main surface active ingredients [12]. SLS and ALS are highly soluble in water at a wide range of pH and temperature, insensitive to water hardness and can generate copious amounts of foam [13]. Both of these surfactants are widely available

and economical. Based on total weight, the anionic surfactant can comprise 8 ÷ 20 wt. % of the shampoo [14].

Nevertheless, no single surfactant can successfully provide proper hair cleaning, easy rinse-off, and desirable hair appearance and texture without chemical damage to the hair. As a result, both shampoos and shampoo conditioners (2-in-1) usually contain a primary surfactant and other surfactants, often referred to as secondary surfactants. The primary surfactant provides cleaning and foaming, while the secondary surfactant may serve another role such as delivery of active ingredients. Most conventional shampoos generally contain SLS in combination with ALS to improve surfactant mixture solubility and to prevent precipitation due to the presence of conditioning agents in a 2-in-1-type formulation [15].

Polymers are large molecules (i.e. macromolecules) composed of many repeating structural units linked by covalent bonds. Surface active or amphiphilic polymers usually contain a large number of hydrophilic ("water-loving") and hydrophobic ("oil-loving") sequences distributed along the polymeric backbone and form micelles by self-association of one or several amphiphilic macromolecules in aqueous solution at the critical micelle concentration (CMC). Amphiphilic polymers are commonly used in formulating personal care products [16-21]. They are often employed to enhance viscosity and consistency, to control rheology of personal care products [22], although the polymer micelles (micellar assemblies) have also been used to impart detergency, solubilization and conditioning to shampoo formulations [23, 24].

Complex shampoo formulations are in close contact with skin and other tissues of the human body, thus, their ingredients are usually deposited on contact areas for indefinite periods of time after application. In some cases, it may cause an allergic reaction, skin irritation or sensitization. For medical safety, the ingredients of shampoos need to be free of any toxic and potentially hazardous components and show no irritation to skin/eye/scalp [25]. In fact, both SLS and especially, ALS possess a degenerative effect on the cell

membranes because of theirs protein denaturing properties. As a result, SLS and ALS may deteriorate the skin's immune system by separating and inflaming outer skin layers. If exposed to these surfactants, young eyes may not develop properly, because of induced protein degradation. Although, the skin absorption of anionic surfactants is reported to be low [26], even a low concentration of toxic ingredients can pose health threats. High levels of skin penetration may occur at even low use concentration of these surfactants.

The use of natural product ingredients is currently a major trend in global cosmetics. The development of new environmentally friendly natural ingredients is more prevalent in the personal care area than in any other segment of the surfactant market. Some types of polymeric surfactants from renewable sources are, for example, alkyl polyglucosides, synthesized by the reaction between a fatty alcohol (derived from vegetable oils) and glucose [27, 28]. For these materials, surfactant properties depend on the alkyl chain length and average degree of polymerization. Other examples include surface active macromolecules from inulin (extracted from chicory roots) and amphipathic graft copolymers produced by modifying the polyfructose backbone with alkyl groups (C_4-C_{18}) [29-30].

Increasing environmental awareness and the utilization of renewable materials provide opportunities to use soybean oil for the production of new surfactants as well, in particular for the synthesis of surface active polymers. Oleo-based surfactants are commonly derived from plant oils, such as coconut and palm oil, or from animal fats, but no soy-based polymeric surfactants are widely reported and used in personal care products.

Recently, we synthesized and characterized novel soybean oil-based polymeric surfactants (SBPSs) using cationic copolymerization of a vinyl ether monomer derived from soybean oil and tri(ethylene glycol) ethyl vinyl ether. Such SBPSs are considered to be 'naturally-derived' as they are synthesized partially based on natural raw material – soybean oil, as well as 'dioxane-free' for the 1,4-dioxane is not a part of development

process. It is uncertain if such SBPS could be nominated as 'PEG-free' composition as it contains ethylene glycol units in sequences of less than 5, however there is no sign of presence of ethylene oxide, 1,-4-dioxane, heavy metals or polycyclic aromatic compounds in sourced monomer composition.

It was demonstrated that these SBPSs form micelles and effectively solubilize hydrophobic molecules in an aqueous environment. It was also shown that micellar "capacity" (size of the micellar interior) increased with increasing SBPS concentration and temperature.

To assure applicability of the environmentally friendly SBPSs in shampoos, either as a single component or in combination with the common anionic surfactant, SLS, the quality control tests including physicochemical properties, visual assessment and performance of model shampoo formulations were carried out in this study. Primary criteria for modern shampoos - cleaning and foaming, conditioning, visual/aesthetic appeal – were all investigated for shampoos based on SBPS and SBPS/SLS mixtures as a surfactant component and the results compared to commercially available shampoos.

6.3. Materials and Methods

6.3.1. Materials

Hair samples (hair tresses of up to 2 g Caucasian brown hair) (L'Oreal, Clark, U.S.A.). Before conducting experiments, the tresses were washed with 15 wt. % aqueous SLS (Sigma-Aldrich, Saint-Louis, MO). Nile Red (TCI America, Portland, OR), pyrene (Alfa Aesar, Ward Hill, MA) and copper (II) sulfate pentahydrate (VWR International, Randor, PA) used as received. Deionized water was obtained from a Millipore Milli–Q system (Millipore, Bedford, MA). Aloe Vera extract was isolated from a gel (Fruit of the Earth, Fort Worth, TX). All other reagents and solvents were supplied by Sigma-Aldrich, Saint-Louis, MO. All chemicals used were of analytical reagent grade and used without additional purification.

6.3.2. Methods

6.3.2.1. SBPS synthesis and characterization.

6.3.2.1.1. SBPS Synthesis

The soybean oil-based vinyl ether monomer, 2-(vinyloxy)ethyl soyate (2-VOES), was synthesized as described elsewhere [32]. The hydrophilic vinyl ether monomer, penta(ethylene glycol) ethyl vinyl ether (PEGEVE), was synthesized by first producing the tosylate of tri(ethylene glycol) ethyl ether (TsTEGEE) and reacting it with diethylene glycol vinyl ether (DEGVE). TsTEGEE was synthesized as follows: In a 200 mL beaker, 8 g of sodium hydroxide (NaOH) was dissolved in 40 mL of deionized (DI) water and 30 mL of tetrahydrofuran (THF). Next, in a 500 mL round-bottom flask, 22 g of tri(ethylene glycol) ethyl ether was dissolved 30 mL of THF before adding the NaOH solution. This solution was then chilled to 0 °C using an ice bath. A solution of 22.5 g of tosyl chloride in 70 mL of THF was then added dropwise to the rapidly stirring solution at a rate that allowed the reaction temperature to be maintained at 0 °C. Once the addition was complete, the reaction mixture was allowed to stir for 2 hour at 0 °C. The reaction mixture was then transferred to a separating funnel and 100 mL of ice water was added. The product was extracted with 100 mL of CH_2Cl_2, which was done twice. The two CH_2Cl_2 solutions were combined and then washed with DI water (150 mL) twice, followed by a wash with 150 mL of brine solution. The solution was then dried with $MgSO_4$ and the product isolated by vacuum stripping the solvent. The yield of TsTEGEE was 95%.

The procedure for the synthesis of PEGEVE was as follows: To a three-neck, round-bottom flask, 1.5 g of NaH was dissolved in 75 mL of THF and the flask placed in an ice-bath. The flask was equipped with an addition funnel and nitrogen inlet and outlet. Next, a solution of 6.25 g of DEGVE dissolved in 30 mL of THF was added dropwise to the rapidly stirring NaOH solution. Once the addition was complete, the solution was stirred for an hour, which was long enough to observe the cessation of hydrogen gas evolution from the

solution. The reaction mixture was then allowed to warm to room temperature, and the flask was further equipped with a condenser. Next, a solution of 15 g of TsTEGEE in 45 mL of THF was added dropwise to the reaction mixture, and the temperature was raised to 60 °C. The reaction was continued for 20 hours before cooling down to room temperature. Once cooled, 150 mL of diethyl ether and 100 mL of THF were added to the flask and the precipitate removed by filtration. The product was isolated from the solution by vacuum stripping all volatiles. The crude product was then dissolved in 100 mL of CH_2Cl_2, transferred to a separating funnel and washed with DI water twice. The solution was then dried with $MgSO_4$ before isolation by vacuum stripping the CH_2Cl_2. The yield of PEGEVE was 85%.

Using cationic polymerization, a copolymer of 2-VOES and PEGEVE was produced inside a glove box equipped with a heptane bath and chiller [33]. The initiator for the polymerization was 1-isobutoxyethyl acetate, which was produced using the method of Aoshima and Higashimura [34]. 2-VOES and PEGEVE were dried with MgSO4 prior to use, and all glassware was baked at 200 °C and allowed to cool to room temperature inside the glove box. A 500 mL round-bottom flask equipped with an overhead stirrer was charged with 3 g of 2-VOES, 17 g of PEGEVE and 74 mg of IBEA dissolved in 120 mL of dry toluene. This reaction mixture was chilled to 0 °C before the polymerization was initiated by the addition of 2.52 mL of the coinitiator, $Et_3Al_2Cl_3$ (25 wt. % in toluene). The reaction was terminated after 18 h by the addition of 120 mL of chilled methanol. The mixture was then transferred to a 500 mL separating funnel and washed twice with 50 mL of DI water. The toluene layer was dried with $MgSO_4$ before isolating the purified copolymer by vacuum stripping the toluene. The copolymer was isolated as a viscous liquid.

The molecular weight of the copolymer was determined using gel permeation chromatography (GPC) and polystyrene standards. The GPC system was from Waters Corporation and consisted of a Waters 515 HPLC pump, a Waters 2410 Refractive Index

detector and a set of two 10 μm PL-gel mixed-B columns. The column temperature was set at 40 °C, and tetrahydrofuran (THF) was used as the carrier solvent. Fourier transform infrared spectra of the SBPS copolymer were recorded using a Nicolet 8700 (Thermo Scientific) spectrometer with a resolution of 4 cm^{-1}. ^{1}H NMR spectra of the copolymer were recorded in acetone-d6 using a JEOL ECA 400 MHz NMR spectrometer.

6.3.2.1.2. SBPS critical micelle concentration

Critical micelle concentration for the SBPS was measured using a pyrene fluorescent probe and the method previously reported [35]. The spectra were taken using a Fluoromax-3 Fluorescence Spectrometer (Jobin Yvon Horiba) with 90° geometry and a slit opening of 0.5 nm. For fluorescence excitation spectra, λ_{em} = 390 nm was chosen. Spectra were accumulated with an integration time of 0.5 nm/s. Critical micelle concentration values were determined after fitting the semi-logarithmic plots of intensity ratio $I_{336.5}/I_{332.5}$ versus log concentration to the sigmoidal curve.

6.3.2.1.3. Solubilization of Nile Red (hydrophobic dye) by SBPS micelles

Micellar dyes were prepared by the thin film method [36]. According to this method, 0.1 g of SBPS and 0.5 mL of an acetone solution of Nile red (1 mg/mL) were dissolved in 10 mL of acetone. The solvent was removed by rotary evaporation at 60 °C for 1 hour to obtain a film of the dye dispersed in the SBPS. Residual acetone remaining in the dye/SBPS mixture was evaporated overnight under vacuum. The resultant thin film was hydrated with 10 mL of Millipore water and dye aggregates removed by filtration through a 0.45 μm filter. Optical spectra were recorded using a Cary UV-vis-NIR optical spectrometer.

6.3.2.2. SBPS-based model shampoo formulations and evaluation

6.3.2.2.1. Model shampoo preparation

Two groups of model shampoos were used in this study (Table 6.1). Model formulations of Group 1 comprise only deionized water and a surfactant ingredient, either SBPS or a SBPS/SLS mixture. The model formulations of Group 2 were prepared by adding

the most frequently used commercial shampoos additives (Table 6.1) to Group 1 formulations. In testing, Group 1 formulations were employed to study the effect of SBPS as a surfactant on physicochemical properties and performance. To compare these properties with commercially available shampoos (Herbal shampoo, Nature's Gate, Chatsworth, Ca, and Jonson's Baby Shampoo, J&J), Group 2 formulations were applied.

Table 6.1. The model shampoo formulations used. The values in the table represent weight percent.

	Group 1					**Group 2**		
	1A	**1B**	**1C**	**1D**	**1E**	**2A**	**2D**	**2E**
Deionized water	90	90	90	90	90	72.3	72.3	72.3
SLS	10	9	7.5	5	–	10	5	–
SBPS	–	1	2.5	5	10	–	5	10
Base composition*	–	–	–	–	–	8/8/1/ 0.5/0.2	8/8/1/ 0.5/0.2	8/8/1/ 0.5/0.2

*Base composition (as listed): cocamidopropyl betaine, Polyquaternium-7, xanthan gum, 1,3-bis(hydroxymethyl)-5,5-dimethylimidazolidine-2,4-dione (DMDM Hydantoin), and 2,2',2'',2'''-(ethane-1,2-diyldinitrilo)tetra acetic acid (disodium EDTA).

6.3.2.2.2. Cleaning action

The Thompson method was used to evaluate cleaning ability of the model formulations [37]. For this purpose, sample hair tresses were initially soiled using artificial sebum. The artificial sebum was similar to actual sebum [37]: 5 wt. % squalene, 5 wt. % cholesterol, 6 wt. % stearic acid, 7 wt. % linoleic acid, 12 wt. % oleic acid, 12 wt. % paraffin, 13 wt. % palmitic acid, 20 wt. % coconut oil, 20 wt. % olive oil. Before testing, each hair tress was washed with 15 wt. % aqueous SLS solution and dried in an oven to a constant weight, then equilibrated at room temperature for 12 h.

Artificial sebum was deposited onto hair tresses from a 10 wt. % hexane solution by immersion of each tress into a beaker with sebum solution for 1 h. After immersion, excess solution was gently squeezed from the hair tress and the tress dried using a laboratory heat-gun operating at 40 °C. After the tresses were equilibrated at room temperature, each tress was treated with 10 ml of Millipore water and subsequently with 2 ml of a 10 wt. % aqueous solution of a model shampoo formulation using a thumb-rubbing washing procedure (adapted from [37]). After the washing, tresses were rinsed with 3 x 500 ml of deionized water, dried using a laboratory heat-gun operating at 40 °C and equilibrated at room temperature. Five parallel tests were performed for each hair tress. For every experimental batch, a control sample was produced. Production of the control sample involved following same procedure but without treatment with a model shampoo formulation. Cleaning action results were evaluated gravimetrically and calculated using the following equation:

$$\varphi = \frac{M_w - M_w^0}{M_d} \cdot 100\% \tag{6.1}$$

where M_w and M_w^0 is the weight of the sebum washed off the treated hair tress and the control sample, respectively. M_d is the weight of initially deposited sebum.

SBPS-based model shampoo foaming ability

SBPS-based model shampoo foaming ability was evaluated using the Ross and Miles test [38], which has been widely accepted for measuring foaming performance of shampoos, and the Hart and De George method [39], which includes foam drainage time. Consistent with the Ross and Miles technique, 200 ml of a 1 wt. % aqueous solution of each model formulation was carefully placed into a 500 ml graduated cylinder. Next, 50 ml of the same solution was dropped to the cylinder from a fixed height using a funnel. Foaming ability was evaluated by measuring the height of the foam generated in the cylinder. To

determine effect of sebum on foam formation, 0.5 g of olive oil was added and foaming ability in presence of the oil compared to the foaming without sebum.

Additionally, consistent with the Hart and De George method, a kitchen blender was used to generate foam. 50 ml of a 1 wt. % aqueous solution of each model formulation was poured in a 500 ml plastic beaker and subsequently beaten with a blender at 700 rpm for 3 minutes. Formation of a thick, creamy foam was evaluated gravimetrically by weighing 50 ml of the foam. To determine foam drainage, 50 ml of the blender-generated foam was placed inside a sintered glass funnel and the time required for the material to pass through the funnel into a graduated cylinder determined.

6.3.2.2.3. Dirt dispersion

One drop of ink was added to 10 ml of a 10 wt. % aqueous shampoo solution in a 10x100 mm glass test tube. Samples were tightly closed and shaken by hand for 15 seconds. Tinting severity of the foam produced in each test tube was visually determined and graded on a scale: slight-moderate-severe.

6.3.2.2.4. Protein loss measurement

To determine hair protein loss caused by shampooing, a modified version of the Lowry method was employed [40]. First, for calibration, eleven sets of 10 x 100 mm glass test tubes were washed and dried in an oven at 100 °C for 4 h. To each test tube, an aliquot of bovine serum albumin (BSA, 1 mg/ml) was added. Aliquot sizes were 0, 10, 20, 30, 40, 50, 60, 70, 80, 90 and 100 µl. 2 ml of incubation mixture (48 ml 2 wt. % Na_2CO_3 in 0.1 N NaOH, 1 ml 1 wt. % NaK tartrate in H_2O, 1 ml 0.5 wt. % $CuSO_4$ in H_2O) were added to each tube and incubated for 10 min at room temperature. At this point, 0.2 ml of phenol reagent (50 % v/v Folin-Phenol in H_2O) was added to each test tube, immediately vortexed and incubated for an additional 30 minutes. Absorbance of the samples was recorded at 600 nm using a Cary UV-vis-NIR spectrometer to build a calibration plot. Each sample was measured in triplicate.

Further, 2 ml of a 10 wt. % aqueous solution of each model formulation (containing Aloe Vera extract as a hair conditioner) was applied onto 2 g of hair tress. Each tress was subsequently washed using a thumb-rubbing technique, rinsed with deionized water three times (3 x 500 ml) and combed (wet) using a nylon comb with 8 teeth/cm, 100 times. For every 10 passes through the hair tress with the comb, the comb was dipped into 50 ml of deionzed water to rinse the proteins removed from the hair. After each 20 passes with the comb, the comb and tress were rinsed in the same 50 ml of water and tress was turned to change the side of the tress from subsequent combing. After completing the combing process, 1 ml of the protein colloid produced was collected. To determine protein concentration, the modified Lowry method, described above, was employed.

6.3.2.2.5. Rheological evaluation

Viscosity was determined using a Brookfield CAP 2000 viscometer, cone #3, at 2000 rpm and constant temperature.

6.3.2.2.6. Visual inspection

All formulations prepared were visually inspected in terms of their clarity, fluidity and ability to generate foam by shaking.

6.4. Results and Discussion

6.4.1. SBPS surface activity

The chemical structure of the SBPS used in this study is shown in Figure 6.1. The repeat units derived from 2-VOES possess long aliphatic chains derived from soybean oil that are hydrophobic, while the repeat units derived from PEGEVE possess hydrophilic ethylene glycol units.

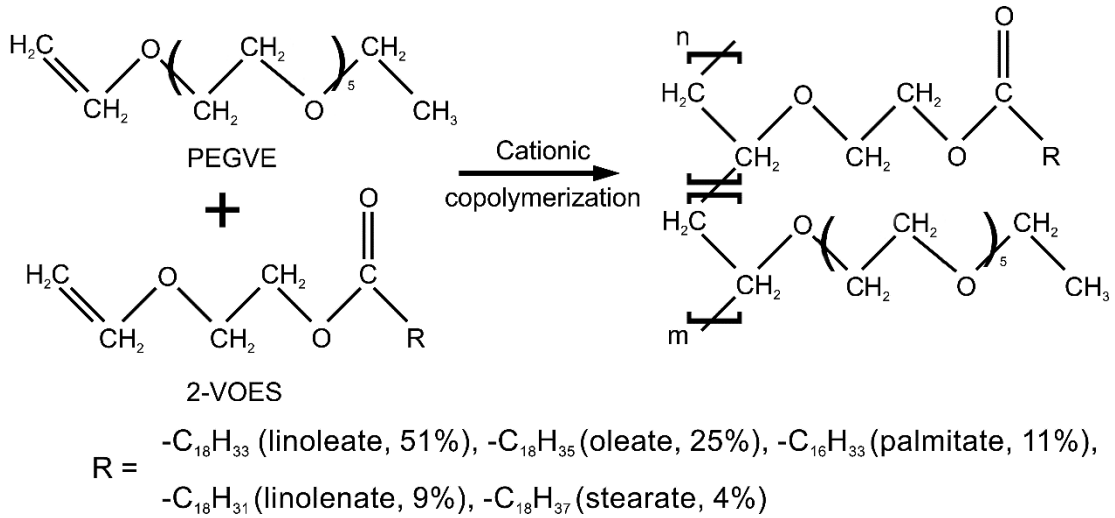

Figure 6.1. Synthesis of the SBPS copolymer (R – soybean oil fatty acid components).

The random copolymer was synthesized using cationic polymerization, and the chemical structure of the poly(2-VOES-ran-PEGEVE) copolymer was confirmed by ^{1}H NMR and FTIR spectroscopy. The ^{1}H NMR spectrum of the copolymer is depicted in Figure 6.2 A. Proton signals from 2-VOES-derived pendant groups, PEGEVE-derived pendant groups, and the polymer backbone are indicated in the ^{1}H NMR spectrum. For the polymerization, the weight ratio of 2-VOES to PEGEVE used was 15/85. Using the peak integration values from the ^{1}H NMR spectrum, it was determined that the composition of the copolymer was the same as the monomer feed ratio, i.e. the content of 2-VOES repeat units was 15 weight percent. For the FTIR spectrum of the poly(2-VOES-ran-PEGEVE) copolymer (Figure 6.2 B), the intense adsorption band at 1112 cm^{-1} corresponds to C–O stretching vibrations, while the narrow band at 1733 cm^{-1} is attributed to the stretching vibrations of C=O bonds of the ester groups. The shoulder absorbance band at 3010 cm^{-1} is due to stretching vibrations of C–H bonds associated with unsaturation in pendant groups derived from 2-VOES.

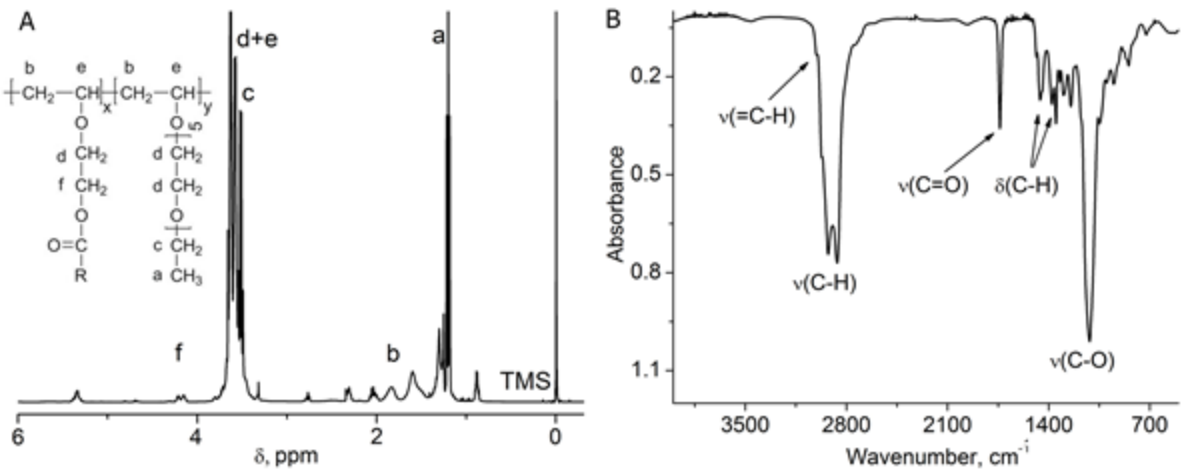

Figure 6.2. The ^{1}H NMR (A) and FTIR (B) spectra of the poly(2-VOES-ran-PEGEVE) copolymer.

To confirm formation of SBPS copolymer micelles in aqueous solution, the CMC was determined using the solubilization of pyrene technique [36] and surface tension measurements. A red shift of the absorption band with enhanced excitation intensity was observed in optical spectra measurements due to the migration of the probe from the hydrophilic to the hydrophobic region of the polymer micelles, depending on the environment of the pyrene (Figure 6.3 A). In our experiments, pyrene excitation spectra were monitored in the wavelength range of 300–360 nm. The intensity ratio ($I_{336.5}/I_{332.5}$) was plotted as a function of SBPS concentration from the pyrene excitation spectra. It is expected that once the copolymer micelles are formed in the aqueous solution, the hydrophilic exterior of the micelles provides stability in water and the hydrophobic interior solubilizes hydrophobic species, for example, dirt, oils, etc. As it was shown in Chapter 5, the size of the micellar interior and, thus, it's "capacity" for extracting the impurities, can be tuned by the number of 2-VOES sequences in the SBPS macromolecules. Upon contact of the SBPS solution with a surface, the "dirt" is extracted and accumulated into the interior of the micelles and can be removed from the surface when the solution is rinsed.

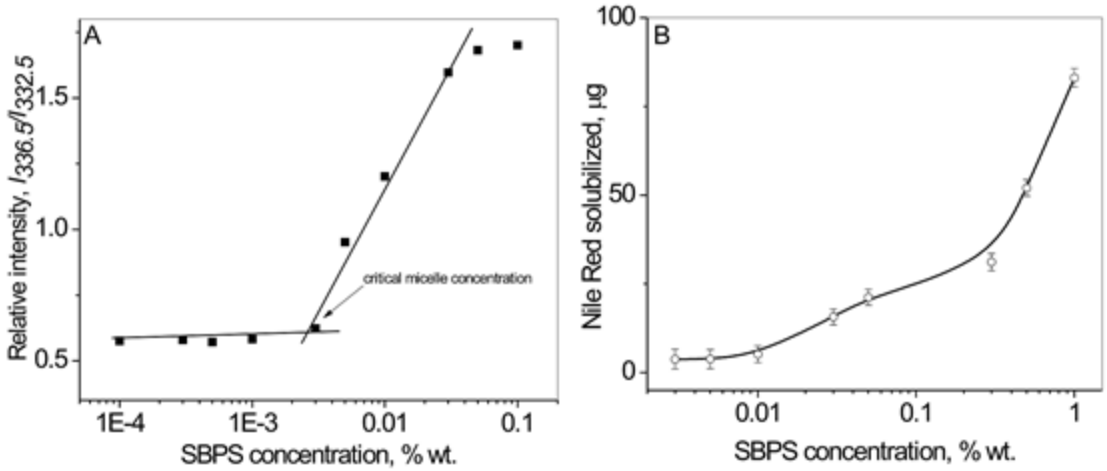

Figure 6.3. The intensity ratio $I_{336.5}$ / $I_{332.5}$ of the excitation spectra of pyrene in SBPS solutions vs. SBPS concentration (A). Solubilization of the insoluble dye by SBPS macromolecules at 25 °C in aqueous solution (B).

Molecular weight, polydispersity index, and CMC (using both pyrene solubilization and surface tension measurements) of the SBPS are shown in Table 6.2.

Table 6.2. Chemical characteristics of the SBPS used for the study.

	M_n	PDI	CMC, mol/L
2-VOES-*ran*-PeEG	12,327	1,45	2.5×10^{-6} * 2.5×10^{-7} **

* using surface tension study,
** using solubilization study.

Next, we determined an ability of SBPS micelles to solubilize poorly water-soluble hydrophobic materials in aqueous solution. Nile red (7-diethylamino-3,4-benzophenoxazine-2-one) is a lipophilic dye that is insoluble in water [41] and provides no absorption in optical spectroscopy measurements of aqueous systems [42]. However, in the presence of a SBPS solution (1% w/v), the dye is immediately solubilized by the SBPS micelles in water (Figure 6.3. B), which confirms the surface activity of SBPS and its potential as a polymeric surfactant. The absorption intensity at 547 nm, which is associated with Nile red, increases with increasing SBPS concentration in water. This fact confirms that polymer micelles provide a microenvironment that is capable of sequestering hydrophobic molecules in water.

6.4.2. Evaluation of model shampoo formulations based on SBPS

To ensure applicability of the novel SBPS macromolecules as polymeric surfactants, testing of physicochemical properties, performance and appearance of SBPS-based model formulations was conducted. This study was carried out for both single surfactant formulations, where the SBPS served as the only surface active ingredient, as well as surfactant mixtures of SBPS and SLS. Both groups of model shampoos were compared to commercial shampoos. The commercial shampoos were the herbal shampoo from Nature's Gate) and Johnson's Baby Shampoo from Johnson & Johnson.

6.4.2.1. Foaming evaluation

Foam generation and foam stability are important criteria to shampoo consumers, even though foam itself has little to do with a cleaning ability [43]. In our study, we applied two different techniques for evaluating foaming ability, namely, the Ross and Miles method and the Hart and De George method. Although the Ross and Miles method has been widely criticized, it still remains a fast and reproducible method that reflects shampoo performance. However, this test produces "airy" foam that does not represent the foam that results during the use of the shampoo by the consumer [44]. In contrast, the Hart and De George blender method results in a thick and creamy foam that is representative of that observed during the shampooing of hair.

Model formulations 2A (10 wt. % SLS), 2D (10 wt. % of a 1:1 mixture of SLS and SBPS) and 2E (10 wt. % SBPS) were chosen to study foaming and foam stability. As seen from Figure 6.4, the model shampoo based on SLS (i.e. 2A) provided the highest foaming ability both in the absence and in the presence of artificial sebum (olive oil). However, the presence of sebum reduced the foaming ability of formulation 2A while the foaming ability of the two SBPS-containing formulations (i.e. 2D and 2E) were essentially unaffected by the sebum.

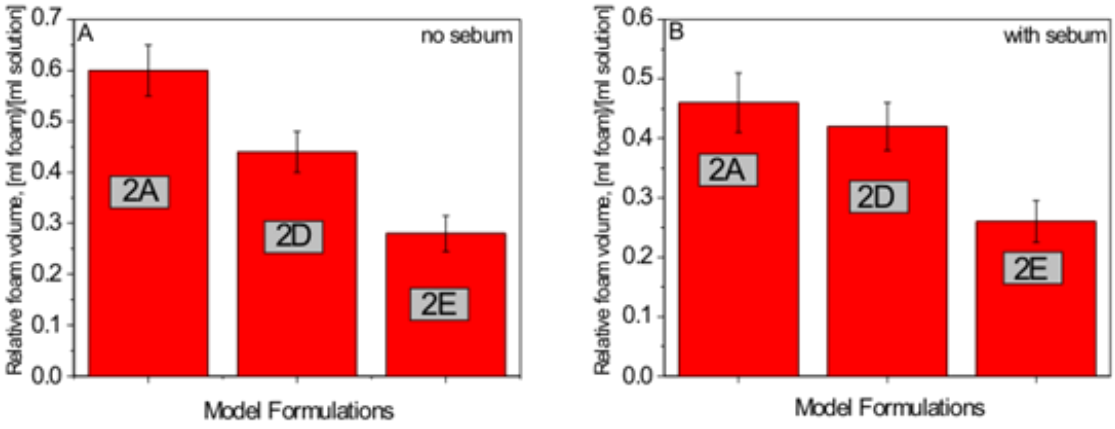

Figure 6.4. Foaming ability as evaluated using the Ross and Miles technique of three model formulations with no added sebum (A) and in the presence of sebum (olive oil) (B).

Using the Hart and De George method, all of the formulations investigated showed similar foaming performance (Figure 6.5 A), indicating that the SBPS can successfully replace almost half of common anionic detergent (on a weight basis) without decreasing its foaming ability.

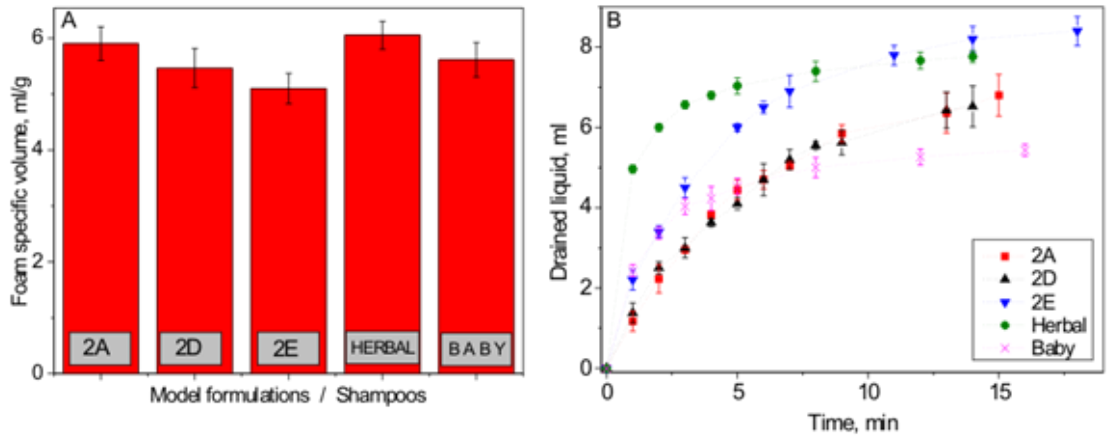

Figure 6.5. Foaming ability as evaluated using the Hart and De George method (A), and foam drainage (B) of three model shampoos and two commercially available shampoos.

Moreover, the presence of the SBPS in a mixture with SLS improves the stability of the foam produced as indicated by the foam stability results shown in Figure 6.5 B.

6.4.2.2. Dirt dispersion

The foaming study was followed by measuring the ability of the SBPS-based formulations to disperse dirt. For this purpose, ink was used as a model for dirt. The ink was dispersed in the Group 2 samples and commercial shampoos. If the shampoo concentrates the ink in the foam, it is considered to be of a low quality. Ideally, the ink should remain in solution where it is easy to rinse away [45]. As shown in Table 6.3, almost no dirt was present in the foam. Interestingly, one of the commercial shampoos displayed the poorest performance of all compositions evaluated.

Table 6.3. Data pertaining to the appearance of foam after exposure of the shampoo to dirt.

Model formulation	Foam tinting by ink
2A	Slight
2D	Slight
2E	Slight
Johnson's Baby	Slight/Moderate
Herbal	Moderate

6.4.2.3. Viscosity testing

Shampoo viscosity is important in defining many properties, such as clarity, ease of flow from the container, stability in the container, spreading etc. [46]. There are also both psychological and practical values of having relatively high viscosity of shampoos, such as the inhibition of dripping through the fingers and slow pouring into the palm of the hand.

We compared the viscosity of the model SBPS-based formulations with commercial shampoos in order to see how the presence of the SBPS impacts viscosity. As shown in Table 6.4, increasing SBPS content within the Group 2 samples (i.e. replacing the SLS with

SBPS) results in a considerable increase of viscosity. The viscosity of SBPS-based formulation (2E) was found to be similar to that of the two commercial shampoos.

Table 6.4. Viscosity of model formulations compared to commercial shampoos.

Formulation	**2A**	**2D**	**2E**	**Herbal**	**J&J Baby**
Viscosity, Ps	0.0468	0.256	0.309	0.135	0.308

6.4.2.4. Protein loss from hair after treatment with different formulations and conditioner

Since hair is a protein-containing material, it was anticipated that possible damage to hair by combing could be measured by determining the amount of protein abraded from the hair after shampooing [47]. This technique can also potentially demonstrate the conditioning/protective efficacy of the modern conditioning shampoos (2-in-1 shampoo and conditioner). In this study we determined if the presence of SBPS in model formulations has an impact on the amount of protein removal caused by combing [48]. In addition to evaluating the effect of SBPS on protein removal, the effect of Aloe Vera extract as a hair conditioning treatment was also evaluated. To determine the effect of the treatment, hair tresses were shampooed with Group 1 formulations with and without Aloe Vera and the protein loss resulting from combing determined using a modified version of the Lowry method.

Table 6.5 indicates that the presence of SBPS in a shampoo formulation decreases the harsh influence of SLS on the hair cuticle. It appears that the presence of SBPS promotes a conditioning effect as indicated by the reduction in protein loss from treated hair tresses. The positive influence of the SBPS is even more pronounced when the common conditioning agent, Aloe Vera extract, is present in the shampoo. Overall, these results indicate that SBPS reduces damage to the hair during wet combing. The shampoo that resulted in the greatest combing-induced loss of protein was the formulation containing only SLS as the surfactant ingredient (i.e. 1A).

Table 6.5. The effect of shampoo composition on protein loss resulting from combing.

Treatment	Protein Loss, μg protein /g Hair	Relative Protein Loss (vs. Control)
Control*	1243	–
1A	1445	+ 16.25 %
1D	1280	+ 2.97 %
1E	1138	- 8.45 %
1A + Aloe Vera	1240	- 0.24 %
1D + Aloe Vera	1170	- 5.87 %
1E + Aloe Vera	946	- 23.89 %

* Hair treated with deionized water only

6.4.2.5. Cleaning ability

The Thompson method was used to evaluate the cleaning ability of SBPS-based model shampoos (Group 1 formulations). Briefly, the hair tresses were first soiled with sebum dissolved in hexane and then washed using the different model shampoos. After drying the shampooed tresses, the remained sebum was determined gravimetrically and the cleaning power calculated.

Figure 6.6 A shows cleanability data for model shampoos based on SLS, various mixtures of SLS/SBPS and SBPS as the surface active ingredient. It can be clearly seen that combining SLS and SBPS as the surface active component, it is possible to optimize and improve cleaning performance. As seen from the results, there is a significant difference in the amount of sebum removed between the different Group 1 formulations. The maximum cleaning ability was obtained when SLS/SBPS ratio was 9/1 ratio.

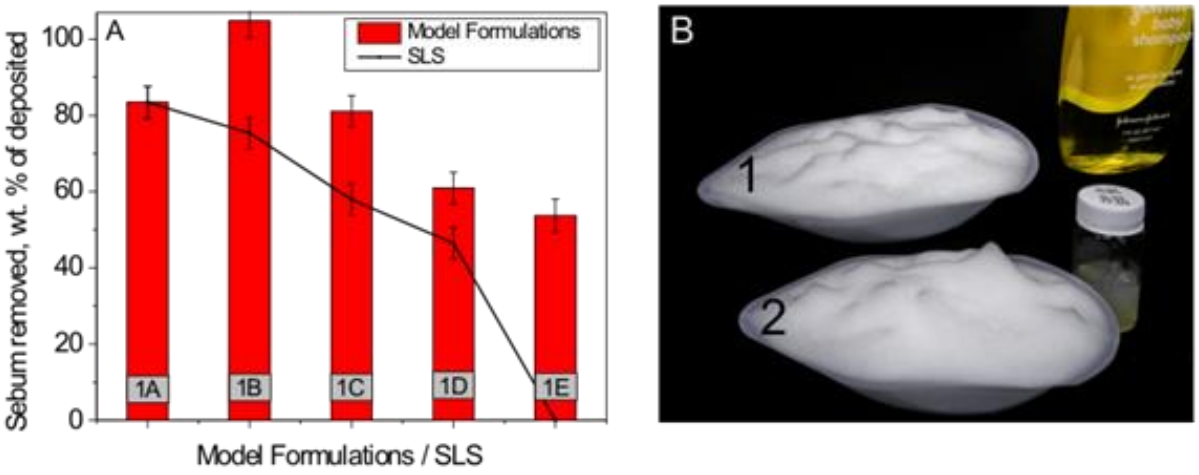

Figure 6.6. Cleaning ability of the different model shampoos determined using the Thompson method (A), and visual appearance of the 9/1 SLS/SBPS-based shampoo (1B) and the foam (B) produced from the (1) Johnson's Baby and (2) SBPS-based (2E) shampoos.

Finally, the visual assessment of both Group 1 and Group 2 formulations was performed. Figure 6.6 B shows the appearance of shampoo formulation 1B (9/1 SLS/SBPS) and the foam produced using the foaming test as well as the foam produced by Johnson's Baby Shampoo used for comparison. The results of visual inspection indicate that the formulations do not change their physical appearance over 6 months of storage at room temperature. The model shampoos remain light yellow and transparent over the 6 month period. In addition, the clarity, fluidity and ability to generate foam by shaking does not change over this period.

Overall, the results show that SBPS positively influences cleaning and foaming ability, as well as the physicochemical properties of model shampoo formulations. The SBPS-based formulations meet major requirements of multifunctional shampoos and are comparable with commercial shampoos.

6.5. Conclusions

A new non-toxic, environmentally friendly soybean oil-based polymeric surfactant was produced and extensively studied for potential application as a surface active ingredient for shampoos. The hydrophobic portions of these surface active macromolecules were derived from soybean oil, while the hydrophilic portions were based on ethylene glycol units. Using both surface tension measurements and fluorescence spectroscopy, high surface activity and the formation of micelles for the SBPS in water was demonstrated.

In order to determine the utility of the SBPS in shampoos, either in combination with SLS or as a single surface active ingredient, the physicochemical properties, cleanability, foaming characteristics, viscosity and appearance of model SBPS-based shampoos were characterized and compared to model shampoos based on SLS as the sole surface active ingredient as well as commercially available, SLS-free part shampoos.

Overall, the results showed that the presence of SBPS improves foaming as well as hair cleaning and conditioning of model formulations. As a result, SBPS-based formulations meet major requirements of multifunctional shampoos, including mild and efficient detergency, foaming comparable with existing retail products, good conditioning, and aesthetic appeal. In general, the model SBPS-based shampoos were found to be comparable with the commercial shampoos used for the study.

By investigating mixtures of SBPS and SLS in model shampoos, it was shown that the presence of the SBPS enabled the concentration of the anionic surfactant, SLS, to be significantly reduced without sacrificing shampoo performance. This result is significant and demonstrates the utility SBPS in shampoos.

6.6. Acknowledgments

The work was supported by the United Soybean Board (USB #1425, #2425) and North Dakota Soybean Council.

6.7. References

1. Butler H. Poucher's Perfumes. Cosmetics and Soaps, Kluwer Academic Publishers, **2000,** 289-306.

2. Mirajkar Y. R. K., Applications of Surfactants in Shampoos, in Handbook of Detergents. Part E: Applications, Ed. U. Zoller, CRS Press: Boca Raton, **2008,** 151-179.

3. Dawar N., Parker P., Marketing universals: Consumers' use of brand name, price, physical appearance and retailer reputation as signals of product quality. *J of Market.* **1994,** 58, 81–95.

4. Creusen M. E. H., Schoormans J. P. L., The different roles of product appearance in consumer choice. *J. Prod. Inn. Man*. **2005,** 22, 63–81.

5. Schramm L. L., Personal care product applications in Emulsions, Foams, and Suspensions. Wiley-VCH: Weinheim, **2006,** 337–346.

6. Baginski L., Barnaby A., Containers Capture Consumer Convenience, *Packaging World Magazine*. **2000,** 60.

7. Product Usage Instructions, Chinese Herb Stimulating Shampoo. www.lamasbeauty.com (accessed 9/27/2014).

8. Furterer R., Naturia Dry Shampoo. www.drugstore.com (accessed 9/27/2014).

9. Home-made Shampoos, Conditioners, Rinses, Baby Shampoo, Chamomile Shampoo. www.greenspun.com (accessed 9/27/2014).

10. Barson D. C., Using consumer research in the development and restaging of personal care products. In *Surfactant in Personal Care Products and Decorative Cosmetics*, Surf. Sci. Ser., 135 Eds. Rhein L.D., Scholssman M., O'Lenick A. and Somasundaran P., Marcel Dekker: New York, **2007,** 95–105.

11. Lin C.-F., Quality-delivery system: A conceptual framework of attribute level-value linkages. *Total Quality Management & Business Excellence*, **2003,** 14, 1079–1092.

12. Edward F., Natural Skin Care Products Toxic Chemicals. www.ghchealth.com (accessed 9/27/2014).

13. Ho Tan Tai L., Nardello-Rataj V., Application of Personal Care Detergent Formulations, in Handbook of Detergents, Part E: Applications. Ed. U. Zoller, CRS Press: Boca Raton, **2008,** 109-135.

14. Reich C., Chupa J., Hair Shampoos. In *Harry's Cosmeticology*, 8th ed. Ed. Rieger M., Chemical Publishing Company: New York, **2000**.

15. Shore S., Berger R., Alcohol and Ether Alcohol Sulfates. In *Anionic Surfactants, Surfactants Science Series*, 7 Ed. Linfield, W., Marcel Dekker: New York, **1976,** 135–217.

16. Bertleff W., Baur R., Gumbel H., Welch M., Schaumarme tenside. In German. *In Weakly foaming surfactants*, SÖFW-Journal, **1997,** 123, 222–233.

17. Nace V.M., Ed., Nonionic Surfactants: Polyoxyethylene Block Copolymers, *Surfactant Science Series*, 60, Marcel Dekker: New York, **1996**.

18. Bolich Jr R.E., Aylor R.B., U.S. Patent 3928251, **1975**.

19. Cardin C.W., Davis J.I., Hart J.L., Schmidt D.G., Antidandruff shampoo compositions. U.S. Patent 5104645, **1992**.

20. Walele I.I., Scarangella N.J., Ansaldi A., Andrews A.M., Benzoate esters of polyalkoxylated block copolymers. U.S. Patent 5271930, **1993**.

21. Andrews J.F., Kure J.T., Medicated shampoo. U.S. Patent 5378731, **1995**.

22. Somasundaran P., Chakraborty S., Qiang Q., Deo P., Wang J., Zhang R. Surfactants, polymers, and their nanoparticles for personal care applications. *J. Cosmet. Sci.* **2004,** 55, S1-S17.

23. Hamley I.W. Introduction to Soft Matter. Synthetic and Biological Self-Assembling Materials, Wiley-VCH: Weinheim, **2007**.

24. Somasundaran P., Chakraborty S., Deo P., Deo N., Somasundaran T., Contribution of Surfactants to Personal Care Products, in Surfactants in Personal Care Products and Decorative Cosmetics. Ed. Rhein L.D., Schlossman M., O' Lenick A., Somasundaran P. CRC press, **2007,** 121-135,.

25. Tadros T., Colloid aspects of Cosmetic Formulations with Particular Reference to Polymeric Surfactants. In *Colloids in Cosmetics and Personal Care*, Vol. 4, Wiley-VCH: Weinheim, **2008**.

26. Reich C., Hair cleaners. In *Surfactants in Cosmetics.* Eds. Reger M.M., Rhein L.D., Marcel Dekker: New York, **1997,** 357-384.

27. Tadros T.F., Applied Surfactants, Wiley-VCH: Weinheim, **2005**.

28. Holmberg K., Jonsson B., Kronberg B., Lindman B., Surfactants and Polymers in *Aqueous Solutions*, John Wiley & Sons Ltd.: Chichester, **2003**.

29. Stevens C. V., Meriggi A., Persiterpoulou M. et al., Polymeric surfactants based on inulin, a polysaccharide extracted from chicory. 1. Synthesis and interfacial properties. *Biomacromolecules*, **2001,** 2, 1256-1259.

30. Hirst E.L., McGilvary D. I., Percival E. G., Studies on fructosans. Part. I. Inulin from dahlia tubers. *J. Chem. Soc.* **1950,** 1297-1302.

31. Alam S, Kalita H., Kudina O., Popadyuk A., Chisholm B. J., Voronov A., Soy-Based Surface Active Copolymers as Safer Replacement for Low Molecular Weight Surfactants. *ACS Sus. Chem. & Eng.* **2013,** 1, 19-22.

32. Alam S., Chisholm B. J. Coatings derived from novel, soybean oil-based polymers produced using carbocationic polymerization. *J. Coat. Technol. Res.* **2011,** 8, 671-683.

33. Chernykh A., Alam S., Jayasooriya A., Bahr J., Chisholm B. J., Living carbocationic polymerization of a vinyl ether monomer derived from soybean oil, (2-vinyloxy)ethyl soyate. *Green Chem.* **2013,** 15, 1834-1838.

34. Aoshima S., Higashimura T., Living cationic polymerization of vinyl monomers by organoaluminum halides. 3. Living polymerization of isobutyl vinyl ether by ethyldichloroaluminum in the presence of ester additives. *Macromolecules* **1989,** 22, 1009-1013.

35. Zhang X., Jackson J. K., Burt H. M., Development of amphiphilic diblock copolymers as micellar carriers of taxol. *Int. J. Pharm.* **1996,** 132, 195–206.

36. Kohut A., Sieburg L., Vasylyev S., Kudina O., Hevus I., Stafslien S., Daniels J., Kislenko V., Voronov A. In *Amphiphiles: Molecular Assembly and Applications*, Ed. Nagarajan R., *ACS Symp. Ser.* Washington, DC, **2011,** 1070, 205–224.

37. Thompson D., Lemaster C., Allen R., Whittam J., Evaluation of relative shampoo detergency. *J. Soc. Cosmet. Chem.* **1985,** 36, 271-286.

38. Ross J., Miles G.D., An apparatus for comparison of foaming properties of soaps and detergents. *Oil Soap* **1941,** 18 (5), 99-102.

39. Hart J. R., DeGeorge M. T., The lathering potential of surfactants – a simplified approach to measurement. *J. Soc. Cosmet. Chem*. **1980,** 31, 223-236.

40. Lowry O. H., Rosenbrough N. J., Faar A. L., Rendall R. J., Protein measurments with Folin phenol reagent. *J. Biol. Chem.* **1951**, 193, 265-275.

41. Deye J. F., Berger T. A., Nile Red as a solvatochromic dye for measuring solvent strength in normal liquids and mixtures of normal liquids with supercritical and near critical fluids. *Anal. Chem*. **1990,** 62, 615-622.

42. Hevus I., Kohut A., Voronov A., Interfacial micellar phase transfer using amphiphilic invertible polymers. *Pol. Chem.,* **2011,** 2, 2767-2770.

43. Mainkar A. R., Jolly C. I., Evaluation of commercial herbal shampoos. *Int. J. Cosm. Sci.* **2000,** 22, 385-39,.

44. Klein K., Evaluating Shampoo Foam. *Cosmetics & Toiletries*, **2004,** 11 (10), 32-35.

45. Deshmukh S., Kaushal B., Ghode S., Formulations and evaluation of herbal shampoo and comparative studies with herbal marketed shampoo. *Int. J. Ph. Bio Sci.* **2012,** 3 (3), 638-645.

46. Sorkin M., Shapiro B., Kass G.S., The practical evaluation of shampoos. *J. Soc. Cosm. Chem.* **1966,** 17, 539-551.

47. Sandhu S. S., Ramachandran R., Robbins C. R., A simple and sensitive method using protein loss measurements to evaluate damage to human hair during combing. *J. Soc. Cosm. Chem.* **1995,** 46, 39-52.

48. 5 benefits of Aloe Vera for hair. www.organiccolorsystems.com/5-benefits-of-aloe-vera-for-hair/ (accessed 9/27/2014).

CHAPTER 7. THERMORESPONSIVE LATEXES FOR FRAGRANCE ENCAPSULATION AND RELEASE

7.1. Abstract

New thermoresponsive polymer particles for fragrance encapsulation were synthesized and characterized, including assessing the performance of particles in triggered release by elevated temperature. Cross-linked latex particles protect the encapsulated fragrance at ambient temperatures, and facilitate the release of cargo at the temperature of the surface of the skin that varies in different regions of the body between 33.5 and 36.9 °C. Poly(stearyl acrylate) (PSA), a polymer with long crystallizable alkyl side chains (undergoes order-disorder transitions at 45 °C), was chosen as the main component of the polymer particles. To obtain network domains of various crystallinity, stearyl acrylate was copolymerized with dipropylene glycol acrylate caprylate (comonomer) in the presence of a dipropylene glycol diacrylate sebacate (cross-linker) using the miniemulsion process. Comonomers and a cross-linker were mixed directly with a fragrance during polymerization. Fragrance release was evaluated at 25, 31, 35, and 39 °C to demonstrate a new material potential in personal/health care skin-related applications. It is also shown, how release profiles can be tuned by temperature and controlled by the amount of loaded fragrance and the ratio of comonomers in the feed mixture.

7.2. Introduction

Important in daily life, fragrances, scent-masking agents, and their mixtures (such as perfume compositions) are widely applied to provide odors for consumer cosmetic, personal care, and household products [1]. The demand for such products is growing, but high volatility of fragrances, as well as low stability in time, often results in a loss of active components during manufacturing, storage, and use [2-4]. Currently, direct admixing of fragrances (in particular, in the presence of surfactants) in product formulation is a main

strategy used to introduce odors to consumer products [5]. However, fragrance volatility and low stability still remain significant drawbacks to this strategy.

It is highly desirable for many fragranced consumer products, such as perfumes, deodorants, moisturizers, shampoos, etc. [6-8], that their active odor components (both less volatile and highly volatile) are released slowly over time (sustained release). This is because the most volatile fragrance components (top notes) are responsible for the so-called fresh-feeling consumer experience. The concentration of top notes in the vicinity of the substrate (headspace concentration) should ideally be constant over a long period of time and characterized by zero-order diffusion kinetics [2, 9].

The direct admixing of fragrances into the product does not impart the desired kinetics of release. By this technique, the headspace concentration increases exponentially and depends on the volatility of the fragrance. The top notes can only be found over a short period of time. It remains highly advantageous to develop an approach to fragrance delivery that will protect the volatile top notes in product formulation and provide their sustained release from various substrates over a longer period (at least 24 hours) of time [2].

A significant amount of research on encapsulation (engulfing the fragrance molecules into confinement within a protective matrix material) has been devoted to improving the sustained release of odor components [10-15]. Although various commercial delivery systems are available for this purpose, many common state-of-the-art materials suffer from low, uncontrolled interaction between the cargo (fragrance molecules) and the carrier (matrix) materials. Many fragrances are hydrophobic substances, as well as often carrier components (waxes, fats, fragments of amphiphilic polymers, etc.). Therefore, carrier hydrophobic fragments steadily discharge hydrophobic volatile fragrance molecules and do not reduce evaporation [2].

Using polymers in the encapsulation of fragrances and their controlled release has been a subject of significant study during recent decades [7, 16-19]. It was shown that the

incorporation of odor components into polymer micro- and nanoparticles could result in novel materials and devices for sustained delivery of these substances [17, 19]. Various polymer-based systems are patented and applied to the commercial development of consumer products, including air fresheners, deodorants, devices for fragrance release in contact with skin, etc. [17, 20, 21]. A wide range of hydrophilic polymers and copolymers can be cross-linked to provide swellable polymer networks (polymer gel particles) for the encapsulation of fragrances. The release rate from such polymer particles is swelling-controlled, whereas the degree of swelling depends on polymer structure and physical properties [6-8, 16, 20]. Moreover, responsive polymeric particles that change their network properties in response to external stimuli can be designed for the encapsulation of hydrophobic odor components [4, 23]. Such particles are considered novel and innovative smart materials for the sustained release of fragrances.

In this study, we developed thermoresponsive cross-linked latex particles for fragrance encapsulation and release. The main component of the particle network is poly(stearyl acrylate) (PSA), a polymer with long crystallizable alkyl side chains (Scheme 7.1). PSA macromolecules undergo reversible order-disorder transitions at 45 °C [22, 24] associated with interactions between the alkyl side chains [25-27]. Below this temperature, the polymer side fragments are ordered in the crystalline lamellar structures that may suppress diffusion of the incorporated volatile molecules and stabilize the fragrance (Scheme 7.1 A). When PSA is heated above 45 °C, the crystalline domains become disordered, and fragrance molecules can diffuse from the polymer and be released (Scheme 7.1 B). Our objective was to synthesize the particles protecting the encapsulated fragrance at ambient temperatures, and to facilitate the release of cargo at the temperature of the surface of the skin, which varies in different regions of the body between 33.5 and 36.9 °C [28].

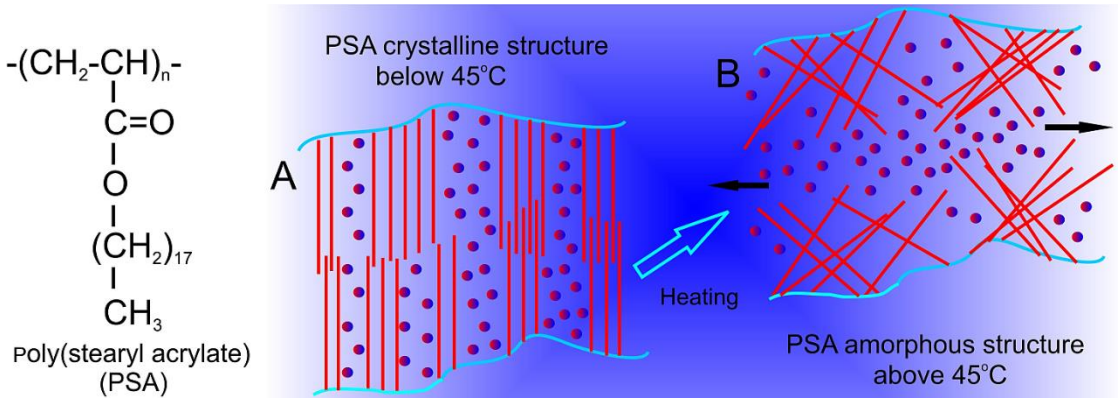

Scheme 7.1. Expected mechanism of release from PSA crystalline domains.

To develop latex particles with fragrances incorporated in the interior, we used miniemulsion free radical polymerization. The miniemulsion method has been widely applied in developing nanocapsules and nanospheres [4, 29-31]. This process is especially convenient for the hydrophobic monomers (as stearyl acrylate) that scarcely diffuse through aqueous phases and, thus, are hardly suitable for conventional emulsion polymerization [32-34].

To obtain domains with a various degree of crystallinity in the network, commercially available stearyl acrylate (SA) was copolymerized with dipropylene glycol acrylate caprylate (DGAC) (a comonomer) in the presence of dipropylene glycol diacrylate sebacate (DGDS) (a cross-linker) (Scheme 7.2). Both DGAC and DGDS were developed in this study. The miniemulsion oil phase was prepared by mixing monomers, cross-linkers and initiator with a fragrance. Cross-linked particles with localized fragrance molecules were formed via free radical miniemulsion polymerization.

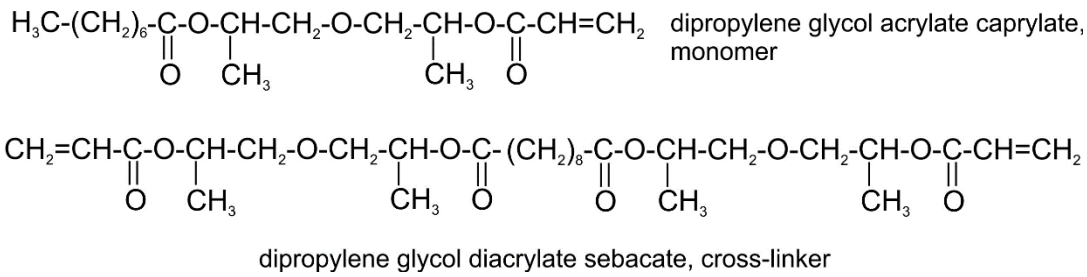

Scheme 7.2. Chemical structure of DGAC and DGDS.

The fragrance release profile from latex particles was evaluated at 25, 31, 35, and 39 °C to demonstrate the potential of the material in a variety of personal and health care (particularly, skin-related) applications.

7.3. Materials and Methods

7.3.1. Materials

Caprylic (octanoic) acid (Alfa Aesar, Ward Hill, MA), sebacic (decanedioic) acid (TCI America, Portland, OR), dipropylene glycol (DPG) (Alfa Aesar, Ward Hill, MA), acryloyl chloride (EMD Millipore, Billerica, MA), 4-dimethylaminopyridine (DMAP) (Alfa Aesar, Ward Hill, MA), trimethylamine (TEA) (Amresco, Solon, OH), Tween 80, absolute ethanol (Sigma-Aldrich, St. Louis, MO), a fragrance composition (Givaudan, Cincinnati, OH), the free radical initiator 2,2'-azobis(2-methylbutyronitrile), VAZO-67 (DuPont, Wilmington, DE) were used as received. Deionized (DI) water was used for the purification steps (MiliQ, 18 MΩ). Other solvents and chemicals were used as received and were of an analytical grade or higher.

7.3.2. Synthetic and analytical methods

7.3.2.1. Synthesis of DGDS

The synthetic route to obtain a cross-linker, DGDS, comprises two steps, i.e., the synthesis of dipropylene glycol sebacate diester (DS) and DS acrylation (Scheme 7.3). To synthesize DS, 170 g of DPG (1.27 mol) were mixed with 30 ml toluene, followed by the addition of 13 g sebacic acid (0.064 mol) and 1 ml of concentrated H_2SO_4 in a 250 ml round-bottom flask fitted with a Dean-Stark condenser. The reaction mixture was heated to

110 °C in an oil bath and stirred at 500 rpm for 12 h. The reaction mixture was then transferred to a separating funnel and 100 mL DI water were added. The product was extracted with 100 mL of CH_2Cl_2, washed with DI water (150 mL) twice, and washed with 150 mL of a brine solution. The resulting solution was passed several times through an Al_2O_3 column and dried with $MgSO_4$. The solvent was removed under reduced pressure. The yield of DS was 90 %.

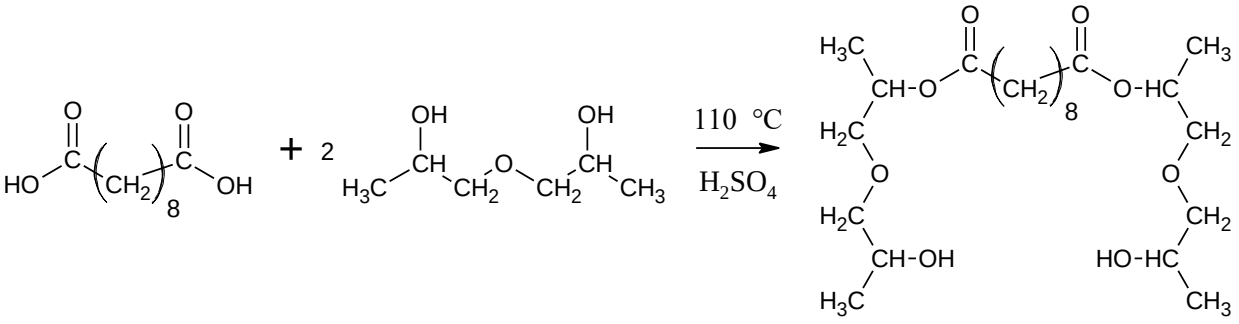

Sebacic acid | di-propylene glycol | di-propylene glycol sebacate

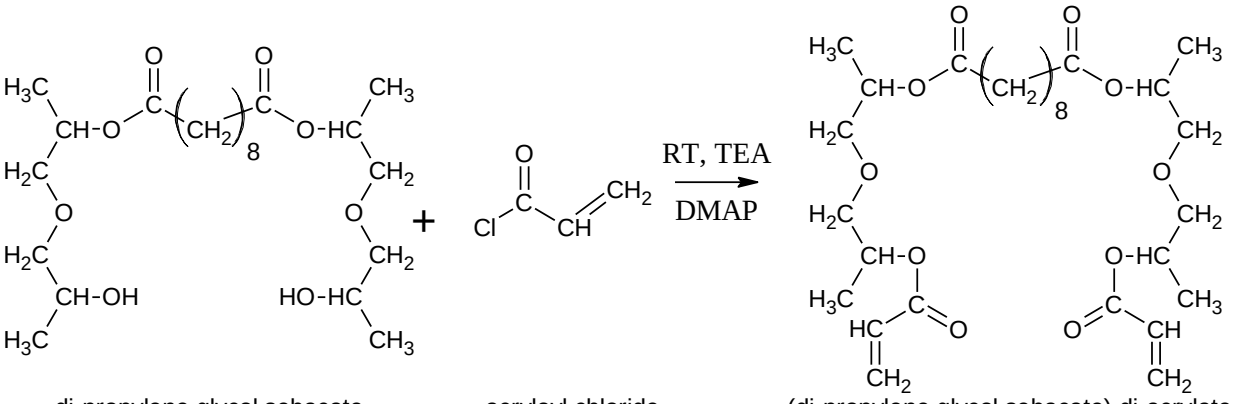

di-propylene glycol sebacate | acryloyl chloride | (di-propylene glycol sebacate) di-acrylate

Scheme 7.3. Synthesis of dipropylene glycol diacrylate sebacate (DGDS) (cross-linker).

The second step, the acrylation of DS, was performed by reacting DS with acryloyl chloride, as follows: 5.7 g of acryloyl chloride (0.063 mol) were added slowly via syringe to a stirring solution of 6.3 g TEA (0.062 mol) and 10 g DS (0.023 mol) in dry CH_2Cl_2 (7 ml). Temperature was kept at 0 °C during addition, and afterwards was allowed to reach room temperature. At this point, a catalytic amount of DMAP was added, and the reaction was stirred for an additional 2 h. The reaction mixture was then admixed with ethyl acetate,

washed with DI water (50 mL) twice, followed by a wash with 50 mL of a brine solution, and filtered. The solvent was removed under reduced pressure. The DGDS yield was 96 %. For storage, 10 ppm of hydroquinone was added to the product, which was stored at –4 °C.

7.3.2.2. Synthesis of DGAC

Synthesis of the DGAC monomer comprises two similar steps as described for the DGDS cross-linker (Scheme 7.4).

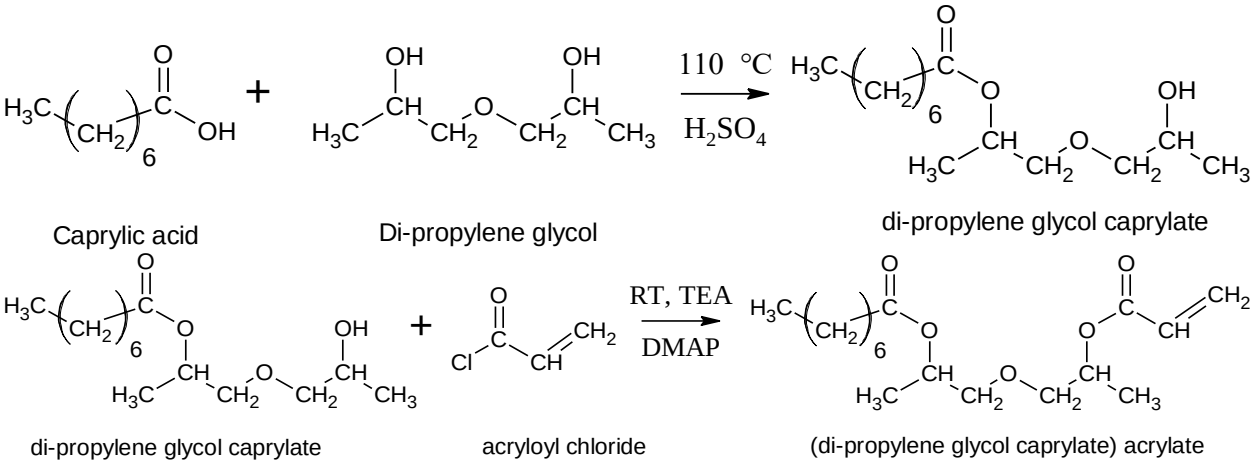

Scheme 7.4. Synthesis of dipropylene glycol acrylate caprylate (DGAC) (monomer).

To obtain dipropylene glycol caprylate diester (DC), 170 g DPG (1.27 mol) were reacted with 15 g caprylic acid (0.104 mol). The DC yield was 99 %. In the second step, acrylation of DC was performed by reacting with acryloyl chloride in a similar way, where 10 g of DC (0.038 mol) were reacted with 4.5 g acryloyl chloride (0.050 mol) and 5 g TEA (0.049 mol) in 7 ml dry CH_2Cl_2. To confirm the chemical structure, the synthesized DS, DGDS, DC, and DGAC were characterized using ESI mode GC-MS mass spectrometry (BioTOF, Bruker Daltonics, Billerica, MA), ^{1}H NMR spectroscopy (ECA 400 MHz JEOL, Peabody, MA,) and FT-IR spectroscopy (Nicolet 8700, Thermo Scientific, Waltham, MA,).

7.3.2.3. Synthesis and characterization of fragrance-loaded latex particles

Fragrance-loaded latex particles were synthesized using a miniemulsion polymerization process. The acrylate monomers SA and DGAC (at 100/0, 85/15, and 70/30 wt. % monomer ratios), the cross-linker DGDS (0.03 mol/l, equal to 1 part per 40 parts of

monomer mixture), and initiator VAZO-67 (1.7 wt. %) were mixed in a fragrance (at total monomer concentrations 50 and 67 wt. %) to obtain 1.5 g of the oil phase. A 16.5 g of aqueous solution of the surfactant, Tween 80 (0.13 wt. %), was added to the oil phase. For pre-emulsification, the mixture was homogenized using a magnetic stirrer for 1 h at 1000 rpm. The miniemulsion was prepared by ultrasonicating the pre-emulsified mixture for 180 s at 90 % amplitude (digital sonicator 500 Watt, 1/2" tip, 20 kHz, QSonica, Newtown, CN) at 0 °C. The polymerization was performed at 72 °C for 8 h under stirring. Solid content was determined gravimetrically by drying the samples at 80 °C. For most polymerization experiments, conversion was 99%. The size distribution of latex particles was measured using a Zetasizer Nano-ZS90 (Malvern, Worcestershire, UK) at a single scattering angle of 90° and temperature of 25 °C.

Transmission electron microscopy (TEM) images were taken using a JEM-2100 (JEOL, Peabody, MA) analytical transmission electron microscope. For the TEM measurements, a drop of latex dispersions was placed onto a copper mesh covered with a thin carbon film.

Scanning electron microscopy (SEM) images were taken using a JEOL 7600F scanning electron microscope. For the SEM measurements, a drop of latex dispersions was placed onto a silicon wafer and dried.

Differential scanning calorimetry (DSC) was measured to determine thermal transitions (melting temperatures) of the latex nanoparticles network using a Q1000/Q2000 Modulated Differential Scanning Calorimeter (TA Instruments, New Castle, DE) in hermetic aluminum pans in a 0–100 °C sweep range with a 10 °C/sec heating rate. To prepare samples for DSC measurements, acrylate monomers, cross-linkers, and initiators were mixed in a fragrance at concentrations used for miniemulsion polymerization. Solutions were sealed in a 5 ml glass ampoule and polymerized at the same conditions used in the miniemulsion process. After polymerization, the ampoules were opened to immediately subject samples to DSC measurements.

The fragrance release profile from particles was determined by quantifying the amount of fragrance remaining in samples that were left in uncovered vials at certain temperature for specified times. Quantification was performed using UV-Vis spectroscopy measurements. For this purpose, 0.35 g of fragrance-loaded particles were placed into a 20 ml glass vial in a thermostat at the experimental temperature. The vials were kept uncovered for 6–48 h to facilitate release. After a specified time, the remaining fragrance was extracted from the sample by mixing the particles with absolute ethyl alcohol in a tightly capped vial. To facilitate desorption of fragrance into alcohol, samples were initially placed on sonic bath for 5 min and then kept under stirring at 36 °C for 24 h with another 5 min sonic bath treatment just before measurements. The fragrance content in the extract was determined by monitoring optical absorbance at 303 nm using UV-Vis spectra recorded on a Cary 5000 UV-Vis-NIR (Varian, Palo Alto, CA) spectrophotometer. The analysis was carried out in triplicate. To assess the remaining concentration of fragrance in the extract, a calibration curve was prepared using known fragrance concentrations in ethanol.

Release profiles from latex particles were compared to the corresponding unencapsulated (direct admixed) sample of fragrance. The unencapsulated samples were prepared by adding 2.6 and 4 wt. % fragrances into 0.28 wt. % SDS aqueous solution and thorough stirring. Three unencapsulated samples were prepared for each experiment, left opened, and then subjected to extraction and optical absorbance analysis to determine the released amount of fragrance.

7.4. Results and Discussion

7.4.1. Synthesis and characterization of fragrance-loaded latex particles

When macromolecules consist of a main backbone with branch points and linear side chains, it is said to be a graft polymer [35]. Such poly(acrylates) are often classified as graft (co)polymers with differing physical properties if compared to polymers with no side fragments [36]. Due to interactions between the side chains, the graft polymers are able to

form crystalline domains when the length of the side chain is above eight carbon atoms. The crystallization is not favored for four- to eight-atom-long side fragments, and such polymer structures remain amorphous [37].

We chose two acrylates with a different nature and length of side fragments to synthesize a graft copolymer network of thermoresponsive cross-linked latex particles. Such a combination was chosen in order to obtain crystalline and amorphous domains in the cross-linked polymer structure. Scheme 7.5 shows the formation of the network by the copolymerization of stearyl acrylate (17 methylene fragments in the alkyl group) and dipropylene glycol acrylate caprylate with six methylene groups in alkyl fragment in the side chain. A three-dimensional network was formed by a radical copolymerization reaction of monomers and cross-linkers. At the same time, the longer stearyl fragments form ordered (crystalline) domains (Scheme 7.5), whereas shorter fragments of the DGAC remain disordered and form amorphous phases (domains).

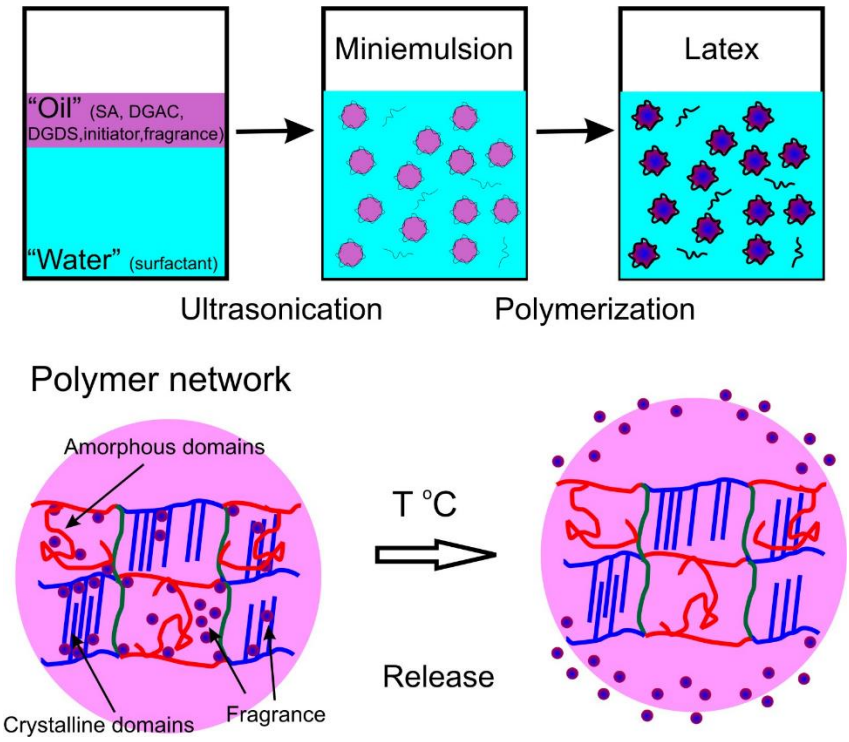

Scheme 7.5. Miniemulsion polymerization (top) and the anticipated temperature-controlled release mechanism (bottom).

The chemical structures of the synthesized monomer, DGAC, and the cross-linker, DGDS, were confirmed

DS and DC syntheses were conducted in 10 fold molar excess of hydroxyl functional groups in order to ensure consumption of carboxylic functional groups and suppress formation of high molecular weight oligomers. Structure of DS, DC, DGDS, and DGAC were confirmed by ^{1}H NMR spectroscopy and GC-MS spectrometry (observed monoisotopic masses were within <7 ppm threshold of theoretical structures).

The structure of the synthesized monomers was confirmed using FT-IR spectroscopy (Figure 7.1, 7.2), ^{1}H NMR spectroscopy (Figure 7.3, 7.4), and mass spectrometry (Figure 7.5, 7.6).

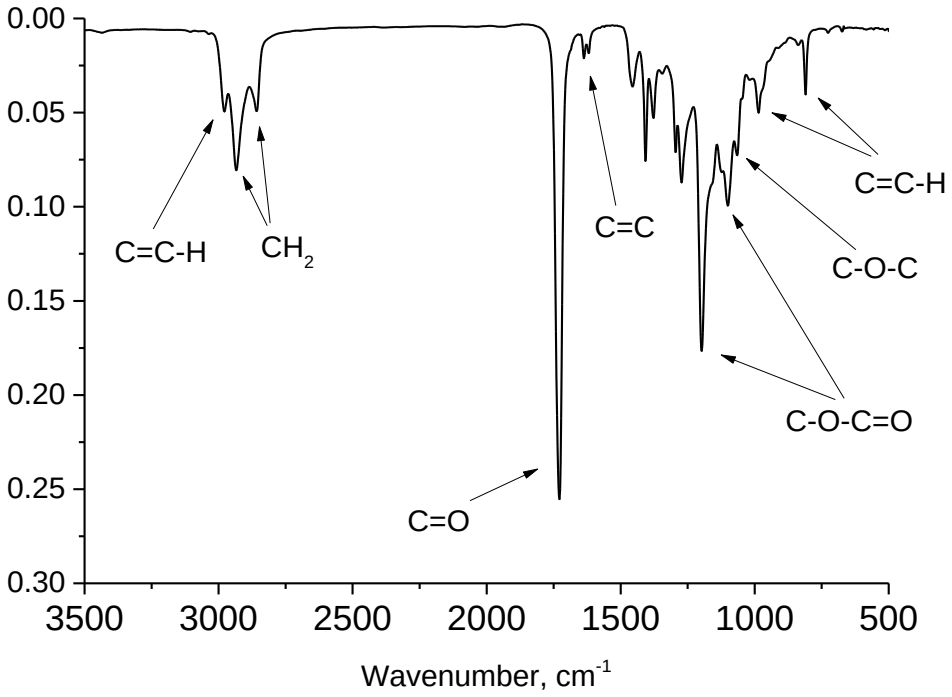

Figure 7.1. FTIR spectrum of DGDS.

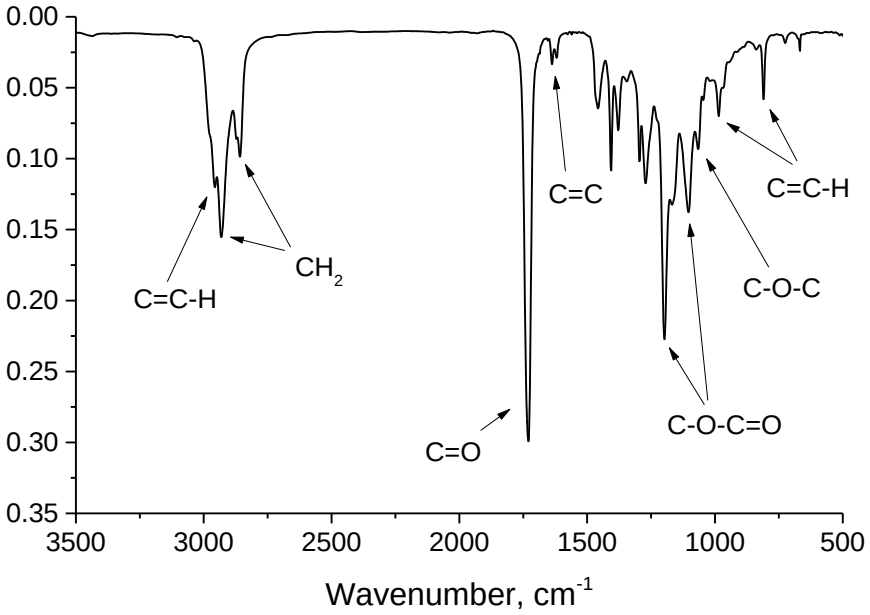

Figure 7.2. FTIR spectrum of DGAC.

The presence of an ester group was confirmed by the presence of several characteristic adsorption bands in the FTIR spectra of DGDS and DGAC. Valence vibrations of the ester C=O bond result in an intense adsorption band at 1727 cm^{-1}. A doublet of adsorption bands at 1198-1101 cm^{-1} is caused by valence vibrations of ester C-O bonds. The spectrum shows a doublet of absorption bands in the range of 2858–2933 cm^{-1} (valence oscillations) that are characteristic of CH_3, CH_2, and CH groups. Finally, the presence of carbon-carbon double bonds was confirmed by the adsorption bands at 2977 cm^{-1} (C=C–H), 1637 cm^{-1} (C=C), as well as 809 and 985 cm^{-1} (C=C–H).

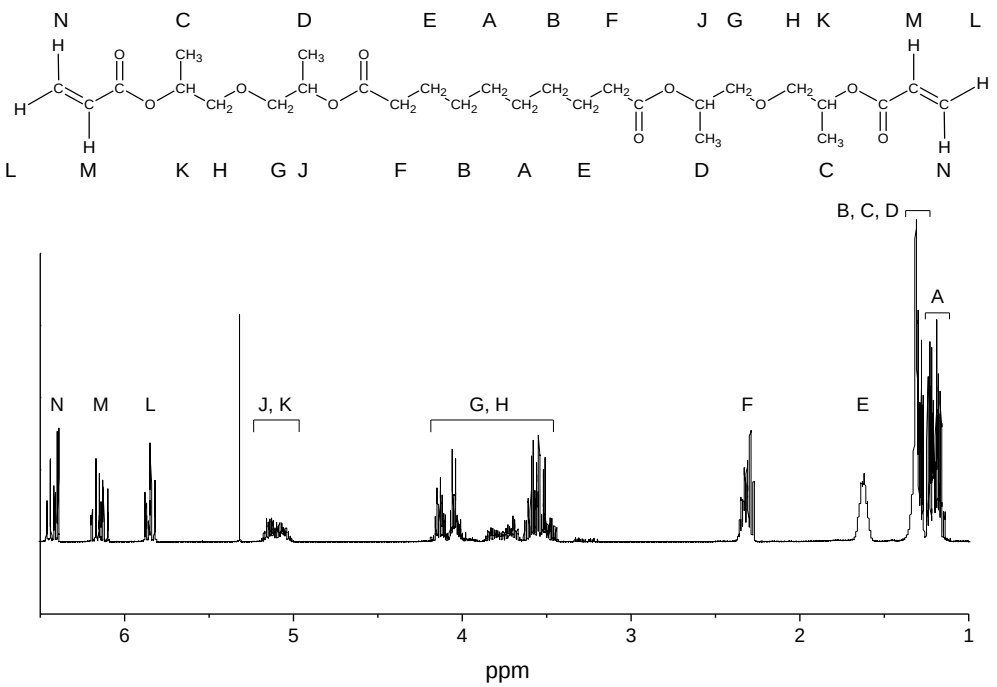

Figure 7.3. ^{1}H NMR spectrum of DGDS.

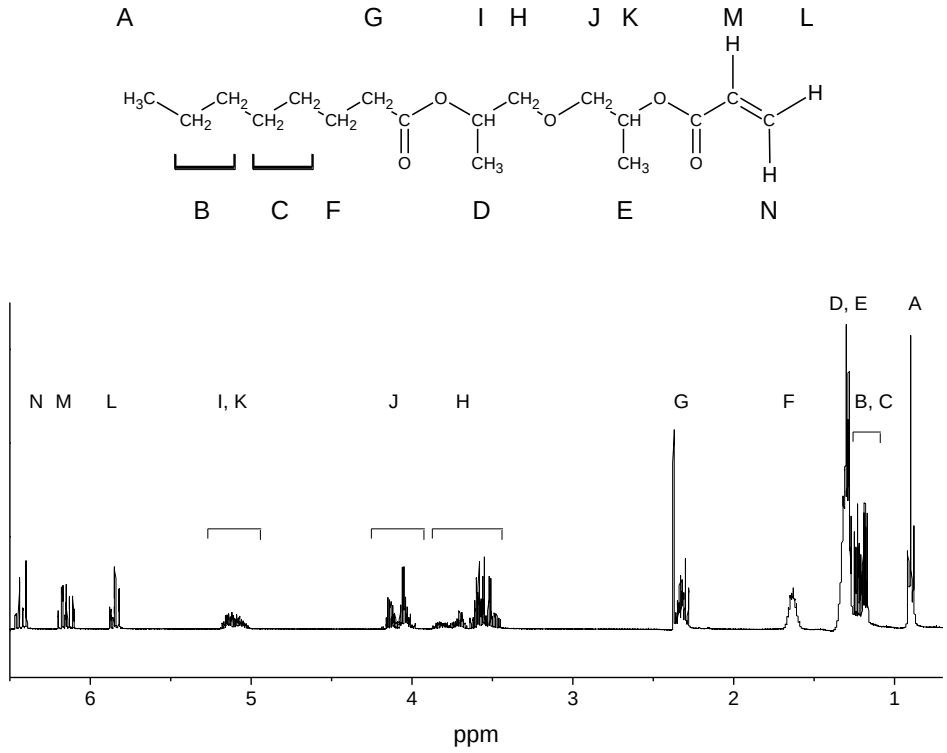

Figure 7.4. ^{1}H NMR spectrum of DGAC.

In the ^{1}H NMR spectrum of dipropylene glycol diacrylate sebacate (DGDS) (Figure 7.3), peaks appeared at A ppm (m, 4H, $(C\underline{H}_2)_2$) and B ppm (m, 4H, $C\underline{H}_2CH_2CH_2COO$), which were in agreement with those of sebacic acid. The spectrum shows multiplet peaks at F and E ppm corresponding to the methylene groups in an α- and β-position in relation to the carbonyl groups in sebacic acid moieties (4H, $CH_2C\underline{H}_2COO$ and 4H, $C\underline{H}_2CH_2COO$, respectively). At J and K ppm, multiplet absorption peaks that can be contributed to the methyne protons of the acylated dipropylene glycol end unit was observed (m, 4H, $COOC\underline{H}$). Other protons of the dipropylene glycol fragments reveal themselves as multiplet peaks at C and D ppm (12H, $C\underline{H}_3$) and G and H ppm (8H, $C\underline{H}_2$). The signals of acrylate moieties are found at L ppm (2H, $C\underline{H}_2$=CH), M ppm (2H, CH_2=$C\underline{H}$), and N ppm (2H, CH_2=$C\underline{H}$).

In the ^{1}H NMR spectrum of dipropylene glycol acrylate caprylate (DGAC) (Figure 7.4), peaks appeared at A ppm (t, 3H, $C\underline{H}_3$), B and C ppm (m, 8H, $(C\underline{H}_2)_4CH_2CH_2COO$), which were in agreement with those of caprylic acid. The spectrum shows multiplet peaks at G and F ppm corresponding to the methylene groups in an α- and β-position in relation to the carbonyl groups in caprylic acid moieties (2H, $CH_2C\underline{H}_2COO$ and 2H, $C\underline{H}_2CH_2COO$, respectively). At I and K ppm, multiplet absorption peaks that can be contributed to the methyne protons of the acrylated dipropylene glycol end unit was observed (m, 2H, $COOC\underline{H}$). Other protons of the dipropylene glycol fragments reveal themselves as multiplet peaks at D and E ppm (6H, $C\underline{H}_3$) and H and J ppm (4H, $C\underline{H}_2$). The signals of an acrylate moiety are found at L ppm (1H, CH_2=$C\underline{H}$), M ppm (1H, CH_2=$C\underline{H}$), and N ppm (2H, $C\underline{H}_2$=CH).

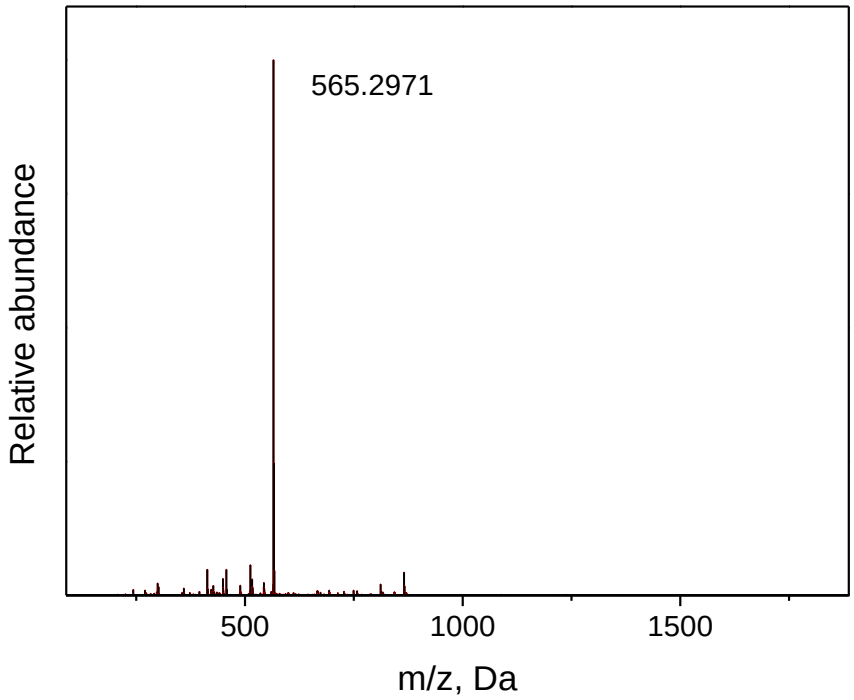

Figure 7.5. Mass-spectrometry of DGDS (monoisotopic M= 565.2988, difference 3 ppm).

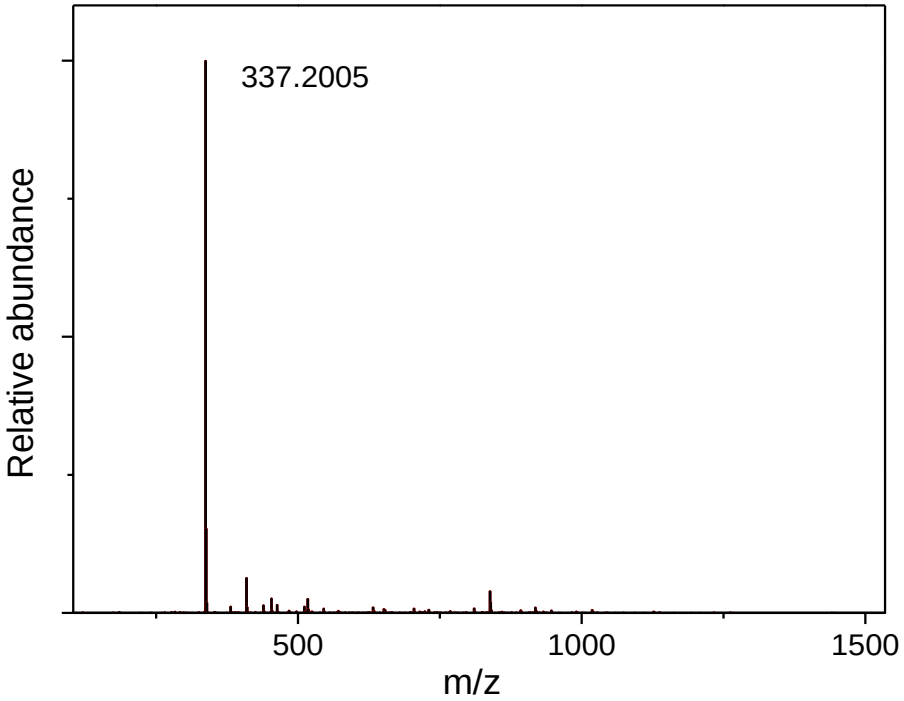

Figure 7.6. Mass-spectrometry of DGAC (monoisotopic M=337.1991, difference 4 ppm).

Fragrance molecules were loaded into the hydrophobic polymer network using the miniemulsion process (Scheme 7.5, top). Monomers, cross-linkers, and initiators of radical polymerization were mixed in a fragrance to obtain the oil phase of the emulsion. The mixture was sonicated in a surfactant-containing aqueous phase to form miniemulsion. Polymerization started by increasing the temperature and resulted in a stable latex formation. The structure of the synthesized latex particles represents a polymer network of various crystallinity with fragrance loaded into the particle matrix. It was expected that the variation of crystallinity provides particles with temperature-controlled release of fragrance.

Fragrance-loaded latex particles of six different compositions (S1f–S6f in Table 7.1) were synthesized. For the purpose of various crystallinity of the network, a long side chain monomer, SA, was copolymerized with a comonomer, DGAC, at two different ratios (S2f, S3f, S5f, S6f), as well as homopolymerized (no DGAC) (S1f, S4f). To monitor whether different fragrance loading in the particles influences the release profile and facilitates temperature-sensitive properties of particles, the amount of fragrance in the reaction mixture was varied (33 wt. % of fragrance in S1f–S3f and 50 wt. % in S4f–S6f). It was expected that both cargo loading and monomer ratios will contribute to release profiles of fragrances at different temperatures.

Table 7.1. Polymerization mixtures and estimated Tm of fragrance-loaded and dried copolymers.

	S1f	**S2f**	**S3f**	**S4f**	**S5f**	**S6f**
SA/DGAC, mol	1.8/-	1.5/0.3	1.2/0.6	1.35/-	1.15/0.2	0.95/0.4
DGDS, mol/L	0.047	0.047	0.047	0.034	0.034	0.034
Initiator, mol/L	0.084	0.084	0.084	0.064	0.064	0.064
Fragrance, wt.%	33	33	33	50	50	50
T_m (with fragrance), °C	36	29	23	30	24	19
	S1	**S2**	**S3**	**S4**	**S5**	**S6**
T_m (no fragrance), °C	44	38	30	43	36	30

SEM and TEM analysis indicate that particles of a spherical shape are formed (Figure 7.7). Dynamic light scattering measurements reveal an average latex particle size between 170 and 200 nm (Table 7.2). No significant effect of monomer ratio and fragrance loading on latex particles size distribution was observed. Miniemulsion polymerization results in a formation of stable latexes. The obtained cross-linked polymer latex particles remain stable during storage over at least several months in the lab (Figure 7.7, top inset).

Table 7.2. Characteristics of latex particles.

	S1	S2	S3	S4	S5	S6
Particles diameter, nm	173±21	176±24	183±27	180±19	184±24	208±26
Estimated loading, mg/g	330	330	330	500	500	500

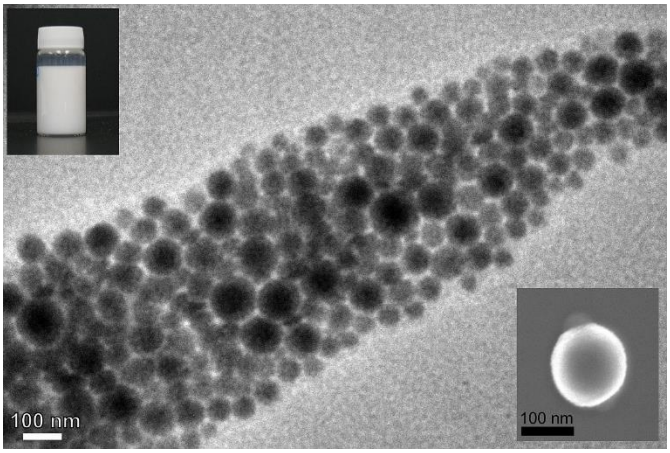

Figure 7.7. TEM and SEM images of fragrance-loaded latex nanoparticles, and latex appearance.

7.4.2. Thermal properties of polymer networks from psa and dgac formed in the presence of DGDS

In this study, the feasibility of the temperature-sensitive release of fragrance from the cross-linked latex particles was targeted. It was expected that the crystallinity of PSA, as a main component of the particle network, determines the thermal properties of the material – T_m (melting temperature [38]) and release performance of the particles.

In order to study the thermal properties of polymer networks, copolymer samples were synthesized via copolymerization of SA with DGAC in the presence of a DGDS cross-linker and an initiator in solution (Table 7.1). The resulting polymers were used to characterize the thermal properties of the network by determining the T_m in DSC measurements. Figure 7.8 A compares the results for the fragrance-loaded sample (corresponds to S1f in Table 7.1) and material where the fragrance was removed from the network by washing with ethanol and drying S1 in Table 7.1. Using point of inflection on the

plots we determined that the T_m of the dried network S1 is 44 °C, whereas the T_m of S1f was 36 °C. Lower T_m of loaded samples can be attributed to the ability of incorporated fragrance molecules to reduce intermolecular interactions between stearic fragments in the cross-linked polymer, and, thus, to decrease the network crystallinity.

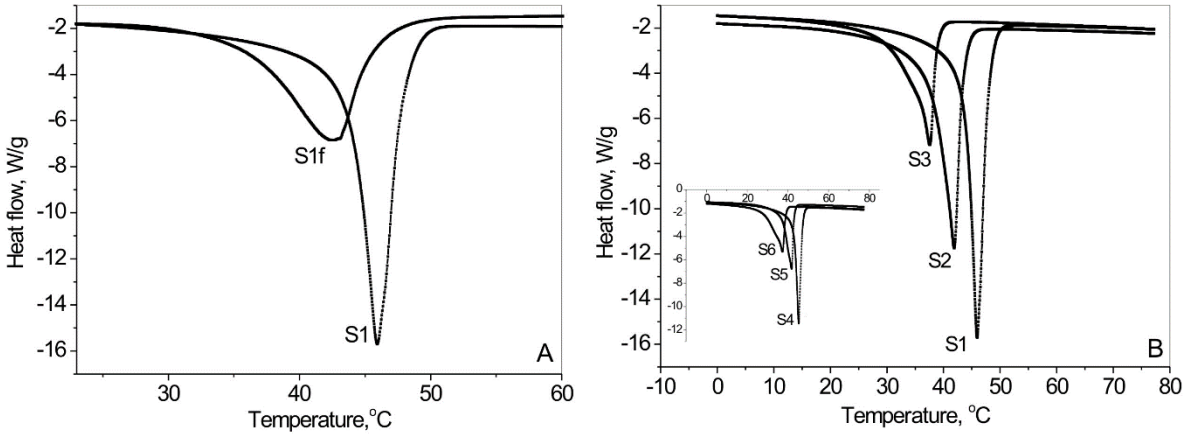

Figure 7.8. Temperature-dependant heat flow for fragrance-loaded S1f, dried S1 (A) and dried S1, S2, S3 (B) polymers. The inset shows data for S4, S5 and S6 compositions (Table 7.1).

Using the DSC, an effect of monomer ratio and the amount of loaded fragrance on the T_m of the network was determined. It is evident that the T_m of a dried copolymer samples decreases by increasing the amount of DGAC comonomer in the monomer feed (Figure 7.8 B). When the concentration of the DGAC short-side chain comonomer in the reaction mixture was 30 wt. %, the T_m of the dried network dropped from 44 °C to 30 °C. At the same time, the T_m of dried samples did not change by increasing the amount of loaded fragrance from 33 to 50 wt. % (S1 and S4 in Figure 7.8 B, Table 7.1). This indicates that the crystallinity of the resulting polymer network does not depend on a fragrance amount during polymerization.

In general, T_m is lower for the fragrance-loaded network if compared to the dried material without the fragrance. It differs noticeably when the ratio of monomers in a feed mixture and amount of loaded fragrance are varied (S1f–S6f in Table 7.1). Contrary to the polymers without incorporated fragrance, the T_m of the loaded samples depends on the

amount of cargo (33 or 50 wt. %) encapsulated in the polymer network. Based on DSC data, the PSA/DGAC ratio and fragrance loading can be both essential in ensuring the feasibility of latex particles for temperature-sensitive release.

7.4.3. Fragrance release from latex particles

It was expected that PSA crystalline-to-amorphous transition (as demonstrated by DSC) will trigger cargo release from the fragrance-loaded latex particles by elevated temperatures. The presence of the encapsulated fragrance molecules, as well as including a smaller fraction of DGAC comonomer that forms amorphous domains in the latex network, can reduce the particles' crystallinity and, thus, enhance the triggered release. To this end, the effect of both factors, fragrance loading, and monomers ratio, on release behavior was considered.

Figure 7.9 shows the release profiles of fragrance in terms of released amount per weight of latex in time. For each sample, release was studied at 25, 31, 35, and 39 °C, gradually approaching the T_m = 44 °C of poly(stearyl acrylate), the main polymer component in the latex network. Release profiles were compared for the particles prepared from 100 (Figure 7.9 A,D), 85 (Figures 7.9 B, E), and 70 wt. % (Figures 7.9 C, F) of stearyl acrylate mixed in a monomer feed, respectively, with 0, 15, and 30 wt. % of DGAC in 33 (Figures 7.9 A–C) or 50 wt. % (Figures 7.9 D–F) of fragrance.

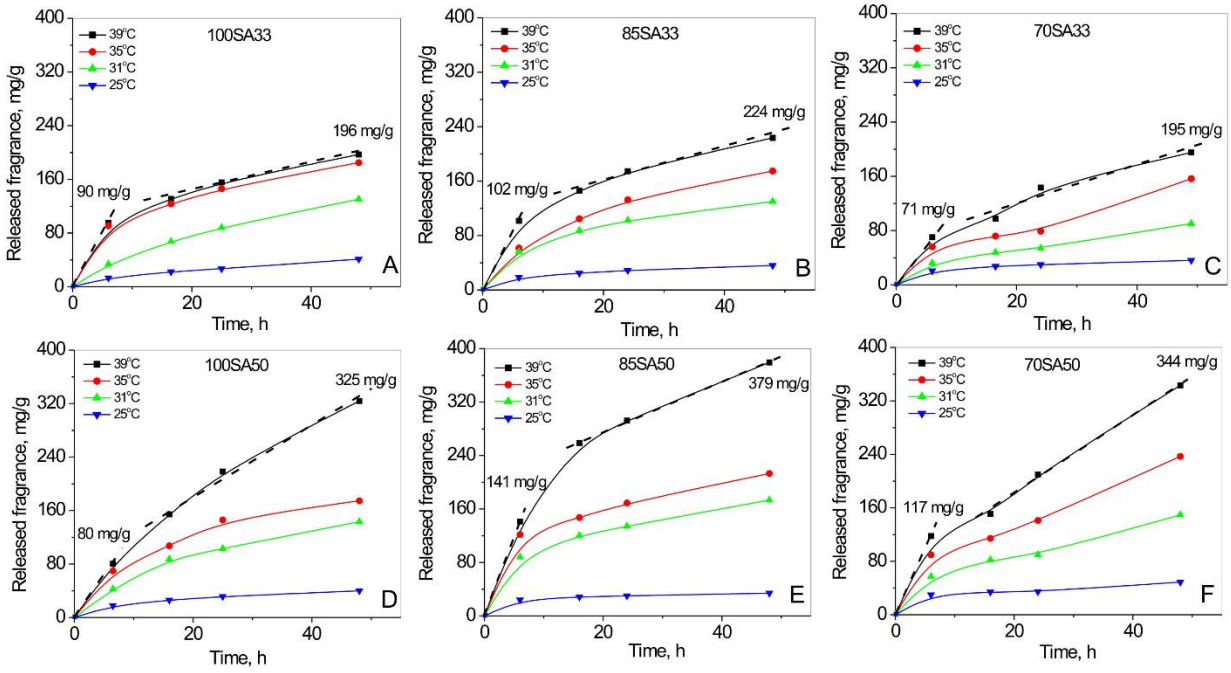

Figure 7.9. Release of fragrances from latex particles depending on copolymer composition, temperature, and fragrance loading (two numbers on each plot provide the amount of fragrance released after 6 and 48 h of the experiment).

Some general conclusions can be drawn from the obtained data. The encapsulation into the latex particles protects the fragrance with respect to release at 25 °C. At this temperature, most of the encapsulated material remains inside the particles (Figure 7.9 – the fragrance release is about 10 mg/g regardless of copolymer composition), preventing rapid volatilization and loss of cargo. Within the same period of time, a considerable amount of cargo was lost at 25 °C if the fragrance was emulsified (admixed) by an SDS aqueous solution (Figure 7.10 A – the fragrance release is about 50 mg/g).

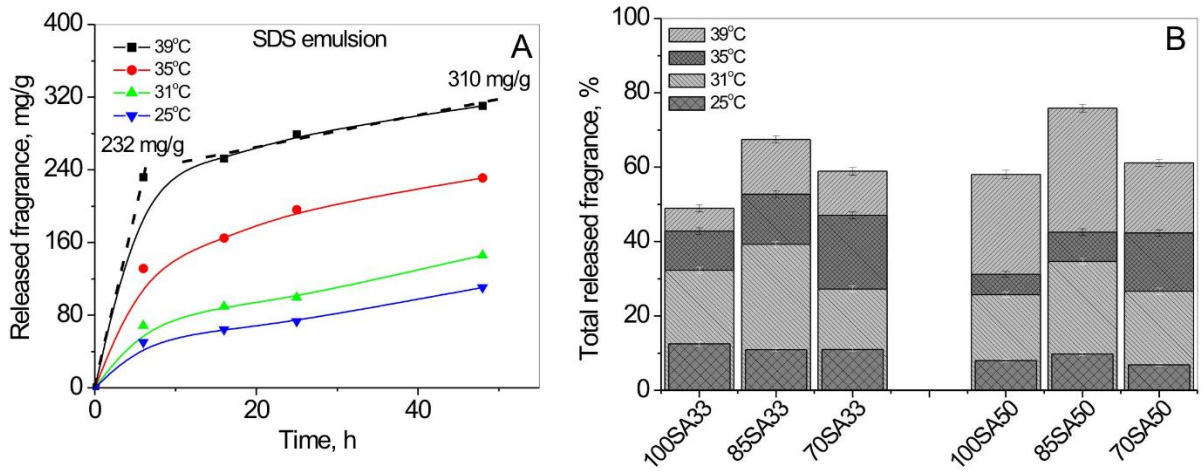

Figure 7.10. The release of fragrance from an SDS aqueous emulsion (A) and total fragrance release from latex nanoparticles after 48 h (B) (two numbers on plot A provide the amount of fragrance released after 6 and 48 h of the experiment).

The amount of released fragrance increases over time for all samples when the latex particles are subjected to heating. The total amount of the released material grows when the temperature increases. Interestingly, the total release was similar for all samples with the same fragrance loading after 48 h of heating (Figure 7.10 B – about 200 mg/g for 33 wt. % of fragrance and about 350 mg/g for 50 wt. % of fragrance). However, all samples have one general feature, namely that their release plots display two clearly distinguishable slopes (Figure 7.9). The first slope corresponds to a rapid increase of the released amount over 6 h (the "fast" period), and the second one indicates a subsequent decrease of release rate (the "prolonged" period). Hence, it is evident that the cross-linked latex particles are able to facilitate controlled release of the fragrance. Currently, direct admixing of fragrances (in particular, in the presence of surfactants) in product formulation is a main strategy used to introduce odors to consumer products [5]. As evidenced by Figure 7.10 A, a large fraction of cargo is released within a few hours in the case of SDS formulation; thus, sustained release is hardly possible.

As can be seen from Figure 7.9 A and D, the released amount during the period of "fast" release from particles from PSA homopolymer does not depend on the amount of

loaded fragrance. However, this factor becomes essential when fragments of the PSA in network are partially replaced by amorphous DGAC (Figure 7.9 B and E). As expected, the presence of short side chain fragments enhances "fast" release both at the same and increased temperatures. This observation is in agreement with DSC data indicating that enhanced release can be explained by decreased polymer network crystallinity due to the formation of amorphous domains of DGAC (Figure 7.8, Table 7.1).

Contrariwise, the second slope ("prolonged" release) is noticeably determined by fragrance loading and does not depend on polymer composition (Figure 7.9, A–C compared to D–F). Interestingly, the latex particles from the copolymer containing 30 wt. % of amorphous DGAC release the cargo slower than the particles from the copolymer containing 15 wt. % of DGAC (Figure 7.9 C and F). The total release from such particles decreases as well if compared to the particles from 15 wt. % DGAC (Figure 7.10 B).

We attribute this finding to the fact that fragrance molecules might have stronger physical interactions with DGAC domains in the polymer network. When the temperature increases and crystalline-to-amorphous transition occurs, the release of cargo from DGAC domains is delayed due to these interactions. Either higher temperature or longer heating time was needed to release fragrance localized in amorphous domains, causing changes in the release profiles that were observed in Figure 7.9 C and F in comparison to Figure 7.9 B and E.

7.5. Conclusion

New thermoresponsive polymer latex particles for fragrance encapsulation were synthesized and characterized, including the performance of particles in triggered release by elevated temperature. Poly(stearyl acrylate), a polymer with long crystallizable alkyl side chains (undergoes order-disorder transitions at 45 °C), was chosen as the main component of the particles' polymer network. To obtain network domains of various crystallinity, stearyl acrylate was copolymerized with propylene glycol acrylate caprylate (comonomer) in the

presence of di-propylene glycol di-acrylate sebacate (a cross-linker) using the miniemulsion process. Comonomers and cross-linkers were mixed directly in fragrances (oil phase) prior to polymerization. The fragrance release was evaluated at 25, 31, 35, and 39 °C to demonstrate new polymer material potential in personal/health care skin-related applications. Particles retain the fragrance at 25 °C. Fragrance release gradually increases at 31, 35, and 39 °C. The crystalline-to-amorphous transition of PSA triggers the release of fragrances from the cross-linked latex particles by increasing their temperature. The inclusion of amorphous fragments in the network reduces the particles' crystallinity and affects fragrance release. The release profile can be tuned by temperature and controlled by the amount of loaded fragrance and the ratio of comonomers in the feed mixture.

Application of biobased latex carriers for fragrance encapsulation potentially reduces environmental impact of the whole cosmetic product composition by providing possible biodegradability.

7.6. References

1. Dreja M., Rybinski D. System for releasing active substances and active agents. DE Patent 10101892 A1, **2002.**

2. Quellet C., Hotz J., Balmer M., Polymeric nanoparticles including active components. US Patent 7,205,340 B2, **2007.**

3. Li Y., Ai L., Yokoyama W., Shoemaker C. F., Wei D., Ma J., Zhong F., Properties of chitosan-microencapsulated orange oil prepared by spray-drying and its stability to detergents. *J. Agric. and Food Chem*., **2013,** 61, 3311-3319.

4. Hofmeister I., Landfester K., Taden, A., pH-sensitive nanocapsules with barrier properties: fragrance encapsulation and controlled release. *Macromolecules*, **2014,** 47, 5768-5773.

5. The Complete Technology Book on Flavors, Fragrances and Perfumes. NPSC Board of Consultants and Engineers, NIIR Project Consultancy Service, **2007.**

6. Calkin R. R., Jelinek J. S., Perfumery: Practice and Principles, Wiley: New York **1994.**

7. Strandburg G., De Lassus P. T., Howell B. A. in Food and Packaging Interactions II, Eds.: Risch S. J. and Hotchkiss J. H. *ACS Symposium Series* 473, ACS, Washington, DC, **1991.**

8. Dorland W. E., Rogers J. A. Jr., The Fragrance and Flavor Industry, Dorland Co., Mendham, New Jersey, **1977.**

9. Peppas N. A., Am Ende D. J. Controlled release of perfumes from polymers. II. Incorporation and release of essential oils from glassy polymers. *J. Appl. Pol. Sci.,* **1997,** 66, 509-513.

10. Edris A., Bergnsthl B., Encapsulation of orange oil in a spray dried double emulsion. *Nahrung*, **2001,** 45, 133–137.

11. Wang C. X., Chen S. L., Fragrance-release property of cyclodextrin inclusion compounds and their application in aromatherapy. *J. Ind. Text.,* **2005,** 34, 157–166.

12. Soper J. C., Kim Y. D., Thomas M. T. Method of encapsulating flavours and fragrances by controlled water transport into microcapsules. US Patent 6,106,875, **2000.**

13. Chang C. P., Dobashi T., Preparation of alginate complex capsules containing eucalyptus essential oil and its controlled release. *Colloids Surf. B: Biointerfaces*, **2003,** 32, 257–262.

14. Wang P., Zhu Y., Yang X., Chen A., Prolonged-release performance of perfume encapsulated by tailoring mesoporous silica spheres. *Flavour Frag. J.,* **2008,** 23, 29–34.

15. Ouall L., Lahoussin D., Process for production nano-capsules containing a fragrance. WO 2006/027664 A2, **2006.**

16. Thies C., Microcapsules for cosmetic applications. *Polym. Mater. Sci. Eng. Proc*., **1990,** 63, 243-244.

17. Pillai J. C., Babar A., Plakogiannis F. M., Polymers in cosmetic and pharmaceutical industries. *Pharm. Acta. Helv*., **1988,** 63, 46-53.

18. Sasaki K., Otani K., Koshiro K., Futaguchi T., Solid perfume composition. *Jpn. Kokai Tokkyo Koho*, Japan Patent, 78 146 744, **1978.**

19. Dross R. D., Polymer compositions allowing controlled release of active constituents. F. Demande (F. Patent) 2 380 328, **1985.**

20. El-Nokaly M., Piatt D., Carpenter B., Polymer Delivery Systems. *ACS Symposium Series* 520, ACS, Washington, DS, **1993.**

21. Peppas N. A., Korsmeyer R. W. in Hydrogels in Medicine and Pharmacy, *CRS Press*: Boca Raton, Florida, **1987.**

22. Tokuyama H., Kato Y., Preparation of thermosensitive polymeric organogels and their drug release behaviors. *Eur. Polym. J.,* **2010,** 46, 277-282.

23. Theisinger S., Schoeller K., Osborn B., Sakar M., Landfester K., Encapsulation of fragrance via miniemulsion polymerization for temperature-controlled release. *Macrom. Chem. and Physics,* **2009,** 210, 411-420.

24. Kimura S., Minamitani K., Gotoh T., Sakohara S., Structure control of thermosensitive porous gels with hydrophobic long side chains and their thermoresponsive properties. *Kobunshi Ronbunshu*, **2000,** 57, 722-729.

25. Matsuda A., Sato J., Yasunaga H., Osada Y., Order-disorder transition of a hydrogel containing an N-alkyl acrylate. *Macromolecules* 27, **1994,** 7695–7698.

26. Osada Y., Matsuda A., Shape-memory in hydrogels. *Nature* **1995,** 376, 6537.

27. Mitsumata T., Gong J. P., Osada Y., Shape memory functions and motility of amphiphilic polymer gels. *Polym. Adv. Technol.,* **2001,** 12, 136–150.

28. Benedict F.G., The Skin Temperature of Humans. *Ergebn. D. Physiol.* **1925,** 24, 594.

29. Tiarks F., Landfester K., Antonietti M., Preparation of Polymeric Nanocapsules by Miniemulsion Polymerization. *Langmuir,* **2001,** 17, 908– 918.

30. Landfester K., Weiss C., Encapsulation by Miniemulsion Polymerization. In Modern Techniques for Nano- and Microreactors/-reactions. Ed.: Caruso F. *Springer*: Berlin, **2010,** 229, 1– 49.

31. Rajot I., Bône S., Graillat C., Hamaide T., Macromolecules. **2003,** 36, 7484–7490.

32. Lau W. Method for forming polymers. U.S. 5 521 266, **1996.**

33. Reinhold J. L., Walker M., Macromol. Chem. Phys., **2002**, 201, 1235– 1243.

34. Agirre A., de las Heras-Alarcón C., Wang T., Keddie J. L., Asua J. M., Waterborne, Semicrystalline, Pressure-Sensitive Adhesives with Temperature-Responsiveness and Optimum Properties. *ACS Appl. Mater. Interfaces*, **2010**, 2, 443–451.

35. Odian G., Principles of Polymerization. 4th edition, *Wiley Interscience*: New York, **2004.**

36. Plate N. A., Shibaev V. P., Comb-like polymers. Structure and properties. *Polym. Sci. Macromol. Rev.*, **1974,** 8, 17-24.

37. Weyland H. G., Hoftyzer P.Y., van Krevelen D.W., Prediction of the glass transition temperature of polymers. *Polymer,* **1970,** 11, 79-87.

38. Turner-Jones A., Crystallinity in isotactic polyolefins with unbranched side chains. *Macromol. Chem.,* **1964,** 71 (1), 1-32.

CHAPTER 8. SYNTHESIS AND FREE RADICAL COPOLYMERIZATION OF A VINYL MONOMER FROM SOYBEAN OIL[4]

8.1. Abstract

A one-step method that converts soybean oil into (acryloylamino)ethyl soyate, a novel acrylic monomer for free radical polymerization, was developed. The synthesized monomer uniquely combines vinyl double bonds (acryloyl functional group) and non-conjugated (isolated) double bonds of fatty acids. The double bond of the acryloyl group is reactive in radical chain polymerization yielding linear macromolecules containing isolated double bonds in side chains. The *Q*-*e* parameters of the new soybean oil-based acrylic monomer (SBA) and monomers reactivity ratios (r_1, r_2) in SBA copolymerization with styrene, methyl methacrylate and vinyl acetate were determined. The results indicate that copolymerization can be described with the classical Mayo-Lewis equation. In terms of polymerizability, the SBA can be classified as a conventional vinyl monomer. The isolated double bonds remain unaffected during polymerization. These double bonds in side chains are capable of further oxidative cross-linking and developing cross-linked polymer coatings.

8.2. Introduction

The design of biobased polymers from renewable resources, including vegetable or plant oils, represents an interesting platform to partially substitute petroleum-based polymers and provide new materials with industrially viable properties and a positive environmental impact [1, 2]. On a cost-performance basis, some of the biobased polymeric

[4]Based on manuscript published in *ACS Sustainable Chem. Eng.,* **2015,** web.
The material in this chapter was co-authored by Andriy Popadyuk, Ihor Tarnavchyk Nadiya Popadyuk and Andriy Voronov. Andriy Popadyuk had primary responsibility for synthetic work, analytical measurements and data interpretation. Andriy Popadyuk was the primary developer of the conclusions that are advanced here. Andriy Popadyuk also drafted and revised all versions of this chapter.

materials can even surpass existing petroleum-based polymers in various possible applications [3, 4]. New biobased macromolecules that compete with existing petroleum-based commodity polymers can be accessed at relatively low cost, which makes plant oils a reliable starting resource (Scheme 8.1 A) [5]. Due to the abundant availability of vegetable oils, they recently became the most important renewable feedstock in the chemical industry, in particular in the production of biobased polymers [6, 10].

The most common renewable resources for synthesizing vegetable oil-based polymers are soybean, linseed, castor and corn oils. Soybean oil (Scheme 8.1 B) is the most abundant and cheap renewable starting material available in large quantities [1].

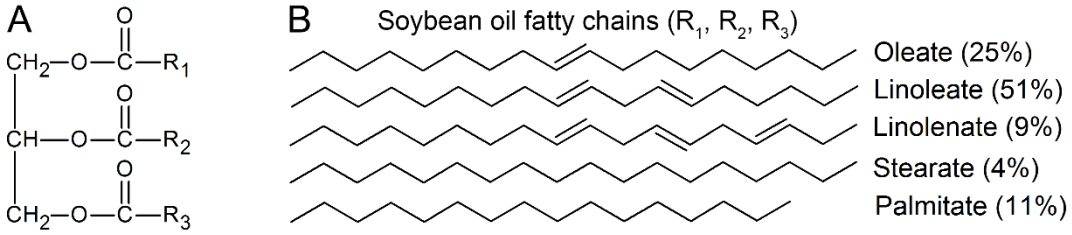

Scheme 8.1. Chemical composition of vegetable oil (A), where R_1, R_2 and R_3 are fatty acid chains. Composition of R_1, R_2 and R_3 in soybean oil (B).

Despite recent progress in the development of renewable polymers, only a small portion (<5%) of biobased polymeric materials are used in the commercial market (largely due to their high cost and mediocre performance), which has motivated thinking about how to prepare low-cost and high-volume polymers from vegetable oils whose properties and performance match those of commodity materials in use, or provide additional benefits [5]. Among polymers from vegetable oils, free radical oxidation polymerization of double bonds of unsaturated triglycerides in atmospheric conditions is the mostly commonly exploited mechanism in coating applications [11, 13]. At the same time, the development of waterborne polymeric materials (emulsions, dispersions, latexes) from vegetable oils remains one of most challenging tasks because of the highly hydrophobic nature of oil [7]. In fact, converting plant oil triglycerides into acrylic monomers for synthesizing latexes, adhesives, etc., *via* classic chain radical copolymerization is challenging. Currently, the

production of fatty acrylates utilizes multistep synthetic procedures [14, 16]. In particular, the production of a fatty monomer, stearyl acrylate, includes the following stages: saponification, neutralization, reduction, acylation and other procedures, thus significantly increasing the monomer cost [17]. Presented approach utilizes one-step transesterification reaction, leading to reduced cost of final monomer.

8.2. Materials and Methods

8.2.1. Materials

Soybean oil (Crisco®, The J.M. Smucker Company, Orville, OH) and N-(hydroxyethyl)acrylamide (HEAAm; TCI America, Portland, OR) were used as received. Azobisisobutyronitrile (AIBN; Sigma–Aldrich, St. Louis, MO) was purified with recrystallization from methanol. Styrene (St; Sigma–Aldrich, St. Louis, MO), methyl methacrylate (MMA) and vinyl acetate (Vac; TCI America, Portland, OR) monomers were distilled under vacuum to remove the inhibitor and stored in a refrigerator. Toluene (Sigma–Aldrich, St. Louis, MO) was distilled prior to use. Other solvents and chemicals, analytical grade or better, were used as received. Deionized water was used for purification purposes (MilliQ, 18 MΩ).

8.2.2. Methods

8.2.2.1. Soy-based Acrylic Monomer (SBA) Synthesis and Characterization

About 115 g of N-hydroxyethyl-acrylamide was added to 150 g of soybean oil, 150 ml of tetrahydrofuran and 0.1 g of 2,6-dimethylphenol in a two-neck 500 ml round-bottom flask equipped with a mechanical stirrer. The reaction mixture was heated up to 40 °C in the presence of a catalytic amount of ground sodium hydroxide slowly added to the reaction mixture with continuous stirring. The reaction mixture was stirred at 40 °C until complete homogenization (approx. 3 hours), and allowed to remain overnight at room temperature. The synthesized product was diluted with CH_2Cl_2, purified by washing with brine, treated with magnesium sulfate and dried under vacuum.

To confirm the chemical structure of the SBA monomer, (acryloylamino)ethyl soyate, ^{1}H NMR spectra were recorded on an AVANCE III HDTM 400 high-performance digital NMR spectrometer (Bruker, Billerica, MA) using $CDCl_3$ as a solvent. The ESI high-resolution mass spectrum of the SBA was obtained using a Bruker Daltonics BioTOF mass spectrometer.

8.2.2.2. Description of FT-IR spectrum of (acryloylamino)ethyl soyate

Figure 8.1 shows the FTIR spectrum of (acryloylamino)ethyl soyate. The appearance of the strong NH adsorption band at 3200-3400 cm^{-1}, the carbonyl (amide I) band at 1670 and the NH (amide II) band at 1540 cm^{-1} indicates the attachment of the acrylamide species to the fatty fragment. The presence of the strong ester bands at 1740, 1245 and 1180 cm^{-1} confirm the ester nature of the synthesized monomer.

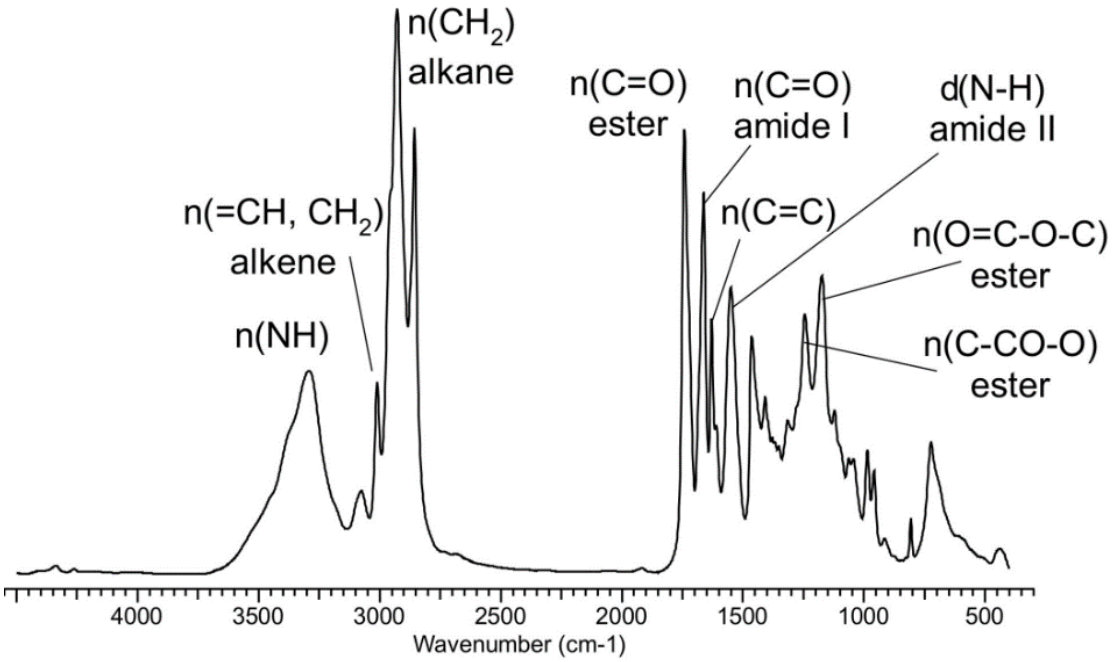

Figure 8.1. FT-IR spectrum of (acryloylamino)ethyl soyate.

FT-IR (film): 3400-3200 cm^{-1} (N-H), 3010 (=CH, CH_2, alkene), 2870-2930 (CH_2, alkane), 1740 (C=O, ester), 1670 (C=O, amide I), 1630 (C=C, vinyl), 1540 (N-H, amide II), 1245 (C-C(O)-O, ester), 1180 (C(O)-O-C, ester).

8.2.2.3. Description of ^{1}H-NMR spectrum of (acryloylamino)ethyl soyate.

Figure 8.2 shows the ^{1}H-NMR spectrum of (acryloylamino)ethyl soyate. The structure of the synthesized monomer is confirmed by the presence of the characteristic peaks of the protons of the acrylic double bond at 6-6.6 ppm, the peaks of the protons of the ethylene linkage between the amide and ester groups at 3.6 and 4.20 ppm, and signals from the fatty acid chains (0.8 to 2.8 ppm).

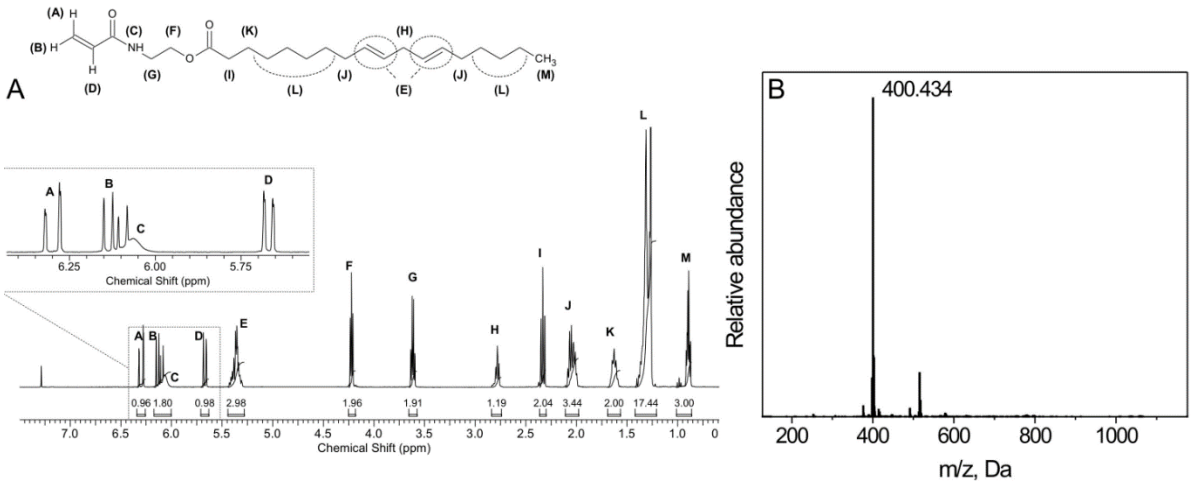

Figure 8.2. ^{1}H NMR spectrum (A) and mass spectrum (B) of SBA.

^{1}H NMR ($CDCl_3$, 400 MHz): δ 0.87 t (3H, CH_3); 1.26 (16-18H, $(CH_2)_{3-9}$); 1.61 (2H, C(O)-CH_2-C$\underline{H}_2$); 2.10 (3-4H, CH_2-C$\underline{H}_2$-CH=); 2.33 dt (2H, C(O)-C$\underline{H}_2$-CH_2); 2.77 (2H, =CH-C$\underline{H}_2$-CH=); 3.6 (2H, NH-C$\underline{H}_2$); 4.2 (2H, C$\underline{H}_2$-O-); 5.35 (2-3H, CH=CH); 5.66 (1H, CH_2=C$\underline{H}$-C(O)); 6.12 (1H, HC$\underline{H}$=CH-C(O)); 6.3 (1H, $\underline{H}$CH=CH-C(O)).

8.2.2.4. SBA free radical polymerization

SBA (0.5 M) and AIBN (0.024 M) were dissolved in toluene and stirred. The reaction mixture was purged with argon at room temperature for 30 min and heated to 60 °C under an argon blanket until 8 h (total monomer conversion of 65 ÷ 85%). The resulting homopolymer was precipitated using a large excess of hexane and purified with multiple precipitations. The purified polymer was dried under reduced pressure at room temperature until a constant weight was obtained.

8.2.2.5. Free radical copolymerization of SBA with St/MMA/Vac

SBA (0.1 ÷ 0.9 mole part), vinyl monomer (St, MMA or Vac) (0.9 ÷ 0.1 mole part) and AIBN (0.024 M) were dissolved in toluene and stirred. The total concentration of monomers was 1-2 M. The reaction mixture was purged with argon at room temperature for 30 min. Copolymerization was carried out under an argon blanket at 60 °C for 2 h until a total monomer conversion of 10 ÷ 15 % was reached. Small samples of the reaction mixture were taken to monitor the progress of the copolymerization reaction using a gravimetric method after precipitation of the copolymer. The resulting copolymer was isolated with precipitation in methanol or hexane and purified with multiple precipitations. The purified polymer was dried under reduced pressure at room temperature until a constant weight was obtained. The resulting copolymers containing 20-80 wt. % of soy-based acrylic units are soluble in acetone, toluene and tetrahydrofuran and non-soluble in methanol and water. The average molecular weight of the copolymers was determined with gel permeation chromatography (M_n = 28,000–37,000 g/mol).

8.2.2.6. SBA-based copolymer characterization

To determine the composition of the SBA-St, SBA-MMA and SBA-Vac copolymers, ^{1}H NMR spectra for the homo- and copolymers were recorded on an AVANCE III HDTM 400 high-performance digital NMR spectrometer (Bruker, Billerica, MA) using $CDCl_3$ as a solvent and phthalic anhydride as an internal reference.

The average molecular weight of the copolymers was determined with gel permeation chromatography (GPC) using a Waters Corporation modular chromatograph consisting of a Waters 515 HPLC pump, a Waters 2410 Refractive Index Detector and a set of two 10 μm PL-gel mixed-B columns; the column temperature was set at 40 °C. Tetrahydrofuran (THF) was used as the carrier solvent.

Figure 8.3 shows the chemical structure of the copolymers synthesized from the SBA and three commodity vinyl monomers, methyl methacrylate (MMA), styrene (St), vinyl acetate (Vac).

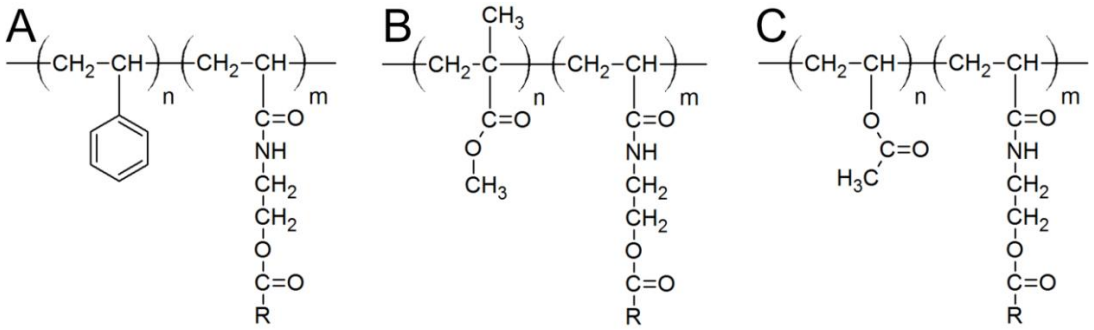

Figure 8.3. Chemical structure of the copolymers from the soy-based acrylic monomer and styrene (SBA-St) (A), methyl methacrylate (SBA-MMA) (B), vinyl acetate (SBA-Vac) (C) (R - fatty acid chains of soybean oil).

The glass transition temperature of the SBA homopolymer as well as the SBA-MMA copolymers was determined via modulated differential scanning calorimetry (MDSC) using a TA Instruments Q1000 calorimeter. Dry nitrogen with a flow rate of 50 mL/min was purged through the sample. The samples were subjected to an underlying heating rate of 10 °C/min.

8.3. Results and Discussion

In this study, we developed a one-step approach for converting soybean oil into acrylic/methacrylic fatty monomers by reacting naturally occurring triglycerides with acrylamide- or methacrylamide-containing alcohols. The direct transesterification reaction allows for the acylation of the hydroxy groups in N-(hydroxyethyl)acrylamide molecules with the acyl groups of triglyceride molecules (Scheme 8.2). It is assumed that the conjugated double bond of the acrylamide functional group is reactive in addition radical chain polymerization and linear macromolecules form from the new (meth)acrylic fatty monomers.

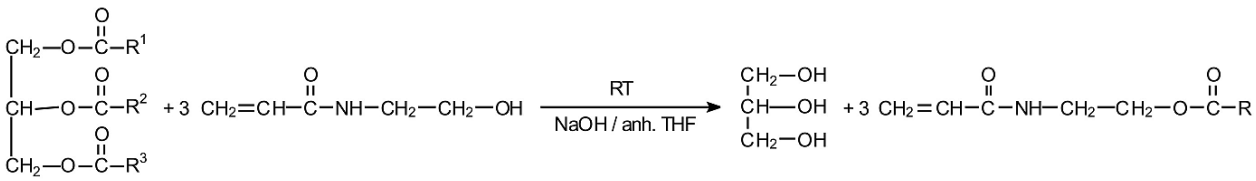

Scheme 8.2. Synthesis of soy-based acrylic monomer (SBA) *via* direct transesterification reaction triglycerides of soybean oil with N-(hydroxyethyl)acrylamide.

At the same time, their non-conjugated double bonds remain unaffected during free radical polymerization, resulting in (co)polymers with unsaturated fatty side fragments. These fragments facilitate (co)polymer oxidative cross-linking, thus enhancing the material's properties and performance and broadening the potential application of the synthesized macromolecules for developing cross-linked polymer coatings.

To yield the (acryloylamino)ethyl soyate monomer, crude soybean oil was reacted in one step with *N*-(hydroxyethyl)acrylamide in the presence of a catalytic amount of sodium hydroxide. Among various solvents, tetrahydrofuran is a suitable reaction medium for high-yield synthesis of the targeted SBA monomer, which depends on the initial concentration of the reactants and the ratio of catalyst (NaOH) to reactants.

The anticipated chemical structure of the synthesized monomer was confirmed using FT-IR spectroscopy (Figure 8.1), ^{1}H NMR spectroscopy (Figure 8.2 A) and mass-spectrometry (Figure 8.2 B). The recorded spectra show that the (acryloylamino)ethyl soyate molecules contain an N-acryloyl fragment that provides monomer reactivity in chain radical polymerization.

To establish the monomer capability in free radical reactions, first homopolymerization was carried out in toluene at 60 °C, an initial monomer concentration of 0.5 M, and a concentration of free radical initiator, AIBN, 0.024 M.

Figure 8.4 shows the ^{1}H NMR spectrum that confirms the formation of the homopolymer from the SBA monomer. The spectrum indicates that polymer backbone is formed through the polymerization of SBA acrylic fragments while the isolated double bonds of the soy-based monomer remain unaffected during the reaction. Reactive in oxidative

polymerization [18, 19], these fragments can be further involved in the free radical processes of the SBA-based macromolecules, in particular the (ambient) cross-linking and formation of the cross-linked polymers. The latter observation distinguishes the SBA monomer from existing vegetable oil-based monomers that do not possess conjugated double bonds (polymerizable in chain radical polymerization) and undergo exclusively free radical oxidation reactions (through isolated double bonds).

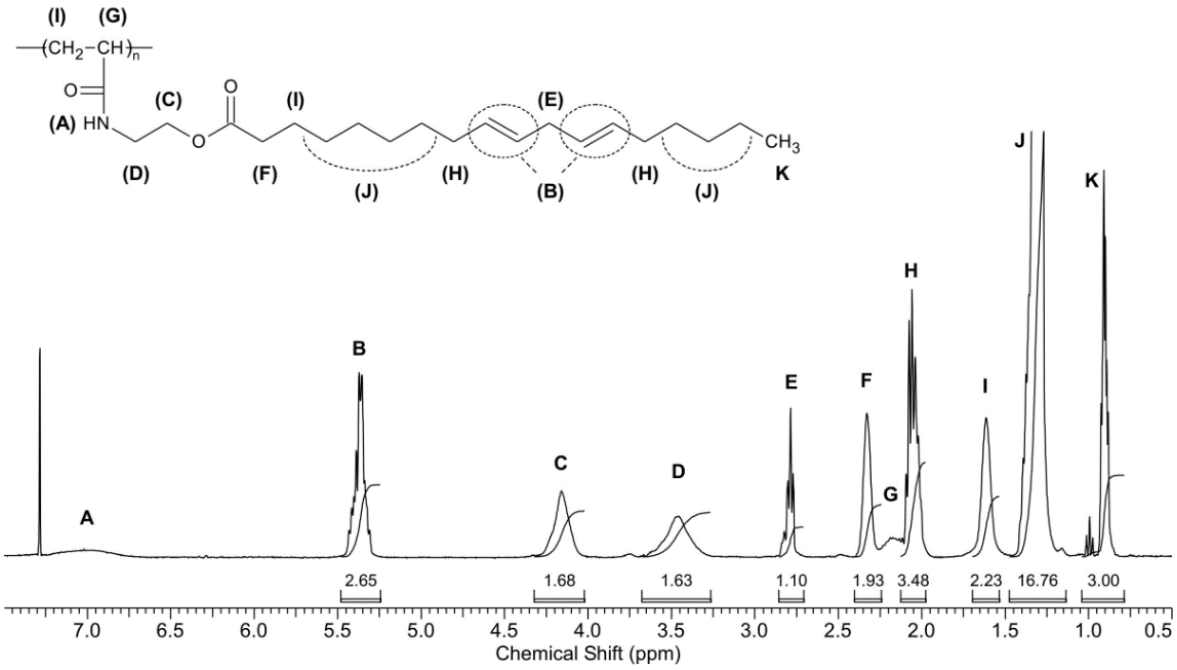

Figure 8.4. ^{1}H NMR spectrum of the SBA homopolymer.

The further focus of this study is to evaluate the reactivity of the SBA acrylic double bond and monomer feasibility in free radical copolymerization. To evaluate monomer reactivity, one should either experimentally determine the r_1 and r_2, reactivity ratios of the monomer pair, showing the tendency of each comonomer to cross-propagation (interaction between the free radical and the "other" monomer) regarding self-propagation (the interaction of the radical and the "own" monomer), or foresee the copolymerization behavior of each monomer using the Alfrey-Price *Q-e* scheme [20]. If the *Q-e* values are available for

each monomer in copolymerization, the Alfrey-Price scheme becomes a useful tool for accessing the potential copolymer composition in a controllable way.

In this work, we performed experiments in order to determine the *Q*-*e* values for a new soy-based acrylic monomer. For this purpose, in copolymerization of the SBA and styrene (St), the r_1 and r_2 were determined experimentally by measuring an instantaneous copolymer composition (with ^{1}H NMR spectroscopy at low monomer conversions) (Figure 8.5) and employing the Kelen-Tudos approach (a differential form of the Mayo-Lewis copolymerization equation) (Equation 8.1) [20-22].

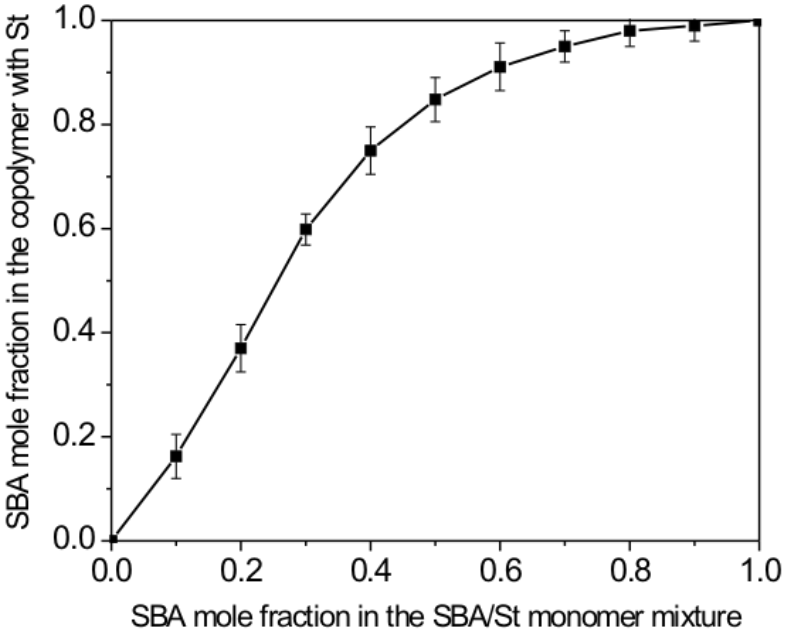

Figure 8.5. Experimental SBA content in the SBA-St copolymer vs. SBA content in the initial feed mixture.

$$y_i = r_1 x_i - \frac{r_2}{a}(1 - x_i) \tag{8.1}$$

$$a = \sqrt{(F_i^2/f)_{min}(F_i^2/f)_{max}};\ \ x_i = \frac{F_i^2/f_i}{a + F_i^2/f_i};\ \ \ y_i = \frac{F_i(f_i - 1)}{f_i(a + F_i^2/f_i)}$$

where F_i is the mole fraction of the monomer in a feed mixture, and f_i is the monomer fraction in the copolymer.

Experimental data of feed composition $F_i = [M_1]_i/[M_2]_i$ and copolymer composition $f_i = [m_1]_i/[m_2]_i$, y_i values were calculated and plotted vs. x_i values [21]. $[M_1]$, $[M_2]$ are each monomer concentration in a feed, and $[m_1]$, $[m_2]$ are each monomer content in a copolymer.

According to the Kelen-Tudos approach, linear approximation of the resulting plot yields the reactivity ratios r_1 and r_2 as follows: $\{x = 1, r_1 = y\}$ and $\{x = 0, r_2 = -ay\}$. Experimental data on r_1 and r_2 for SBA and St are shown in Table 8.1.

Table 8.1. Monomer reactivity ratios and *Q*-*e* values for copolymerization of SBA and MMA, St, Vac.

Comonomer pair	r_1	r_2
SBA (Q = 0.39, e = 0.58) – MMA (Q = 0.78, e = 0.4)20	0.45 ± 0.1	2.15 ± 0.4
SBA - Vac (Q = 0.026, e = -0.22)20	9.43 ± 0.7	0.06 ± 0.01
SBA - St (Q = 1, e = -0.8)20	0.18 ± 0.06	0.85 ± 0.2

Having the experimental r_1 and r_2 for SBA and St, as well as literature data on styrene *Q*-*e* values (Q = 1 and e = -0.8) [20], the Alfrey-Price scheme (Equation 8.2) was applied to calculate the *Q*-*e* of the SBA monomer. This calculation yields Q = 0.39 and e = 0.58.

$$r_2 = \frac{Q_2}{Q_1}\exp\{-e_2(e_2 - e_1)\};\quad r_1 = \frac{Q_1}{Q_2}\exp\{-e_1(e_1 - e_2)\} \tag{8.2}$$

To demonstrate that the *Q-e* values of SBA can be applied to control copolymer composition, an additional studies on copolymerization of the soy-based acrylic monomer with methyl methacrylate (MMA) and vinyl acetate (Vac) were performed.

The chemical composition of each resulting SBA-MMA and SBA-Vac copolymer (ten for each monomer pair) was determined experimentally using ^{1}H NMR spectroscopy, and compared to the theoretical copolymer compositions. The theoretical compositions were assessed using the Alfrey-Price scheme (Equation 8.2) and the *Q-e* values for MMA, Vac (from the literature data for both), and SBA (from our experiments, Table 8.1) to determine r_1 and r_2 for the SBA-MMA and SBA-Vac monomer pairs. In the next step, these r_1 and r_2 were applied to calculate each theoretical copolymer composition using the Mayo-Lewis copolymerization equation (Equation 8.3).

$$\frac{[m_1]}{[m_2]} = \frac{[M_1]}{[M_2]} \cdot \frac{r_1[M_1] + [M_2]}{r_2[M_2] + [M_1]} \tag{8.3}$$

It can be clearly seen in Figure 8.6 that the experimental and calculated plots are in a good agreement, indicating that copolymerization of SBA with Vac (Figure 8.6 A) and MMA (Figure 8.6 B) can be described with the classical Mayo-Lewis copolymerization equation. Additionally, the *Q-e* values of the new monomer provide reliable information on SBA reactivity in free radical copolymerization.

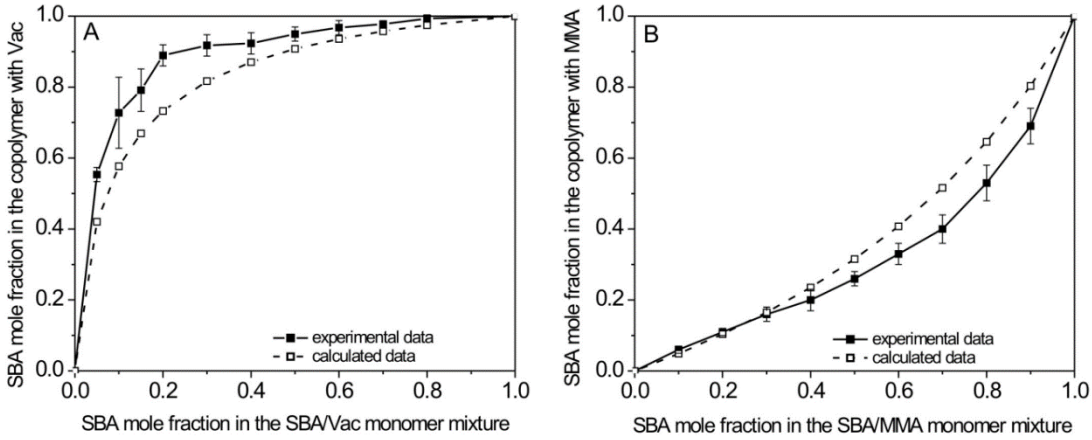

Figure 8.6. Experimental SBA content in SBA-Vac (A) and SBA-MMA (B) copolymers vs. SBA content in the initial feed monomer mixture.

The SBA-based copolymer composition in the fraction of the soybean oil-derived units in the resulting macromolecules can vary within a broad range and in a controlled way by the monomer feed mixture in copolymerization of SBA with three commodity vinyl monomers, styrene, methyl methacrylate and vinyl acetate.

For most free radical copolymerizations, the product $r_1 \cdot r_2$ may be used with discretion for estimating the extent of copolymer randomness [20, 22, 23]. Based on r_1 and r_2 shown in Table 8.1, their product equals 0.96 for SBA and MMA, 0.15 (SBA and St), and 0.56 (SBA and Vac). The obtained data indicate that there is a tendency toward alternation of fragments in the macromolecular backbone of copolymer from SBA and St (the $r_1 \cdot r_2$ value approaches zero). In contrast, the copolymerization of SBA and MMA results in random copolymers (r_1 and r_2 product approaches 1).

To show that the fraction of the soybean oil-derived units in the resulting macromolecules affects the copolymers' properties, the glass transition temperature (T_g) of the SBA-MMA copolymers with varied composition was determined using differential scanning calorimetry (DSC).

The T_g is an important polymer characteristic indicating when the material softens and becomes rubberlike, thus giving direct information about the required polymers' processing conditions and possible various applications. The DSC data (Figure 8.7) indicate that the increasing fraction of the soybean oil-derived fragments in synthesized macromolecules results in decreasing T_g of the copolymers.

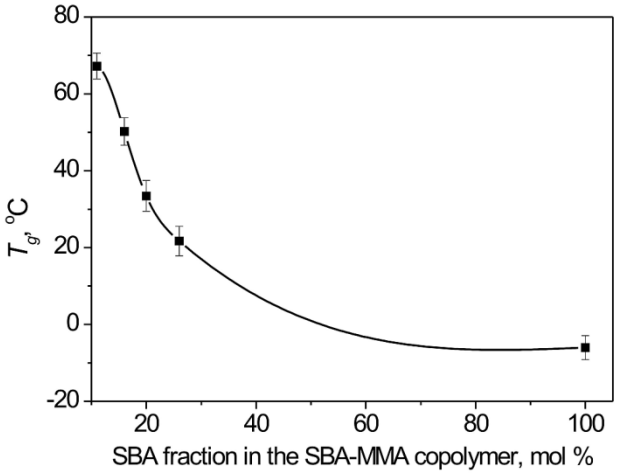

Figure 8.7. Glass transition temperature (T_g) of SBA-MMA copolymers vs. soybean oil-derived fragment content in the macromolecular backbone determined with DSC.

To conclude, the free radical copolymerization of (acryloylamino)ethyl soyate, a biobased acrylic monomer, and commodity monomers can become an important and useful tool in designing new polymeric materials.

8.4. Conclusions

In this work, we demonstrated that in terms of polymerizability, the new monomer behaves as a conventional vinyl monomer. The SBA-based copolymer composition can be varied by the monomers ratio in a feed mixture using the classical Mayo-Lewis copolymerization equation. The physico-chemical properties of such biobased copolymers, including the glass transition temperature, solubility, adhesion, elasticity, chemical reactivity, etc., can vary within wide limits. The SBA monomer could advantageously replace petroleum-based monomers in the production of, in particular, polymer latexes, adhesives and other industrial materials that utilize acrylic monomers and polymers.

8.5. Acknowledgments

The authors would like to thank Dr.Angel Ugrinov, Department of Chemistry and Biochemistry, NDSU, for his help with the mass-spectrometry measurements and interpretation of results.

8.6. References

1. Belgacem M. N., Gandini A., Monomers, Polymers and Composites from Renewable Resources. *Elsevier*: Amsterdam, **2008.**

2. Lu Y., Larock R. C., Novel Polymeric Materials from Vegetable Oils and Vinyl Monomers: Preparation, Properties and Applications. *Chem. Sus. Chem.,* **2009,** 2, 136-142.

3. Williams C. K., Hillmayer M. A., Polymers from Renewable Resources: A Perspective for a Special Issue of Polymer Reviews. *Polym. Rev*., **2008,** 48 (1), 1-10.

4. Gallezot P., Conversion of biomass to selected chemical products. *Chem. Soc. Rev.,* **2012,** 41, 1538-1558.

5. Lligadas G., Ronda J. C., Galia M., Cadiz V., Renewable polymeric materials from vegetable oils: a perspective. *Mat. Today*, **2013,** 16 (9), 337-343.

6. Verhe R. G., Industrial products from lipids and proteins, in Renewable Bioresources: Scope and Modification for Non-Food Applications. Eds.: Stevens C. V., Verhe R. G., *John Wiley & Sons, Ltd*: Chichester, **2004.**

7. Guner F. S., Yagci Y., Erciyes A. T., Polymers from triglyceride oils. *Prog. Polym. Sci.,* **2006,** 31, 633-670.

8. Sharma V., Kundu P. P., Addition polymers from natural oils—A review *Prog. Polym. Sci.,* **2006, *31***, 983-1008.

9. Wool R. P., Sun X. S., Biobased Polymers and Composites. *Elsevier*: Amsterdam, **2005.**

10. Gunstone F., Fatty acid and lipid chemistry, *Blackie Academic & Professional*, New York, **1996.**

11. Bailey A. E., Bailey's Industrial Oil and Fat Products. *Wiley*: New York, **1996.**

12. Norris F. A., Extraction of fats and oils, in Bailey's Industrial Oil and Fat Products. Ed.: Swern D., *Wiley:* New York, **1996.**

13. Johnson R. W., Fritz E. E., Fatty Acids in Industry. *Marcel Dekker*: New York, **1989.**

14. Cayli G., Meier M. A. R., Polymers from renewable resources: Bulk ATRP of fatty alcohol-derived methacrylates. *Europ. J. of Lipid Sci. Technol*., **2008,** 110 (9), 853-859.

15. Biermann U., Friedt W., Lang S., Luhs W., Machmuller G., Metzger J. O., Rüsch gen Klaas M., Schäfer H. J., Schneider M. P., New Syntheses with Oils and Fats as Renewable Raw Materials for the Chemical Industry. *Angew. Chem. Int. Ed.,* **2000,** 39 (13), 2206–2224.

16. Meier M. A. R., Metzger J. O., Schubert U. S., Plant oil renewable resources as green alternatives in polymer science. *Chem. Soc. Rev*. **2007,** 36 (11), 1788-1802.

17. Franz W., Osterburg G., Strehlke G., Process for the production of higher alkylacrylates and methacrylates. US 3887609, **1975.**

18. Derksen J. T. P., Cuperus F. P., Kolster P., Renewable resources in coatings technology: a review. *Prog. Org. Coat*, **1996,** 27, 45.

19. Solomon D. H., The Chemistry of Organic Film Formers. *Wiley*: New York, **1971.**

20. Odian G., Principles of Polymerization. *Wiley*: New York, **1981.**

21. Kelen T., Tudos F., Turcsanyi B., *Polymer Bulletin*, **1980,** 2, 71.

22. Chanda M., Introduction to Polymer Science and Chemistry. A Problem Solving Approach. *Taylor & Francis, CRC Press*: Boca Raton, FL, **2006.**

23. Carraher C. E., Introduction to Polymer Chemistry, 2nd edition. *Taylor & Francis, CRC Press*, Boca Raton, FL, **2010.**

CHAPTER 9. CONCLUSIONS AND FUTURE WORK

9.1. Conclusions

Main goal of this work was to develop novel polymer materials with lower environmental impact, including new biobased materials with properties and performance not sacrificed by presence of renewable content. Synthesis, characterization and feasibility of industrial applications in waterborne systems for such materials are demonstrated.

Chapters 3 and 4 showcase development and application of new copolymer, PM-MA, which combines features of both initiator and surfactant (the inisurf), to be applied in conventional emulsion polymerization. PM-MA was synthesized on the basis of N-[(tert-butylperoxy)methyl]acrylamide monomer, previously developed in our group, and maleic anhydride. It was shown that PM-MA can perform as both surfactant (reduce surface tension, form micelles, solubilize water-insoluble molecules) and initiator of free radical polymerization (decompose at elevated temperature yielding radicals). PM-MA was successfully applied as an inisurf in emulsion polymerization – leading to formation of surface functionalized (peroxidized) polymer latexes. Unlike traditional surfactants, inisurf is covalently grafted onto the latex particle's surface. Extent of in-situ surface functionalization was explored, showing an ability to finely-tune amount of peroxide and carboxyl functional groups on the surface.

Chapter 3 focuses on application of PM-MA functionalized polymer latexes as reactive additives for coatings based on conventional acrylate and styrene-butadiene latexes. It was shown that monodisperse latex particles with a controlled amount of peroxide groups on the surface can be used simultaneously as cross-linker and filler, in latex coatings, effectively improving mechanical properties of the coatings.

Chapter 4 describes a new way of colloidosomes fabrication using functionalized polymer latexes. Discussion is mainly focused on Pickering emulsion formation aspect. Pickering emulsions use PM-MA functionalized latex particles as an exclusive surface active

ingredient to form micron-sized 'soft template' droplets that are further polymerized into colloidosomes.

As a conclusion to work presented in Chapters 3 and 4 it can be summarized that application of PM-MA inisurfs might not only lead to new waterborne polymer materials, but also allows to reduce number of chemicals used in polymer latex production. Usage of PM-MA functionalized latexes can improve properties of current industrial latex materials, opening new possibilities to reduce polymer material environmental impact.

Chapters 5 and 6 are devoted to synthesis, characterization and application of soy-based polymeric surfactants (SBPS) – copolymers of 2-(vinyloxy)ethyl soyate and ethylene glycol ethyl vinyl ether oligomers. Specifically, Chapter 5 describes development of novel environmentally friendly and efficient SBPS for personal-care applications and showcases colloidal properties of SBPS macromolecules - as related to their composition. Notable conclusion drawn from this chapter includes importance of maintaining hydrophilic-lipophilic balance within certain range for SBPS by tailoring chemical structure of ethylene glycol ethyl vinyl ether oligomer and ratio of comonomers in copolymer structure. Evidence of synergetic surface activity in combination with lower molecular weight surfactants (in particular, sodium dodecyl sulfate, SDS) is presented. Solubilization study, where mixture of SDS with SBPS are used, shows higher solubilization abilities of surfactant mixtures than for respective components.

Chapter 6 develops idea of synergy between SDS and SBPS in aqueous solutions. Model SBPS-based hair shampoos are selected as a platform for study and their performance in terms of cleaning efficiency, foaming, conditioning, visual appearance and physicochemical properties was studied. It is shown, that use of environmentally friendly SBPS allows to reduce SDS content of shampoo without sacrificing performance of the formulation. Moreover, SBPS introduces additional desirable property to the shampoo formulations – conditioning, providing protection for hair shafts from protein loss. SBPS

application in shampoo formulations leads to less toxic product and a opens great niche for renewable polymer material applications.

Chapter 7 describes research focused on development of thermoresponsive cross-linked latex particles for fragrance encapsulation and release. The main component of the particle network is a biobased polymer – poly(stearyl acrylate) (PSA), a polymer with long crystallizable alkyl side chains. PSA macromolecules undergo reversible order-disorder transitions at 45 °C associated with interactions between the alkyl side chains. Our objective was to synthesize the particles protecting the encapsulated fragrance at ambient temperatures, and to facilitate the release of cargo at the temperature of the surface of the skin, which varies in different regions of the body between 33.5 and 36.9 °C. In order to be able to control melting temperature of carrier latex particles, additional monomer and cross-linker were developed in this work and copolymerized with PSA to form cross-linked matrix of latex particles. For this, monomers based on caprylic (dipropylene glycol acrylate caprylate) and sebacic (dipropylene glycol diacrylate sebacate) acids were synthesized. As a result, importance of side-chain crystallinity as a triggering mechanism for thermoresponsive fragrance release from carriers was shown. Additionally, effect of interaction between cargo fragrance and different monomer units in structure of matrix is presented. The work concludes that efficient fragrance carriers with thermal trigger release mechanism can be developed on entirely renewable basis, signifying vast improvement in reduction of polymer material environmental impact while fabricating high-performance materials.

Research work presented in Chapter 8 targets development of one-step approach for converting soybean oil into acrylic/methacrylic fatty monomers for free radical polymerization by reacting naturally occurring triglycerides with acrylamide- or methacrylamide-containing alcohols. Presently, new renewable monomer obtained via the direct transesterification reaction of N-(hydroxyethyl)acrylamide molecules with soybean oil

triglycerides is disclosed. Synthetic procedure, characterization and application possibilities are presented in details. It is shown, that new monomer (SBA) can be effectively copolymerized with other common vinyl monomers via free radical copolymerization to yield linear macromolecules. Moreover, the obtained results point to ability of controlling such copolymer composition by employing Q-e monomer reactivity scheme. This is demonstrated on the examples of copolymerization of SBA with methyl methacrylate, vinyl acetate and styrene. In fact, as experimental results suggest, SBA proves to be promising as a comonomer for various latex technologies, such as adhesives, paints and coatings, inks etc. SBA brings several invaluable properties into copolymer macromolecules, including high hydrophobicity, fatty acid unsaturations and long side-chain morphology in conjunction with linear backbone. Yet again, development and application of SBA opens vast array of possibilities in reducing polymer material environmental impact – starting from sustainability and ending with reduced volatile organic content waterborne polymers.

9.2. Future work

The future work in view of currently presented research would include several research efforts.

From perspective of Chapter 3, future research would focus mainly on further investigating improvement of coatings via addition of PM-MA functionalized latexes. Specifically, look into Red-Ox systems to facilitate peroxide decomposition at lower temperatures for ambient cross-linking.

As continuation of Chapter 4, colloidosomes synthesis could be modified to utilize plant oil-based monomers for fabrication of renewable carrier systems for agricultural application.

Additional optimization and manufacturing scale-up studies for SBPS copolymers from Chapters 5 and 6 would be carried out. SBPS copolymers presented in this work were synthesized on the basis of custom-made PEG derivatives, however some similar PEG

derivatives are commercially available and it would be appealing if SBPS would be synthesized using them. It was shown in Chapter 5 that surface activity of SBPS depends on balance between content/type of PEG derivative in SBPS macromolecule. Consequently, changing type of PEG derivative could lead to optimization of SBPS structure for better performance.

As for Chapter 7 – there is still some uncertainty as to the initial evaporation kinetics of fragrance from carrier latex. One of the possible additions to experimental studies would include headspace evaporation technique and application of gas chromatography to analyze composition of vapors. This will not only allow us to better optimize carrier matrix composition, but also gives insights on fragrance fractionation during evaporation stage as well as during storage. Another interesting aspect of this work is type and structure of cross-linking monomer – there exists additional possibility to control fragrance protection and evaporation rates by changing density of cross-links throughout matrix.

Chapter 9 opens variety of possibilities for future work – both in terms of monomer development (using other acrylamide derivatives), monomer synthesis scale-up and monomer application in fabrication of waterborne polymer materials. SBA shows promising application opportunities in the field of polymer latexes for coatings and adhesive industries.